REPUBLIC OF TURKEY
ISTANBUL GELISIM UNIVERSITY
INSTITUTE OF GRADUATE STUDIES

Department of Electrical and Electronics Engineering

SPEED AND FLUX CONTROL OF AN INDUCTION MOTOR USING THE V/F METHOD BASED ON THE FUZZY PI TECHNIQUE

Master Thesis

Mohammed AL-EZZI

Supervisor

Assoc. Prof. Dr. Indrit MYDERRIZI

Istanbul– 2022

THESIS INTRODUCTION FORM

Name and Surname	**:**	Mohammed AL-EZZI
Language of the Thesis	**:**	English
Name of the Thesis	**:**	Speed and Flux Control of an Induction Motor using the V/F method based on The Fuzzy PI Technique.
Institute	**:**	Istanbul Gelisim University Institute of Graduate Studies
Department	**:**	Electrical-Electronic Engineering
Thesis Type	**:**	Master
Date of the Thesis	**:**	04.07.2022
Page Number	**:**	85
Thesis Supervisors	**:**	Assoc. Prof. Dr.Indrit MYDERRIZI
Index Terms	**:**	Induction motor, magnetic Flux, fuzzy logic.

Turkish Anstract **:** Asenkron motorlar günümüzde endüstride yaygın olarak kullanılmaktadır, Asenkron motorlar basit ve sağlam yapısı, yüksek verimliliği, iyi güç faktörü ve kendi kendine hareket eden torku vardır. Bu nedenlerle fabrika uygulamalarında ve proseslerde en çok kullanılan motorlardan biridir. Asenkron motorun hızını kontrol etmek için manyetik akının değeri her zaman sabit tutulmalıdır. Bu amaçla farklı yöntemler kullanılabilir. Scalar V/f kontrol sistemi, bir asenkron motorun hızını kontrol etmek için basit ve pratik bir yol sağlar. Bu tez, motor hızını düzenleyerek ve manyetik akı değerini nominal değerde tutarak Skalar V/f kontrol sisteminin

performansını iyileştirmektedir. Matlab-Simulink simülasyonları, sistemin nominal akı değerini korurken yüksek yorumlama ve kararlı motor hızı sağlama yeteneğini doğrulayarak motor verimliliğini artırdı. Matlab-Simulink kullanılarak yapılan simülasyon sonuçları, önerilen sistemin etkinliğini ve motor hızının yüksek stabilitesini elde etme yeteneğini göstermiştir. Motor verimini ve ömrünü artırmaya ve kayıpları azaltmaya katkıda bulunmuştur.

Distribution List **:** 1. To the Institute of Graduate Studies of Istanbul Gelisim University
2. To the National Thesis Center of YÖK (Higher Education Council)

Mohammed AL-EZZI

REPUBLIC OF TURKEY
ISTANBUL GELISIM UNIVERSITY
INSTITUTE OF GRADUATE STUDIES

Department of Electrical and Electronics Engineering

SPEED AND FLUX CONTROL OF AN INDUCTION MOTOR USING THE V/F METHOD BASED ON THE FUZZY PI TECHNIQUE

Master Thesis

Mohammed AL-EZZI

Supervisor

Assoc. Prof. Dr. Indrit MYDERRIZI

Istanbul– 2022

DECLARATION

I hereby declare that in the preparation of this thesis, scientific and ethical rules have been followed, the works of other persons have been referenced in accordance with the scientific norms if used, and there is no falsification in the user data, any part of the thesis has not been submitted to this university or any other university as another thesis.

Mohammed AL-EZZI

…/…/2022

TO ISTANBUL GELISIM UNIVERSITY

THE DIRECTORATE OF INSTITUTE OF GRADUATE STUDIES

The thesis study of Mohammed AL-EZZI titled as Speed and Flux Control of an Induction Motor using the V/F method based on The Fuzzy PI Technique. has been accepted as MASTER THESIS in the department of ELECTRICAL-ELECTRONIC ENGINEERING by out jury.

Director

Assoc. Prof. Dr. Indrıt MYDERRIZI

(Supervisor)

Member

Prof. Dr. Mustafa DOĞAN

Member *Assoc. Prof. Dr. Aydemir ARISOY*

APPROVAL

I approve that the signatures above signatures belong to the aforementioned faculty members.

… / …. / 2022

Prof. Dr. İzzet GÜMÜŞ

Director of the Institute

SUMMARY

Today, induction motors are widely used in the industry. They have a simple, robust structure, high efficiency, good power, and self-starting torque. For these reasons, they are preferable motors in factory applications and processes. The value of the magnetic Flux must always be kept constant while controlling the induction motor`s Speed. For this purpose, different methods can be used. The Scalar V/f control system provides a simple and practical way to control the speed of the induction motor. In this thesis, work is done to improve the performance of the Scalar V/f control system by regulating the motor speed and maintaining the value of the magnetic Flux at the nominal value. The simulation results in Matlab-Simulink showed the effectiveness of the proposed method and the ability of the control system to provide high performance in regulating the motor speed while maintaining a constant value of the magnetic Flux, which contributes to increasing the motor efficiency and reducing losses.

Keywords : Induction motor, magnetic Flux, fuzzy logic.

ÖZET

Asenkron motorlar günümüzde endüstride yaygın olarak kullanılmaktadır. Asenkron motorlar basit ve sağlam yapısı, yüksek verimliliği, iyi güç faktörü ve kendi kendine hareket eden torku vardır. Bu nedenlerle fabrika uygulamalarında ve proseslerde en çok kullanılan motorlardan biridir. Asenkron motorun hızını kontrol etmek için manyetik akının değeri her zaman sabit tutulmalıdır. Bu amaçla farklı yöntemler kullanılabilir. Scalar V/f kontrol, bir asenkron motorun hızını kontrol etmek için basit ve pratik bir yol sağlar. Bu tezde, motor hızını düzenleyerek ve manyetik akı değerini nominal değerde tutarak Skalar V/f kontrol performansını iyileştirmeye yönelik çalışma yapılmıştır. Matlab-Simulink'teki simülasyon sonuçları, önerilen yöntemin etkinliğini ve kontrol sisteminin, motorun verimliliğini artırmaya ve kayıpları azaltmaya katkıda bulunan sabit bir manyetik akı değerini korurken motor hızını düzenlemede yüksek performans sağlama yeteneğini göstermiştir.

Anahtar Kelimeler : Asenkron motor, manyetik akı, bulanık mantık**.**

TABLE OF CONTENTS

CHAPTER FOUR
CONTROL OF IM USING FUZZY LOGIC

CHAPTER FIVE
CONCLUSIONS AND RECOMMANDATION

ABBREDIVATIONS

V/F	**:**	Voltage over frequency
FLC	**:**	Fuzzy Logic controller
PI	**:**	proportional-integral controller
SPWM	**:**	Sinusoidal pulse width modulation
THD	**:**	Total Harmonic Distortion
IGBT	**:**	Insulated-Gate Bipolar Transistor
IM	**:**	Induction Motor
SVPWM	**:**	Space vector pulse width modulation

LIST OF TABLES

LIST OF FIGURES

PREFACE

I would like to thank Assoc. Prof. Dr. Indrit MYDERRIZI, for his encouragement and support in preparing this thesis. I would also like to express my appreciation and thanks to Prof. Dr. Mustafa DOĞAN, Assoc. Prof. Dr. Aydemir ARISOY and all the staff of Istanbul Gelişim University, including the knowledgeable professors and colleagues who accompanied us during our academic journey. I also thank my family for being a source of motivation throughout my thesis period.

I dedicate my thesis with appreciation to our homeland Iraq and the lovely Turkey, which embraced our scientific experiment and cooperated in making it possible for me to graduate in such a splendid way.

INTRODUCTION

Electrical motors nowadays can be found in many products. Induction motors are widely used around the world. One of their most uses is for industrial purposes because they have simple, robust construction, high efficiency, good power factor, high power/weight ratio, low cost, easy maintenance, and a self-starting torque. (Agrawal et al., 2019;Bharti et al., 2019;Pena & Diaz et al., 2017;Sudaryanto et al., 2020). The speed of an induction motor is proportional to the voltage, frequency, and the number of poles, but considering that the electromagnetic moment of an induction motor is directly proportional to the ratio of the voltage and voltage frequency, the best way to change the motor speed would be by changing the voltage and frequency together in a constant ratio (Devi et al., 2014; Mohammed & Ghoneim et al., 2021; Sudaryanto et al., 2020). Induction Motor drive depends on two major methods of control system: scalar control and vector control (Hannan et al., 2018; Lee & Han et al., 2022; Mikhael et al., 2016). The scalar V/f control methodology maintains a constant ratio between voltage and frequency, which provides a simple, practical way of controlling induction motor speed. This controlling way can be implemented in a closed-loop or open-loop system. This methodology provides a satisfactory response in the steady-state, but the dynamic performance in the transient conditions is usually low, especially at low speeds (Bharti et al., 2019; Pena & Diaz et al., 2017).The control techniques used in the Scalar control system range from traditional controllers to expert and intelligent control techniques. (Divyasree & Binojkumar et al., 2017 ;El-Zohri & Mosbah et al., 2020;Hannan et al., 2018). Proportional–integral (PI) controllers are commonly used in scalar V/F control systems for induction motors (Bharti et al., 2019; Suetake et al., 2011; Verma et al., 2018). A proportional-integral (PI) controller has a simple structure, low cost, and easy implementation, but they have many shortcomings (El-Zohri & Mosbah et al., 2020; Hannan et al., 2018; Lesani et al., 2013; Suetake et al., 2011).

1- They cannot provide the available ability to achieve the performance specifications simultaneously.
2- PI controllers may not be able to achieve good performance when there is a change in the parameters of the controlled system.

3- The constants of PI controllers must be calculated after knowing the mathematical model of the controlling system to obtain good performance when using these controllers, and this matter may not be available.

Efficient controlling techniques are necessary for Induction motors related to Industrial applications. To get a good dynamic performance of the controlled system, it can adopt a fuzzy logic methodology to build the controller. Fuzzy logic controllers have advantages over PI controllers: a shorter rise time, a shorter settling time, and more decreasing electromagnetic torque oscillations (Arulmozhiyal et al., 2009; Mohammed & Ghoneim et al., 2021).

One effective way to implement the fuzzy logic controller for regulating motor speed is the hybrid fuzzy PI controller, where the controller's input signals are speed error (the difference between the reference speed and the measured speed) and error change (the difference between the error value at the present moment and the error value at the previous moment) and then, the control system must generate both the voltage and frequency of the sinusoidal pulse width modulation (PWM) inverter. (El-Zohra & Mosbah et al., 2020; Lesani et al., 2013; Verma et al., 2018).

CHAPTER ONE
PURPOSE OF THE THESIS

1.1. Literature Survey

(El-Zohri et al., 2020) Designed a scalar V/F control system to regulate speed induction motor by using the concept of fuzzy logic like PI; the control system was dependent on the Space vector pulse width modulation (SVPWM) technique, which is used to produce switching pulses for the inverter of insulated-gate bipolar transistor (IGBT) related to its low Total Harmonic Distortion (THD) for the output voltage. The results in their paper using MATLAB/Simulink showed that the hybrid fuzzy PI controller performed better than the PI controller in terms of setting time and harmonic content of Induction motors. The settling time for using PI ranged between 0.16-0.35sec, and THD was equal to 0.47-0.77, while in order to use fuzzy logic, it ranged between 0.12-0.225sec, and THD was equal to 0.44-0.75. However, the study did not consider the regulation of magnetic flux to determine the time to overcome the load torque.

(Setae et al., 2011) presented in their paper a hybrid fuzzy PI system based on a digital signal processor for the scalar speed drive of the induction motor. The experimental results showed that the performance of the fuzzy PI controller was satisfying in relation to load-torque change with constant speed. However, the settling time was 0.3sec. While the study did not compute the consumed time to overcome the load torque.

(Verma et al., 2018) presented a comparison between PI controller and Fuzzy PI Logic controller for scalar control of induction motor. The simulation results showed that the Fuzzy PI controller achieved a shorter rise time which was equal to 1.5sec., and a shorter settling time which was equal to 3.5sec.

In their paper (Bharti et al., 2019), there was an attempt to implement some modifications in the PI controller and compare it with the standard PI controller in order to reduce error and improve performance and harmonics. The settling time was equal to 0.4sec, and the time to overcome the torque load time was equal to 1sec.

The V/f control system for the speed of the induction motor in open-loop and closed-loop was implemented successfully (Pena & Diaz et al., 2017).

The simulation results showed that the speed response was good with a setting time equal to 0.2sec. The motor's performance for applying load torque was tested, and the overcoming time was two seconds.

(Ping & Landing et al., 2006) presented an integral sliding-mode controller for controlling of induction motor, which is based on a vector control system. The motor speed used in the speed feedback loop was estimated by an adaptive algorithm. The control technique provided a fast dynamic response (settling time is equal to 0.3sec) with high performance against parameters changes and external disturbances.

In (Diabase & Inukjuak et al., 2017), the induction motor was controlled using vector control, and space vector pulse width modulation (SVPWM) technology which was used to produce gating pulses to drive the inverter to feed the motor. The design of several PI controllers is also detailed. To avoid deep saturation, anti-windup PI controllers are used. This minimizes the time taken for speed and flux to respond. The coupling between torque and flux is broken. The system performs better in terms of dynamic response with a setting time of 1.8 sec.

(Mugler & Kerion et al., 2021) proposed an optimized Fuzzy PI controller. A simplified rule-based Fuzzy PI controller is developed, and it is compared to a conventional PI controller. The simulation results in MATLAB/SIMULINK showed that the performance of the simplified Fuzzy PI controller is superior to that of the traditional PI controller, as the settling time for the Fuzzy PI controller is 0.98sec, while for the traditional PI controller, it is 1.4 sec.

The application of optimal control for vector control of an induction motor was proposed by (Chen & Zhang et al., 2015). The simulation results in MATLAB/Simulink showed that the designed controller has a good ability to track different speed commands and is robust against load torque changes.

Many studies have been presented on the scalar V/F control system of the induction motor, some of which we mentioned, the aspect of magnetic flux regulation has not been considered, while other research has confirmed that it has great importance (especially research related to vector control). As the magnetic flux

regulation contributes to improving the dynamic performance of the motor and increasing its efficiency, this is what we will seek to apply during this research.

1.2. Problem Statement

The induction motor is the most widely used element in industrial applications. Improving the performance of the induction motor will directly contribute to improving the production performance of the industrial facility and increasing its efficiency. Hence the need to develop an induction motor drive system to increase the speed of response and overcome load changes during the operation of induction motors and work to improve the efficiency of the induction motor and reduce the value of economic and electrical losses.

The issue of maintaining magnetic flux at nominal value is important in an induction motor for the following reasons:

1- A decrease in the value of the magnetic flux will directly affect the value of the electromagnetic torque produced by the motor.

2- An increase in its value leads to thermal heating in the machine, and therefore the voltage applied to the motor must be reduced, and as a result, the value of the speed at which the induction motor can operate will decrease.

3- Regulating the flux value will make the motor highly dynamic, as the motor will produce the required torque and thus increase the response speed and speed in overcoming the load torque.

The scalar V/f control method is based on the fact that changing the value of the voltage and frequency together maintains a nominal value of the magnetic flux, but this assumption is based on neglecting the voltage drop on the resistance of the constant, and therefore the performance of this control method is bad in transient cases as well as when working at low speeds. This issue has been solved by applying vector control methods such as field-oriented control or direct torque control, but these methods are difficult to implement compared to the scalar control method (Chen & Mhelliah et al., 2017; Lee & Han et al., 2022; Mikhael et al., 2016; Pena & Diaz et al., 2017). In this research, we seek to improve the performance of the induction motor and overcome the problems related to transient conditions or working the motor at a

low speed by developing a scalar V/f control method by modifying the control law to regulate the speed and magnetic flux.

1.3. Aims and Objective

The present work aims to develop a scalar control system for a three-phase induction motor, to improve the time response characteristics (reducing settling time and overshot) and increase the motor's ability to overcome changes in load torque and reduce oscillations of the induced torque in addition to improving the efficiency of the motor and reducing the value of losses consumed during motor operation.

This work will be done according to the following steps:

1. Study the mathematical model of the induction motor and build the dynamic model in MATLAB-Simulink.
2. Design a scalar control system using the PI controller in MATLAB-Simulink.
3. Design a scalar control system using the fuzzy PI controller in MATLAB-Simulink.
4. Optimizing the performance of the last control system by regulating the magnetic flux.

1.4. Thesis Organization

The thesis is composed of five chapters.

Chapter One

This chapter provides general information about the induction motor, control systems, control technologies, the problem statement, and the objective of the thesis.

Chapter Two

In this chapter, the structure and working principle of an induction motor are explained, the mathematical model in MATLAB-Simulink is studied and simulated, and the operation of the motor is discussed in an open-loop system.

Chapter Three

In this chapter, methods of controlling the speed of an induction motor and designing a scalar control system to control the speed using PI controllers are studied.

Chapter Four

In this chapter, an explanation of fuzzy logic is presented, and then a scalar V/F control system is designed using a fuzzy PI technic to regulate the speed and magnetic flux of the induction motor.

Chapter Five

In this chapter, Conclusions and future work are presented.

CHAPTER TWO
INDUCTION MOTOR IN OPEN LOOP SYSTEM

2.1. Introduction

The three phase induction motor, invented by Nikola Tesla in 1886, is the most widely used in the industry, and this is due to its advantages such as durability, simplicity of installation, and low cost compared to other motors (Chen & Mhelliah et al., 2017; Lee & Han et al., 2022; Li et al., 2019; Satariano et al., 2020).

2.2. Structure of induction motor

An induction motor consists of two main sections separated by an air gap. These two sections are:

• Stator

It is a group of thin plates made of electromagnetic iron and insulated on both sides with a thin layer of varnish to reduce Foucault's cyclonic currents. There are regularly distributed slots on the inner surface of the stator core, within which are located three similar coils (Hannan et al., 2018).

• Rotor

It is a group of thin plates made of electromagnetic iron and insulated on both sides with a skinny oxide layer. These plates are combined and pressed together to form the core of the rotor. On the outer surface of the rotor, there are evenly distributed slots. They are located within these slots in either three-phase coils with ends assembled in a star or delta. Then it is called a wound rotor (metal rods either of aluminum or copper) that are shortened from both ends by palace rings, and then it is called a rotor with a squirrel cage (Bharti et al., 2019; Sharma G et al., 2020). Thus, the rotor has two electrical structures, but we can accept that these two structures are electrically equivalent.

2.3. Working principle of induction motor

When a three-phase sinusoidal alternating frequency voltage is applied to the stator coils, sinusoidal currents of the same frequency will pass through the coils. These currents generate a magnetic field with a uniform sinusoidal distribution and a constant amplitude, so this magnetic field is rapidly rotating at speed known as the synchronous speed. This rotating magnetic field is transmitted through the air gap and, by scanning the rotor coils, incites an electromotive force according to Faraday's law. Since the rotor coils are shorted, this induced electrical force generates currents in the rotor coils. These currents generate a magnetic field of the same direction and speed as the magnetic field of the stator; these two fields constitute the total magnetic field. Due to the mutual influence between the currents of the rotor and the magnetic field, mechanical effects are generated on the rotor coils, and this causes an electromagnetic moment according to Maxwell's law, this torque rotates the rotor quickly and in the same direction as the magnetic field of the stator, and then the speed of the electrical quantities of the rotor becomes (Bharti et al., 2019; Li et al., 2019).

$$\omega_{\mathrm{sl}} = \omega_s - \omega \tag{2.1}$$

Where ω_{sl} (rad/sec) is the electrical angular speed of the electrical quantities in the rotor (voltages, currents, flux), ω_s (Rad/sec) is the electrical angular speed of the electrical quantities in the stator (voltages, currents, flux). ω (rad/sec) is the electrical angular speed of the rotor, which is given according to the relationship:

$$\omega = p\Omega \tag{2.2}$$

Where Ω (rad/sec) is the mechanical angular speed of the rotor is given according to the relationship:

$$\Omega = \frac{2\pi n}{60} \tag{2.3}$$

Where n (r.p.m) is given as:

$$n = \frac{60*\mathrm{f}}{p} \tag{2.4}$$

Where p is the number of pole pairs of the machine.

2.4. Equivalent circuit of an induction motor

When studying the induction motor, dealing with the real machine is not preferable. Rather, it is preferable to represent the machine with an equivalent electrical circuit that enables us to derive and study the equations that describe the machine. This circuit allows us to study the properties of the motor in different operating conditions. Figure 1 shows the equivalent circuit of a single phase of the induction motor.

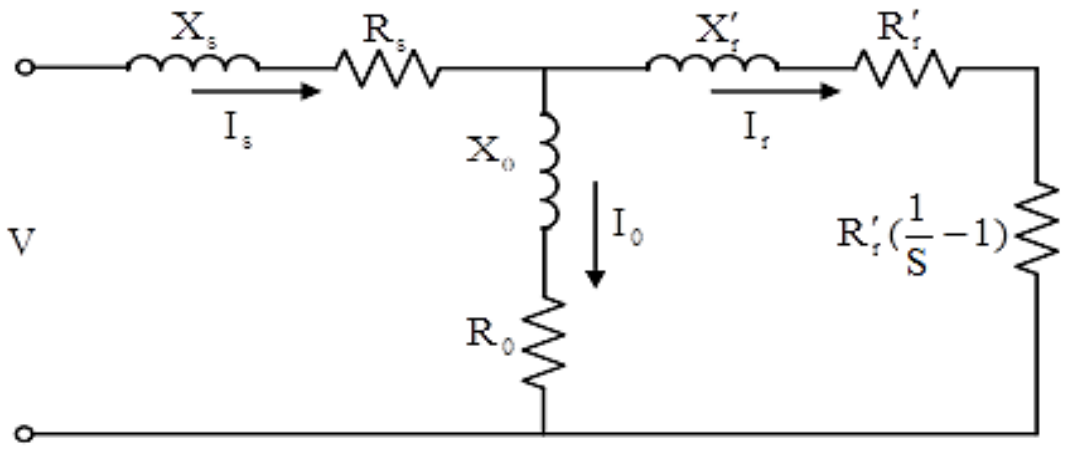

Figure 1. Equivalent single-phase circuit for a three-phase induction motor (Lee & Han et al., 2022; Pedra J et al., 2009).

Where s is slip, R_s, X_s are stator resistance and reactance. $R_r^{`}, X_r^{`}$ are rotor resistance and reactance relative to the stator.

Slip can be defined as:

$$s = \frac{\omega_s - \omega}{\omega_s} \tag{2.5}$$

From this circuit, the rotor current is given by:

$$I_r^{`} = \frac{V}{|Z|} = \frac{V}{\sqrt{(R_s + \frac{R_r^{`}}{s})^2 + (X_s + X_r^{`})^2}} \tag{2.6}$$

The relationship gives the equivalent impedance of one phase:

$$Z = (R_s + \frac{R_r^{`}}{s}) + J(X_s + X_r^{`}) \tag{2.7}$$

Part of the power supplied to the stator coils is spent as iron losses and copper losses, and the remaining part is electromagnetic power transmitted through the air gap to the rotor, and this power is given by the relationship:

$$P_{em} = 3I_r^{`2}\frac{R_r^{`}}{s} \qquad (2.8)$$

When this power reaches the rotor, part of it is spent as electrical and mechanical losses, and the remaining power is a mechanical power given by the relationship:

$$P_{mech} = (1-s)P_{em} \qquad (2.9)$$

2.5. Torque-Speed Relationship

The electromagnetic torque is given by:

$$T = \frac{P_{em}}{\omega_s} \qquad (2.10)$$

Substituting values P_{em} , $I_r^{`}$ into the torque relationship, the following relationship is obtained:

$$T = 3\frac{V^2}{\omega_s}\left[\frac{\frac{R_r^{`}}{s}}{(R_s+\frac{R_r^{`}}{s})^2+(X_s+X_r^{`})^2}\right] \qquad (2.11)$$

Equation (2.11) represents the torque-speed relationship, which is a non-linear relationship; by plotting this relationship, figure 2 was obtained.

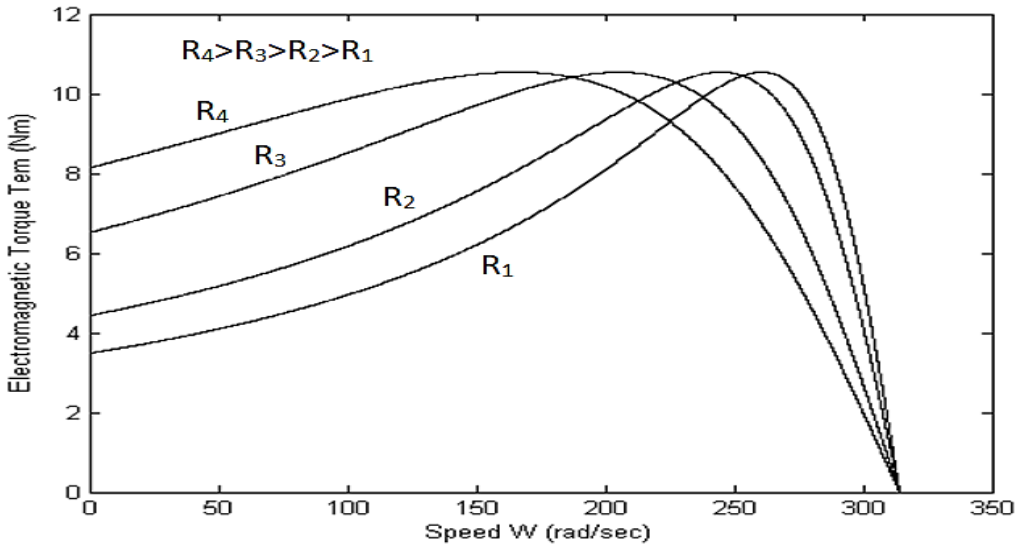

Figure 2. Torque-speed characteristics at different values of rotor resistance (Pedra J et al., 2009), (Verma et al., 2018)

Based on Figure 2, it can be seen that the value of the electromagnetic torque is large at starting, and the motor speed is zero; therefore, slip g=1. When the motor reaches the speed corresponding to the value of slip, approximately g=0, the value of the electromagnetic torque becomes equal to zero. These changes in the value of torque are during starting to occur within a brief period. Also, it can be seen that there is a maximum value of the torque called the critical value, and increasing the rotor resistance leads to an increase in the starting torque; it does not affect the value of the critical torque. This can be used to increase the starting torque by using an external variable resistance connected to the rotor circuit and then shorted after starting (Diyoke et al., 2016; Pedra J et al., 2009).

2.6. Mathematical Model of Three Phase Induction Motor

The mathematical model includes the equations that describe the work of the motor in the steady-state and transient state, and therefore the first step to studying the induction motor is modeling and simulation the motor using computers. Then drive systems can be developed to regulate the motor speed.

To conclude the general mathematical model of the induction motor, the following has been assumed (Pena & Diaz et al., 2017).

• The air gap is regular; that is, it has a fixed width.

• Neglecting the magnetic saturation, magnetic leakage, and iron losses.

• Sinusoidal distribution of the magnetic field along the air gap.

• The complete symmetry of the stator and the rotor windings, i.e., the resistors and inductors of the windings, are equal.

2.6.1 Electrical Equations of an induction motor in a,b,c frame

An induction motor's stator and the rotor contain three windings spaced apart at an angle$2\pi/3$. When applying three-phase voltages to the stator coils, the currents passing through each stator and the rotor and the resulting magnetic flux are also three-phase (Bharti et al., 2019. Sharma et al., 2020). Therefore we can represent the motor in the electric space schematically by six coils, where the electrical quantities (voltages, currents, fluxes) are vectors, and the phases of the stator and the rotor are shifted from each other at an angle, as shown in the following Figure 4.

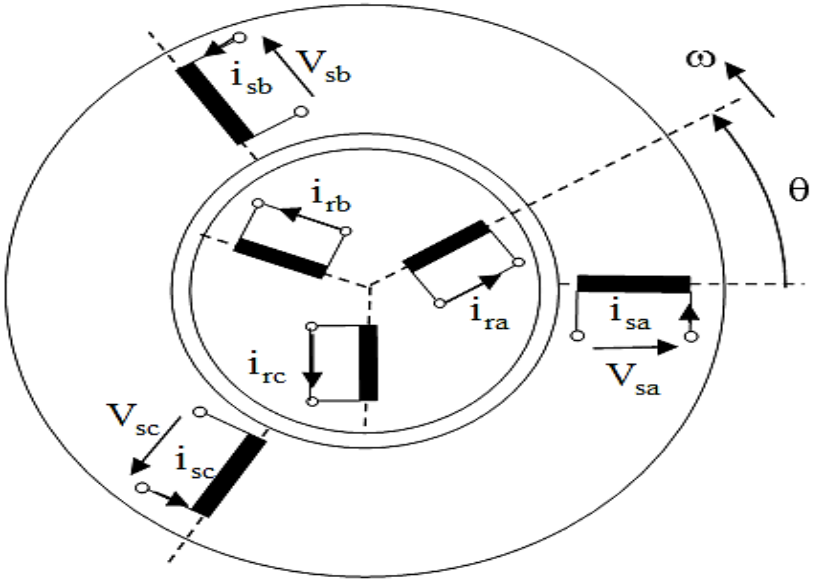

Figure 3. Schematic representation of the induction motor in a,b,c frame (Sharma et al., 2020)

From Figure 3, the voltage equations for the stator phases can be written assuming the same phase resistances as:

• The voltage equation for phase a:

$$V_{\mathrm{sa}} = R_s I_{\mathrm{sa}} + \frac{d\Phi_{\mathrm{sa}}}{\mathrm{dt}} \tag{2.12}$$

The voltage equation for phase b:

$$V_{sb} = R_s I_{sb} + \frac{d\Phi_{sb}}{dt} \tag{2.13}$$

• The voltage equation for phase c:

$$V_{sc} = R_s I_{sc} + \frac{d\Phi_{sc}}{dt} \tag{2.14}$$

In the same way, the voltage equations for the rotor phases can be written assuming the same phase resistances as

• Voltage equation for phase a:

$$\mathrm{V_{ra}} = \mathrm{R_r I_{ra}} + \frac{\mathrm{d\Phi_{ra}}}{\mathrm{dt}} \tag{2.15}$$

• Voltage equation for phase b:

$$V_{rb} = R_r I_{rb} + \frac{d\Phi_{rb}}{dt} \tag{2.16}$$

• Voltage equation for phase c:

$$V_{rc} = R_r I_{rc} + \frac{d\Phi_{rc}}{dt} \tag{2.17}$$

the above equations can be written in matrix form as:

• Voltage equation of stator windings:

$$[V_{sabc}] = [R_s][i_{sabc}] + \frac{d}{dt}[\Phi_{sabc}] \tag{2.18}$$

• Voltage equation of rotor windings:

$$[V_{rabc}] = [R_r][i_{rabc}] + \frac{d}{dt}[\Phi_{rabc}] = 0 \tag{2.19}$$

$$[V_{s(r)abc}] = \begin{bmatrix} V_{s(r)a} \\ V_{s(r)b} \\ V_{s(r)c} \end{bmatrix} \tag{2.20}$$

$$[\mathrm{i_{sabc}}] = \begin{bmatrix} \mathrm{i_{s(r)a}} \\ \mathrm{i_{s(r)b}} \\ \mathrm{i_{s(r)c}} \end{bmatrix} \tag{2.21}$$

$$[\Phi_{s(r)}] = \begin{bmatrix} \Phi_{s(r)a} \\ \Phi_{s(r)b} \\ \Phi_{s(r)c} \end{bmatrix} \tag{2.22}$$

$$[R_{s(r)}] = \begin{bmatrix} R_{s(r)} & 0 & 0 \\ 0 & R_{s(r)} & 0 \\ 0 & 0 & R_{s(r)} \end{bmatrix} \tag{2.23}$$

Where: $[V_{s(r)\text{abc}}]$ are stator (rotor) voltages, $[i_{s(r)\text{abc}}]$ are stator (rotor) currents, $[\Phi_{s(r)}]$ are stator (rotor) fluxes, and $[R_{s(r)}]$ are stator (rotor) Resistors.

2.6.2. Park Transformation Matrix

The voltage equations for the stator and the rotor contain variables that change with time, making modeling these equations very difficult, so a reference α^k , β^k frame rotating with speed ω_k has been defined instead of the system of three axes (Fereka et al., 2018; Mohammed & Ghoneim et al., 2021).

This new reference frame can convert three-phase stator and rotor windings into orthogonal two-phase equivalent windings, as shown in figure 5.

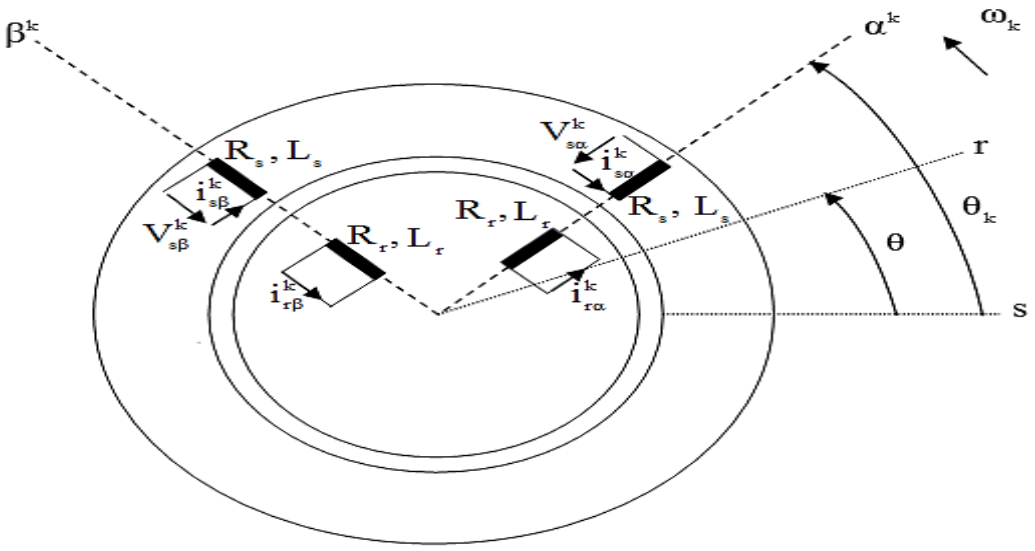

Figure 4. Schematic representation of a three-phase induction motor in α, β frame, (Li et al., 2019)

The following matrix, which can be deduced from figure 4, is used to convert the electrical quantities from a,b,c frame to α, β frame rotating at the speed ω_k. (Sharma et al., 2018).

$$\begin{bmatrix} X_\alpha^k \\ X_\beta^k \end{bmatrix} = \sqrt{3/2} \begin{bmatrix} \cos(\theta_k) & \cos(\theta_k - \frac{2\pi}{3}) & \cos(\theta_k + \frac{2\pi}{3}) \\ -\sin(\theta_k) & -\sin(\theta_k - \frac{2\pi}{3}) & -\sin(\theta_k + \frac{2\pi}{3}) \end{bmatrix} \begin{bmatrix} X_a \\ X_b \\ X_c \end{bmatrix} \quad (2.24)$$

In the special case of a fixed frame($\omega_k = 0$), the process of moving from a,b, and c frame to α_s, β_s frame takes place according to the following matrix equation (Sudaryanto et al., 2020):

$$\begin{bmatrix} X_\alpha^k \\ X_\beta^k \end{bmatrix} = \sqrt{3/2} \begin{bmatrix} 1 & -0.5 & -0.5 \\ 0 & \sqrt{3}/2 & -\sqrt{3}/2 \end{bmatrix} \begin{bmatrix} X_a \\ X_b \\ X_c \end{bmatrix} \quad (2.25)$$

The transposon of the matrix in the previous equation is used to move oppositely. (Hannan et al., 2018; Sharma et al., 2020).

2.6.3. Dynamic Model of the Induction Motor in (α, β) frame

The mathematical model of a three-phase induction motor that uses two components of a rotor flux vector and two components of a stator current vector as state variables is given in a reference α , β frame($\omega_k = 0$): (Hinkkanen et al., 2022; Shiravani et al., 2022; Sabir & Ibrir et al., 2018; Trabelsi et al., 2012).

$$i_{s\alpha} = -a_5 i_{s\alpha} + \omega_k i_{s\beta} + a_3 \Phi_{r\alpha} + a_4 \omega \Phi_{r\beta} + b v_{s\alpha} \quad (2.26)$$

$$i_{s\beta} = -\omega_k i_{s\alpha} - a_5 i_{s\beta} - a_4 \omega \Phi_{r\alpha} + a_{3_{r\beta}} + b v_{s\beta} \quad (2.27)$$

$$\dot{\Phi}_{r\alpha} = a_2 i_{s\alpha} - a_1 \Phi_{r\alpha} - \omega \Phi_{r\beta} \quad (2.28)$$

$$\dot{\Phi}_{r\beta} = a_2 i_{s\beta} + \omega \Phi_{r\alpha} - a_1 \Phi_{r\beta} \quad (2.29)$$

$$\dot{\omega} = (G_1 \Phi_{r\alpha} i_{s\beta} - G_1 \Phi_{r\beta} i_{s\alpha} - T_d) - (f/J)\omega \quad (2.30)$$

Where:

$$a_1 = R_r / L_r \quad (2.31)$$

$$a_2 = L_m R / L_r \quad (2.32)$$

$$a_3 = L_m R_r / (\sigma L_s L_r^2) \quad (2.33)$$

$$a_4 = L_m/(\sigma L_s L_r) \quad (2.34)$$

$$a_5 = (L_r^2 R_s + L_m^2 R_r)/(\sigma L_s L_r^2) \quad (2.35)$$

$$b = 1/(\sigma L_s) \quad (2.36)$$

$$G_1 = (PL_m/L_r) * (P/J) \quad (2.37)$$

$$\sigma = 1 - L_m^2/(L_s L_r) \quad (2.38)$$

Where $v_{s\alpha}$, $v_{s\beta}$ are stator voltage vector components; $i_{s\alpha}$, $i_{s\beta}$ are stator current vector components; $\Phi_{r\alpha}, \Phi_{r\beta}$ are the rotor flux vector components; L_m is the magnetizing inductance; L_s is the stator inductance; L_s is the rotor inductance; J is rotor inertia, f is friction coefficient; and T_d Is load torque.

The stator flux vector components can be evaluated as:

$$\Phi_{s\alpha} = \int (v_{s\alpha} - i_{s\alpha} R_s) \quad (2.39)$$

$$\Phi_{s\beta} = \int (v_{s\beta} - i_{s\alpha} R_s) \quad (2.40)$$

The amplitude of the stator flux vector can be calculated as:

$$|\Phi_s| = \sqrt{\Phi_{s\alpha}^2 + \Phi_{s\beta}^2} \quad (2.41)$$

2.6.4. System stability

By substituting the values of the system parameters around a zero balance point, the dynamic model of the motor in state space can be written as:

$$\begin{bmatrix} i_{s\alpha} \\ i_{s\beta} \\ \dot{\Phi}_{r\alpha} \\ \dot{\Phi}_{r\beta} \\ \dot{\omega} \end{bmatrix} = \begin{bmatrix} -a_5 & 0 & a_3 & 0 & 0 \\ 0 & -a_5 & 0 & a_3 & 0 \\ a_2 & 0 & -a_1 & 0 & 0 \\ 0 & a_2 & 0 & -a_1 & 0 \\ 0 & 0 & 0 & 0 & -f/J \end{bmatrix} \begin{bmatrix} i_{s\alpha} \\ i_{s\beta} \\ \Phi_{r\alpha} \\ \Phi_{r\beta} \\ \omega \end{bmatrix} + \begin{bmatrix} b & 0 \\ 0 & b \\ 0 & 0 \\ 0 & 0 \\ 0 & 0 \end{bmatrix} \begin{bmatrix} v_{s\alpha} \\ v_{s\beta} \end{bmatrix} \quad (2.42)$$

Then, the property values of matrix A are (-309.3 -16.77 -309.3 -16.77 -1). Thus, the system is stable.

2.7. Modelling the induction motor in Matlab\Simulink

This section describes the block diagrams needed to model and simulate a three-phase induction motor in MATLAB-Simulink. Figure 5 shows the block diagram of three phases induction motor, which includes:

1- Block diagram of three-phase induction motor in α, β frame, in Figure 6.

2- The block diagram of Park Transformation, which converts a,b, and c signals into α, β, signals, is shown in Figure 7.

3- Block diagram of Invers Park Transformation, which converts α , β signals into a,b, and c signals, shown in Figure 8.

4- Block diagram of the stator flux observer, shown in Figure 9.

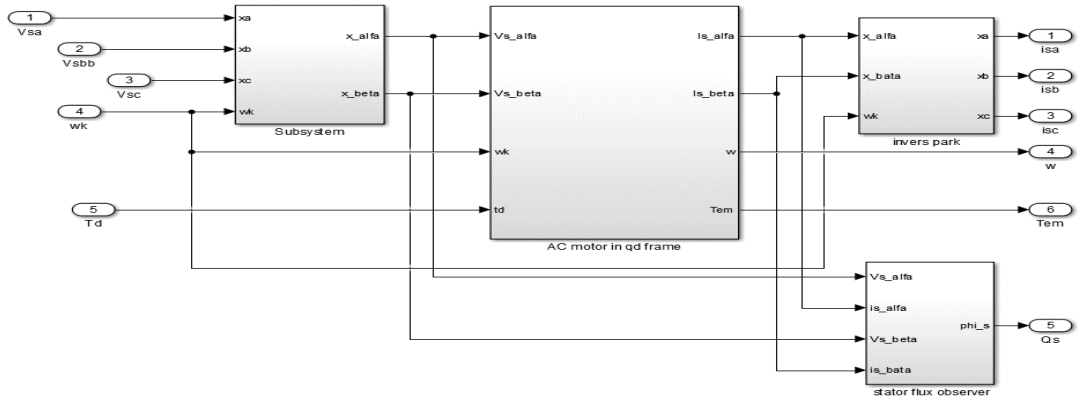

Figure 5. Block diagram of three phases Induction motor in Matlab-Simulink

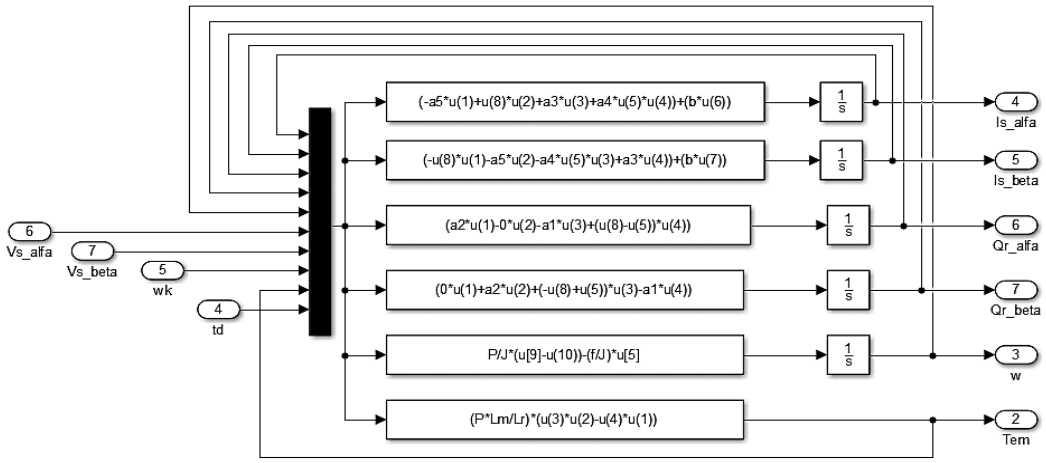

Figure 6. Block diagram of Induction motor in α,β frame

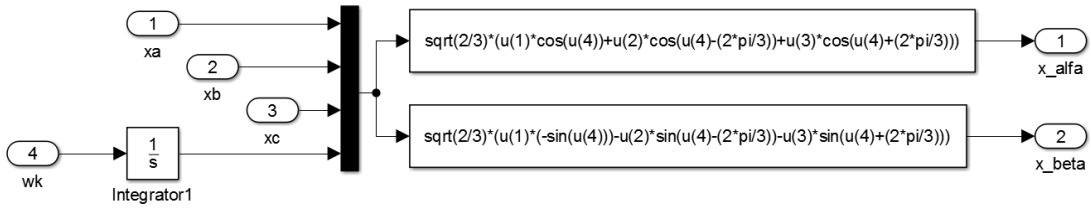

Figure 7. Block diagram of Park Transformation

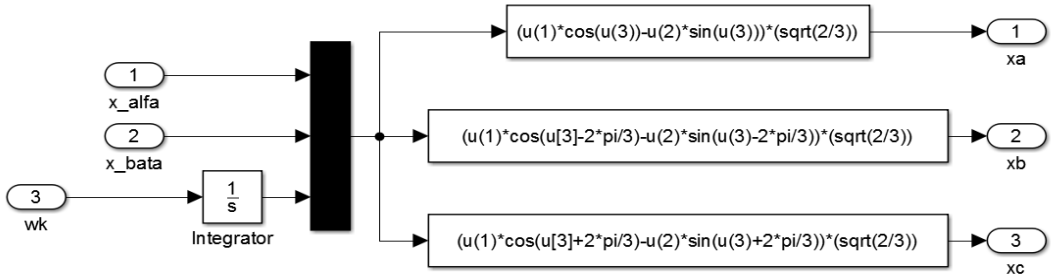

Figure 8. Block diagram of Inverse Park Transformation

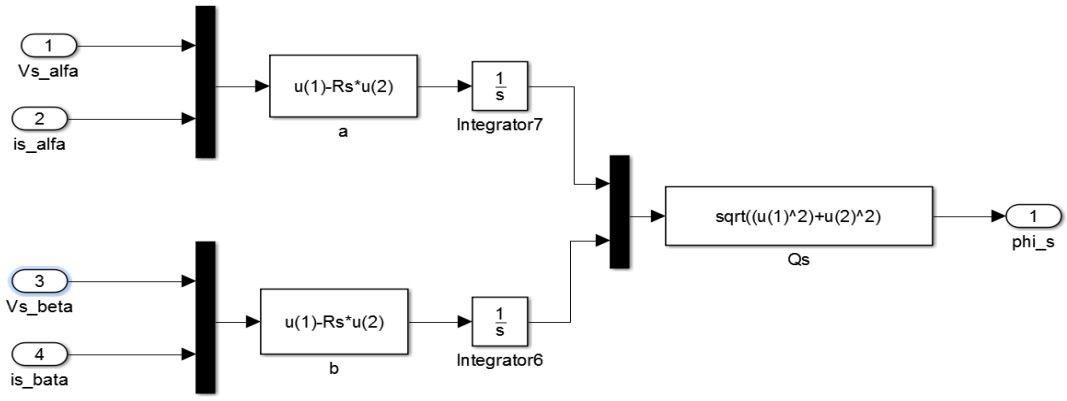

Figure 9. Block diagram of stator flux observer

2.8. Simulation results for the operation of an induction motor in an open-loop system

The dynamic model of the induction motor in the open-loop system in MATLAB-Simulink is simulated, according to the parameters shown in Table 1, to validate the mathematical model and check the values from the nominal current and speed to find out the nominal flow value.

Table 1. Physical parameters of the studied IM (Pena & Diaz et al., 2017)

parameter	value
R_r, R_s	31Ω, 45.83Ω
L_r, L_s	1.11H, 1.24H
L_m	1.054H
J	1e-3Kg.m^2
f	1e-3Kg.m^2/sec
P	2
Power	250W
V_s	Y/Δ 400V/230V
I_s	Y/Δ 0.76A/1.32A
n	1350rpm

The amplitude of the voltages applied to the stator windings has the value of 325v and a frequency 50Hz. Figure 10 shows zoom-in for the stator voltages.

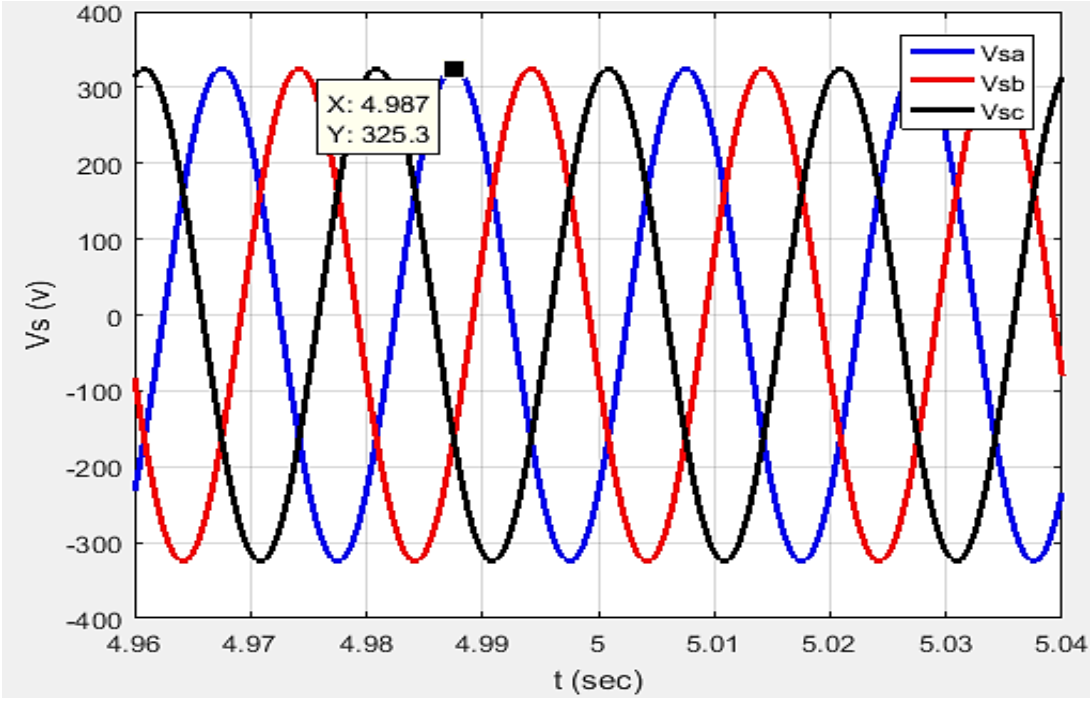

Figure 10. The voltages applied to the stator windings

The load torque is applied at 5 sec, as shown in Figure 11, where we observe that the motor develops an electromagnetic torque (Tem) greater than the load torque (Td) to overcome the friction.

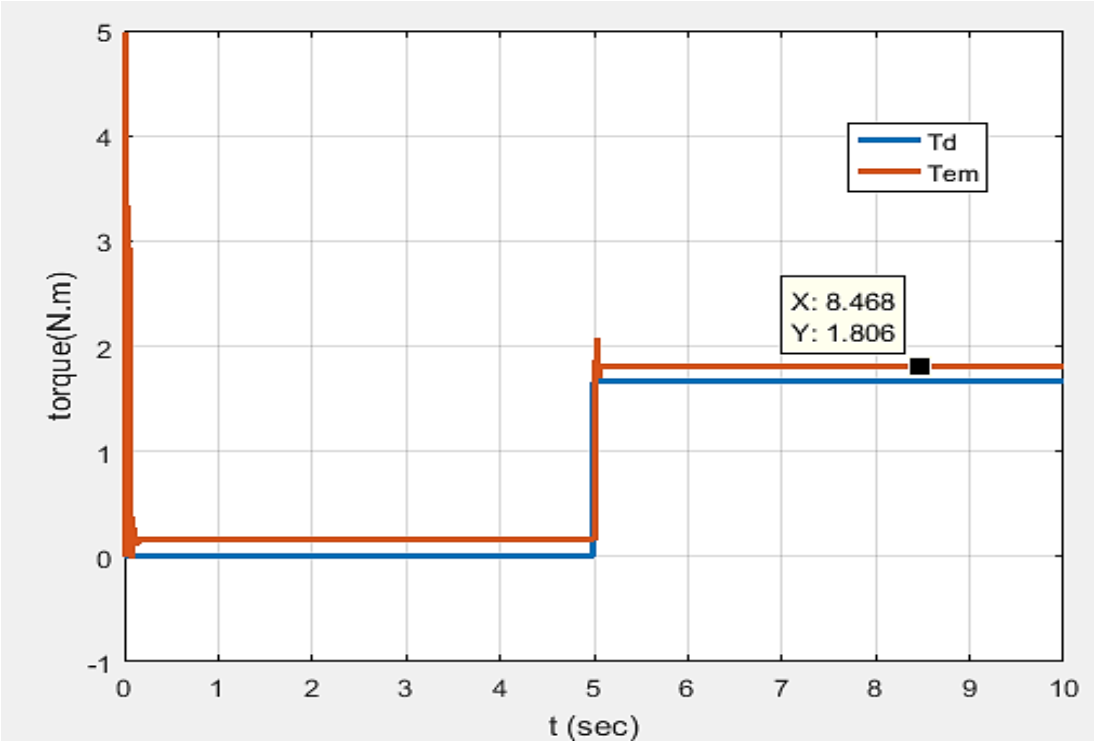

Figure 11. Torque curve

As shown in Figure 12, when the motor works without applying load torque, it consumes current for each phase Is=0.57A to overcome the iron and mechanical losses, and when load torque is applied, the consumed current for each phase will rise from 0.57A to 0.78A to develop an electromagnetic torque sufficient to overcome the load.

Figure 13 shows the currents in the α,β frame, It is noticed that the amplitude of the currents in the α,β frame is greater than the amplitude of the current in a,b,c the frame, and this matter is due to the value of the park coefficient, while these currents have the same frequency as the currents considering$\omega_k = 0$.

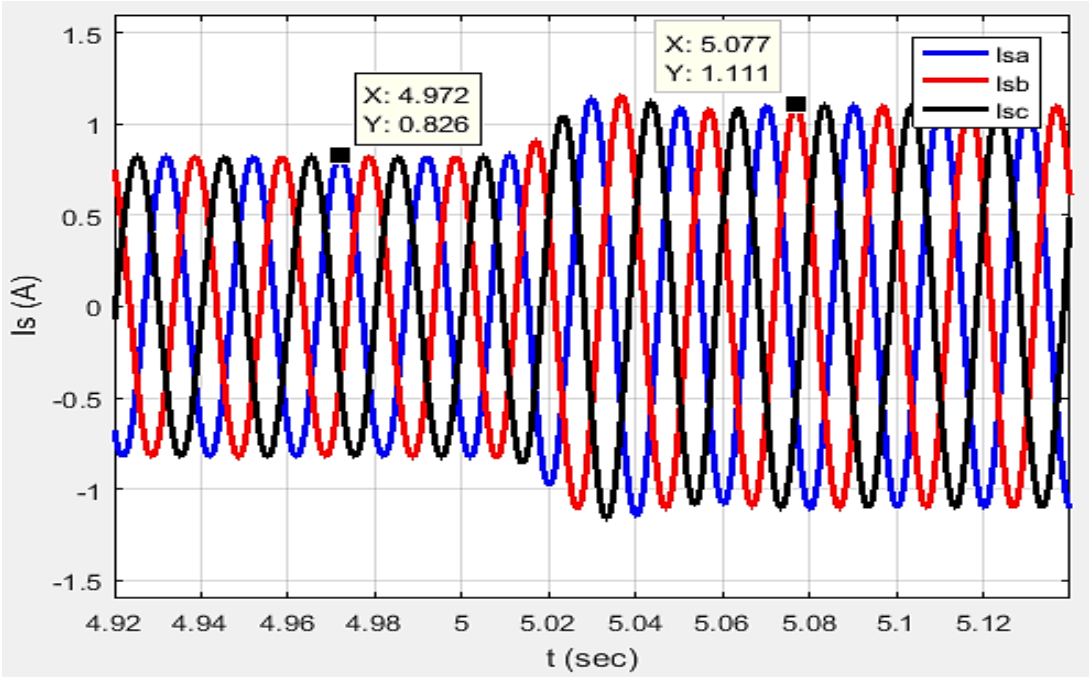

Figure 12. The currents consumed by the motor during the simulation time

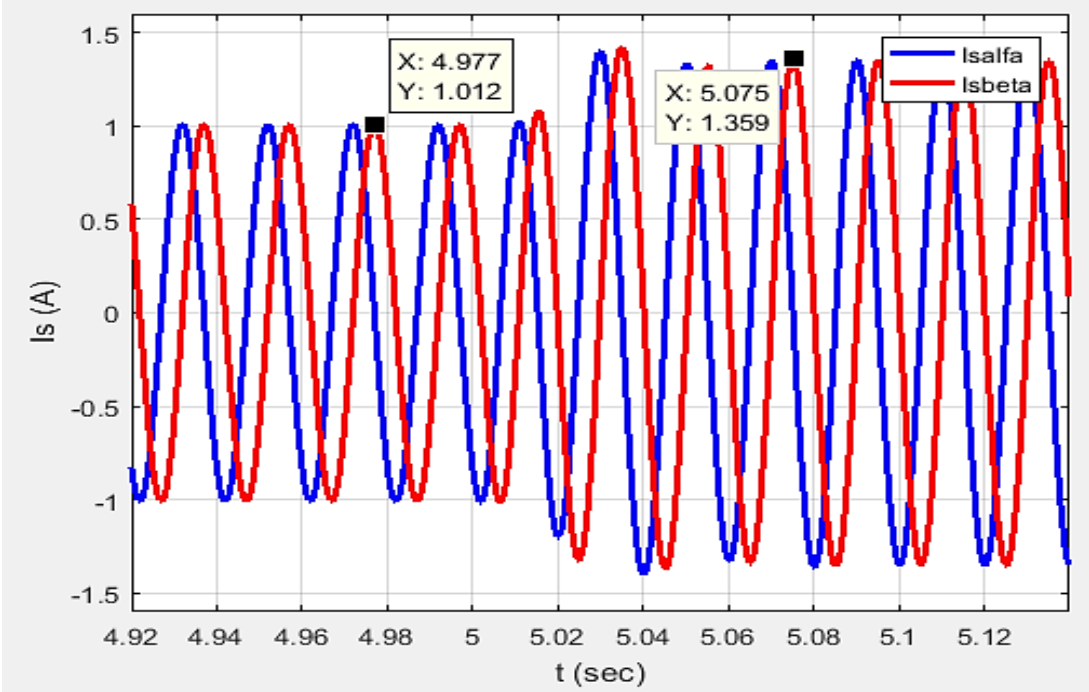

Figure 13. Stator current vector components in α,β frame

When the load torque is applied, the flux amplitude, as shown in figure 14, will decrease from 1.25wb to 1.14wb, the nominal value, and the speed will decrease from 1490 r.p.m to 1350 r.p.m, as shown in figure 15.

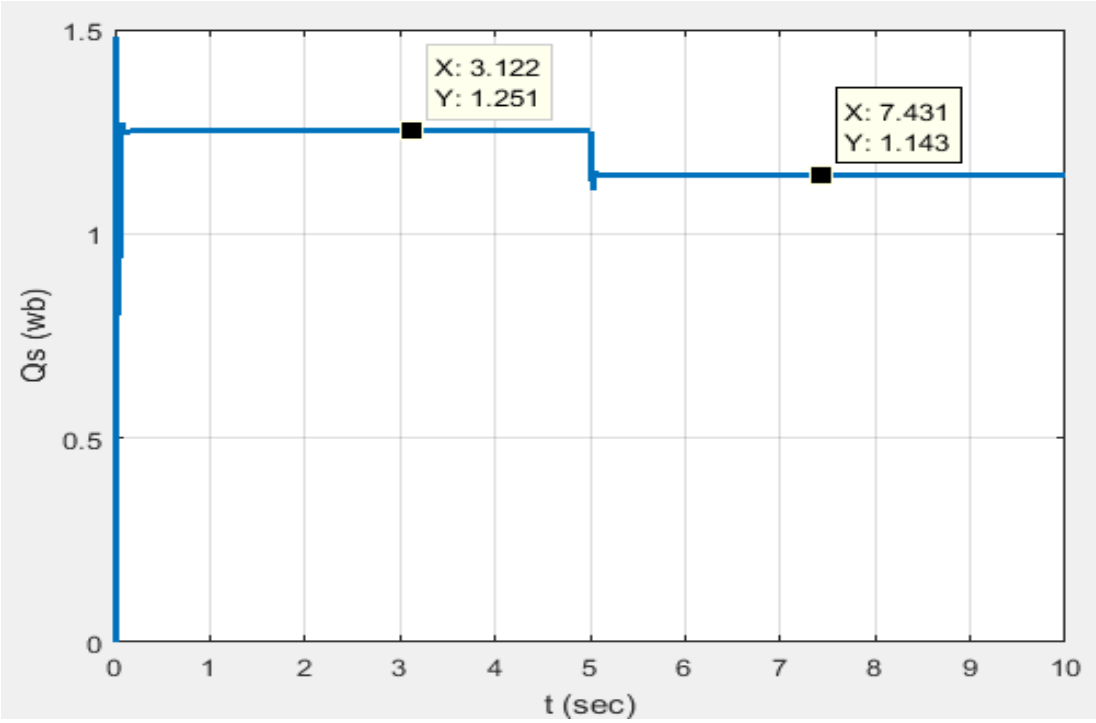

Figure 14. The amplitude of stator flux vector

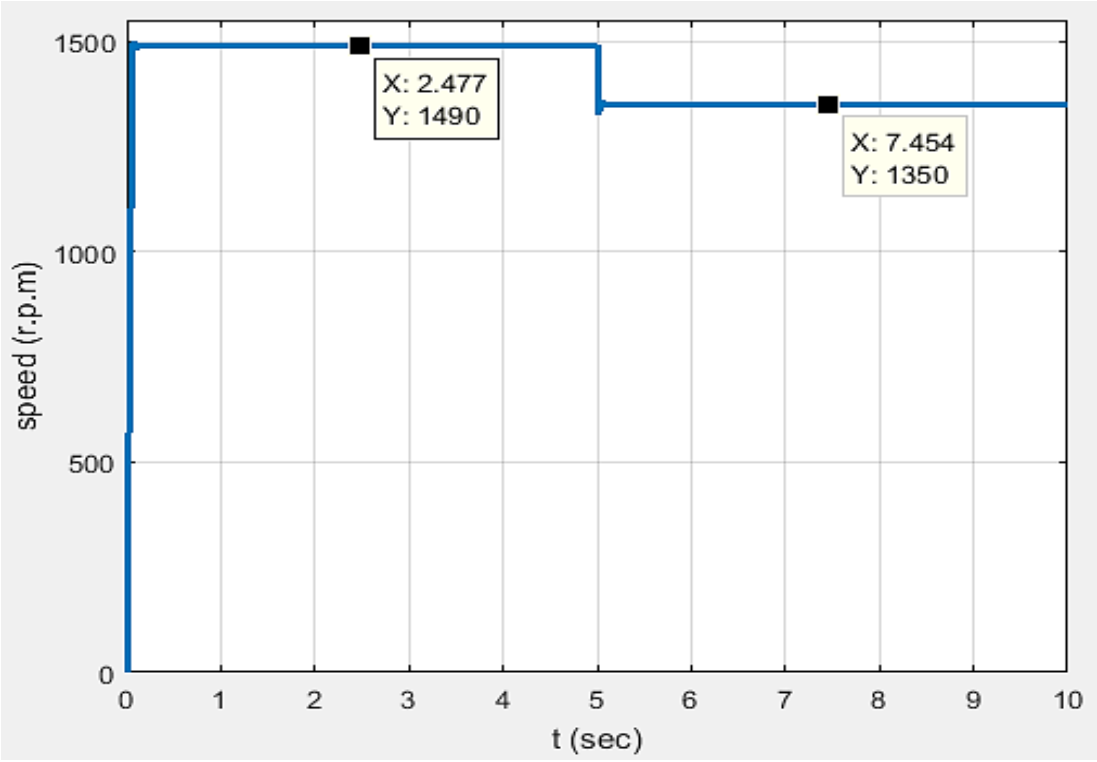

Figure 15. The rotational speed of the motor

CHAPTER THREE
SCALAR CONTROL OF INDUCTION MOTOR

3.1. Introduction

The Scalar V/f control method is simple, easy, and practical. It can be applied in an open-loop or closed-loop system, where the voltage and frequency are changed together to regulate the speed of the induction motor. Traditional regulators, fuzzy logic controllers, or artificial intelligence networks can be used to implement the control system. (Duranay et al., 2020; Harsha et al., 2020; Peña et al., 2017)).

3.2. Induction motor control

The process of controlling the motor speed is complex compared to DC motors. In DC motors - with independent excitation - changing the rotational speed requires changing the value of the voltage applied to the armature coil without affecting the value of the induced torque. As for the induction motor, it must be taken into account that changing the value of the voltage applied to the armature coil will directly affect the torque value, so the voltage and frequency must be changed together to solve this problem and maintain constant torque. (Devi et al., 2014; Sudaryanto et al., 2020).

Induction Motor drive depends on two major methods of control system: scalar control and vector control (Hannan et al., 2018; Nishad & Sharma et al., 2018; Trabelsi et al., 2012; Verma et al., 2018).

The Scalar V/f control keeps the ratio of voltage to frequency constant, which provides a simple, practical way for controlling induction motor speed. This methodology provides a satisfactory response in the steady-state, but the dynamic performance in the transient state is usually low, especially at low speeds. (Harsha et al., 2020;Pena & Diaz et al., 2017;Verma et al., 2018).

3.2.1. The control techniques used in the Scalar control

The control techniques used in scalar control systems range from traditional controllers to expert and intelligent control techniques (Aggarwal et al., 2012; Arulmozhiyal et al., 2009; Hannan et al., 2018). PI controllers are commonly used in scalar V/f control systems for induction motors. PI controllers have a simple structure,

low cost, and easy implementation, but they have many shortcomings (Chen & Zhang et al., 2015; Hannan et al., 2018; Lesani et al., 2013). such as:

1- They cannot provide the available ability to achieve the performance specifications simultaneously.
2- PI controllers may not be able to achieve good performance when there is a change in the parameters of the controlled system.
3- The constants of PI controllers must be calculated after knowing the mathematical model of the controlling system to obtain good performance when using these controllers, and this matter may not be available.

Efficient controlling techniques are necessary for Induction motors related to Industrial applications. To get a good dynamic performance of the controlled system, it can adopt a fuzzy logic methodology to build the controller. Fuzzy logic controllers have advantages over PI controllers: a shorter rise time, a shorter settling time, and more decreasing electromagnetic torque oscillations (Arulmozhiyal et al., 2009; Mohammed & Ghoneim et al., 2021).

One effective way to implement a fuzzy logic controller is a hybrid fuzzy PI controller, which uses the speed error and the speed-error change to generate a sinusoidal PWM inverter's voltage and frequency (Devi et al., 2014; El-Zohri & Mosbah et al., 2020; Hannan et al., 2018).

3.3. Switching techniques

The sinusoidal pulse width modulation technology is adopted to drive the voltage inverter fed the induction motor, which structure is illustrated in figure 17.

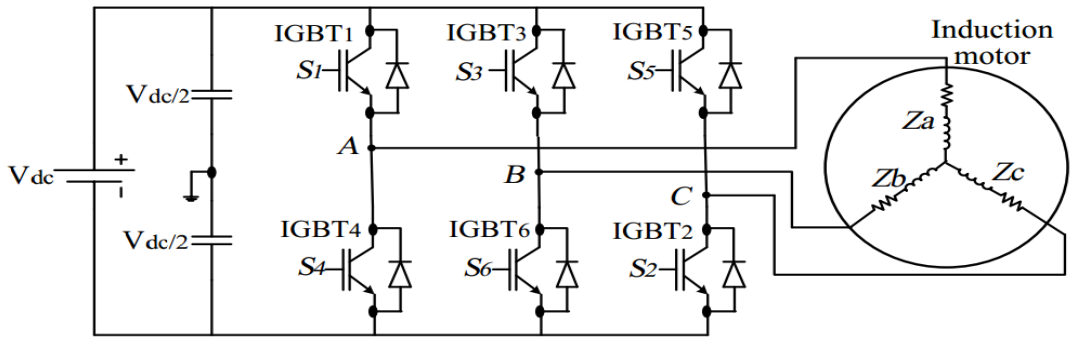

Figure 16. The structure of a 3-ph. voltage inverter with IM (Hannan et al., 2018)

The signal production is shown in figure 18 based on a comparison of the three-phase control waveform and the triangle waveform.

This comparison is based on the criterion $V_{control} > V_{triangle}$, which means S = ON if $V_{control} > V_{triangle}$ is true; otherwise, S = OFF. (El-Zohri & Mosbah et al., 2020), (Hannan et al., 2018), (Suetake et al., 2011).

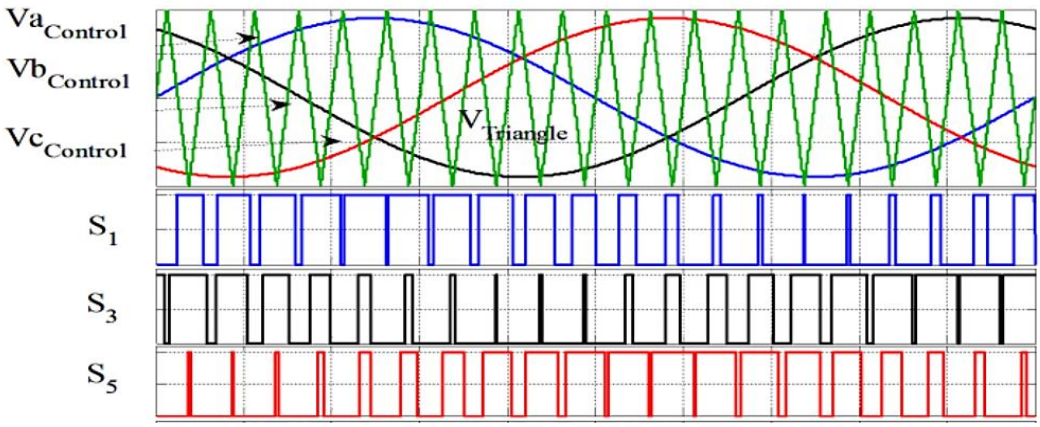

Figure 17. SPWM and voltage waves of a 3-ph. inverter (Harsha et al., 2020)

3.4. The scalar V/F control methodology

Understanding the scalar control methodology must be started from the voltage balance equation, which is given by the following relationship (Lee, 2019; Hannan et al., 2018),

$$\underline{V_s} = R_s \underline{i_s} + \frac{d\underline{\Phi_s}}{\mathrm{dt}} \tag{3.1}$$

Where $\underline{V_s}$ is the stator voltage vector, and $\underline{\Phi_s}$ Is the stator flux vector.

If the voltage drop due to the stator resistance is neglected, the relationship (3.1) becomes as follows:

$$\underline{V_s} = \frac{d\underline{\Phi_s}}{\mathrm{dt}} \tag{3.2}$$

In the steady-state, the magnetic flux vector has a constant amplitude and rotates at a speed of ω_sWhere its relationship is given as:

$$\underline{\Phi_s} = \Phi_{\mathrm{smax}}[\cos(\omega_s t) + \mathrm{J}\sin(\omega_s t) \tag{3.3}$$

By differentiating the previous relationship, the following relationship is obtained:

$$\frac{d\underline{\Phi_s}}{\mathrm{dt}} = \mathrm{J}\omega_s\underline{\Phi_s} \tag{3.4}$$

Substituting the relationship (3.4) into the relationship (3.2), the following relationship is obtained:

$$\underline{V_s} = \mathrm{J}\omega_s\underline{\Phi_s} \tag{3.5}$$

The relationship (3.5) is a vector relationship; without taking the angle into account, it can be written the relationship (3.5) as a scalar relationship-related only to the amplitudes: (Bharti et al., 2019), (Verma et al., 2018):

$$\frac{V_s}{\omega_s} = \Phi_s \tag{3.6}$$

To substitute the values for the studied motor, where (Vs) is equal to 325v and ws is equal to 314 rad/sec, It is obtained that:

$$\Phi_s \approx 1 \tag{3.7}$$

Therefore, the amplitude of the stator voltage vector is calculated as

$$V_s = \omega_s \tag{3.8}$$

3.5. Speed V/F control system using a PI controller

Figure 18 shows the block diagram of the speed V/F control system using a PI controller, where the reference speed is compared with the real speed, and the error signal is processed by the PI controller that gives ω_{sl}which is given as:

$$\omega_{\mathrm{sl}} = \omega_s - \omega \tag{3.9}$$

Therefore, it is added with the motor speed ω to get ω_s, and then the voltage amplitude value is obtained by the relationship (3.8).

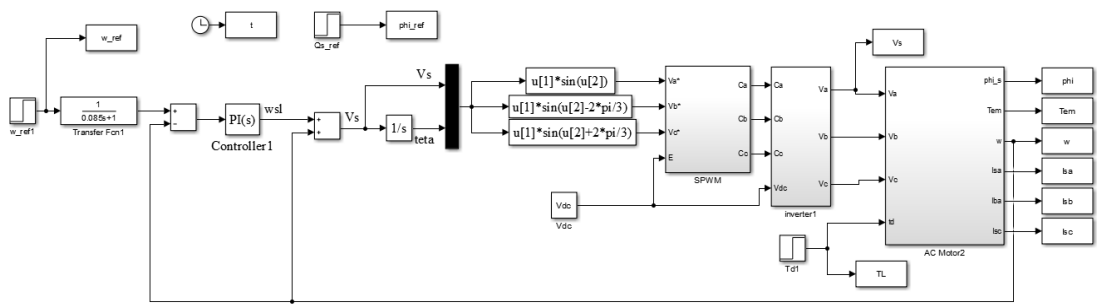

Figure 18.The Block diagram of the speed V/F method using a PI controller

3.5.1. Simulation results of a speed V/F control system based on PI controller at high speed .

A simulation of the speed V/F control system based on the PI controller was carried out to regulate the motor speed at a nominal value equal to 282rad/sec, and the load torque was applied at the moment 2sec.

Figure 19 shows the response time for speed regulation at a nominal value equal to 282rad/sec using a speed V/F control system based on a PI controller.

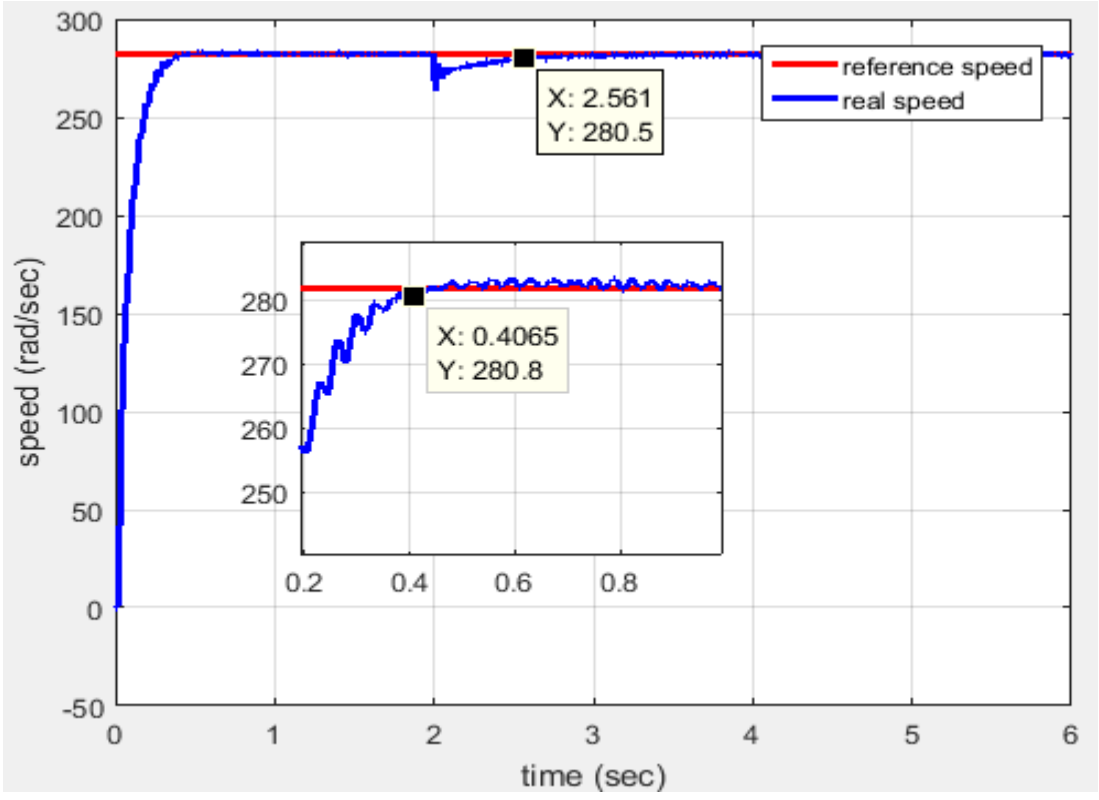

Figure 19. The response time based on the PI controller at 282 rad/sec speed.

It can be seen from figure 19 that the drive system achieves a response with a setting time of 0.4sec, and the motor needs 0.56sec in order to overcome the load torque.

Figure 20 shows the response time for the flux when the speed is regulated at a nominal value equal to 282rad/sec using a speed V/F control system based on a PI controller.

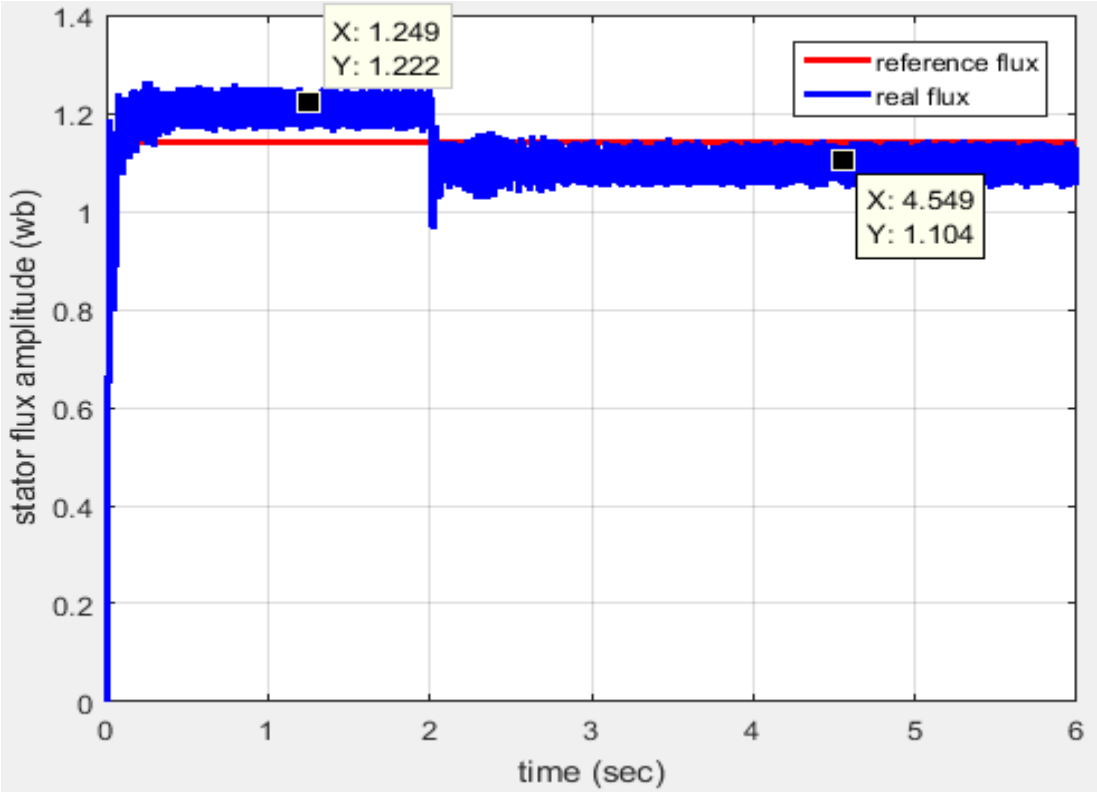

Figure 20. The response time of the flux based on the PI controller at a 282.7rad/sec speed.

Can be seen from figure 20 that the amplitude of the flux changes between the period of work without load and the period of work with load, but it remains at values close to the nominal value of 1.14wb.

Figure 21 shows the response time for the electromagnetic torque when the speed is regulated at a nominal value equal to 282rad/sec using a speed V/F control system based on a PI controller.

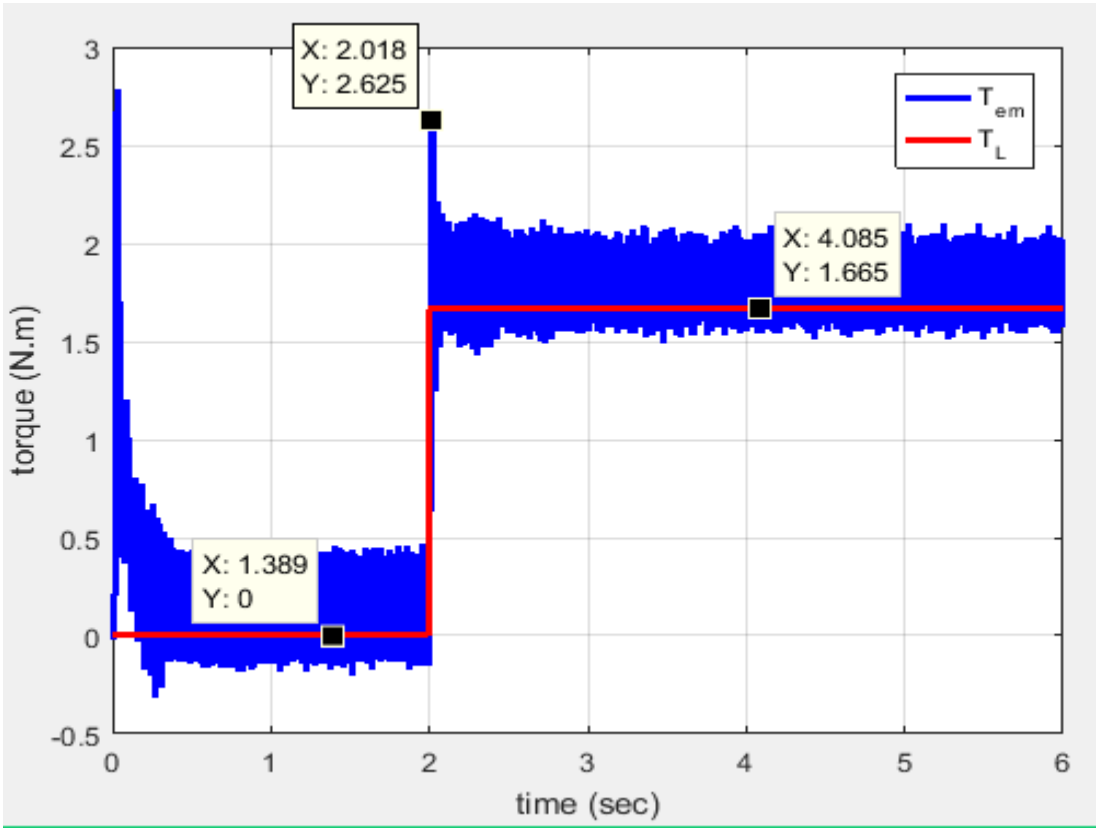

Figure 21. The response time of the electromagnetic torque based on the PI controller at a 282rad/sec speed.

From Figure 21, the electromagnetic torque rises when the load torque is applied to the value of 2.6 N.m; then, it stabilizes at a value close to the load torque.

The voltage wave on the first phase of the motor is shown in figure 22. It can be seen that the values of voltage are within acceptable limits.

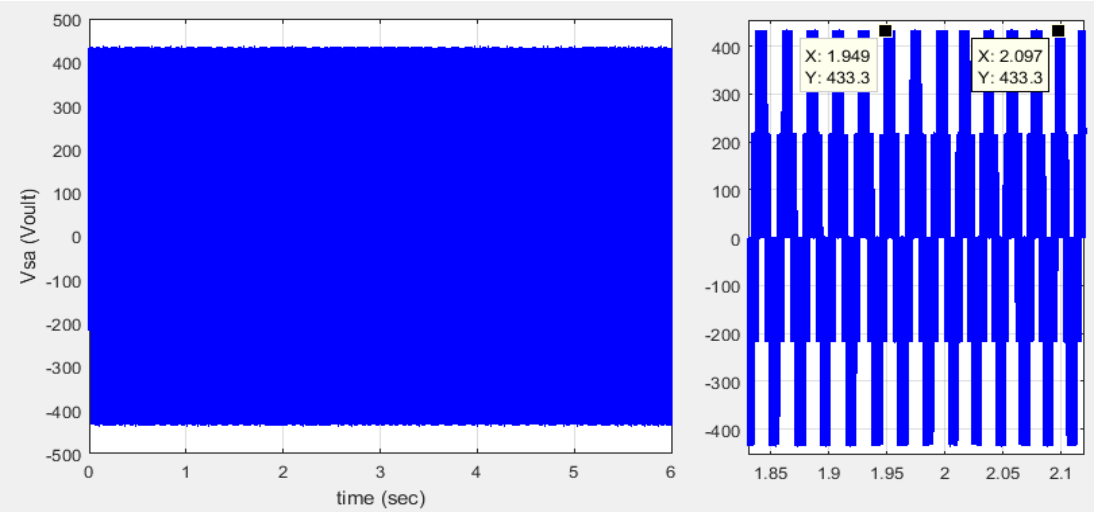

Figure 22. The applied voltages to the stator windings based on the PI controller at 282rad/sec speed.

The current wave of the first phase of the motor is shown in figure 23. It can be seen that the values of current are within acceptable limits.

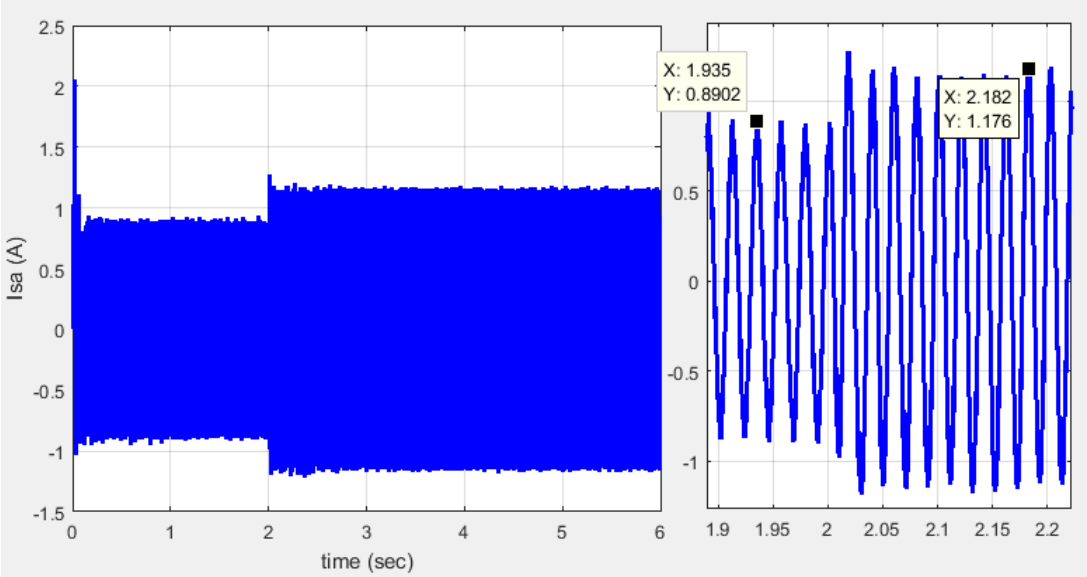

Figure 23. The consumed current by the stator windings based on a PI controller at a 282rad/sec speed.

3.5.2. Speed Simulation results using V/F method based on PI controller at a low speed.

A simulation of the speed V/F control system based on the PI controller was carried out in order to regulate the motor speed at the value of 50rad/sec, and the load

torque was applied at the moment 2sec. Figure 24 shows the response time for speed regulation at a low value using a speed V/F control system based on a PI controller.

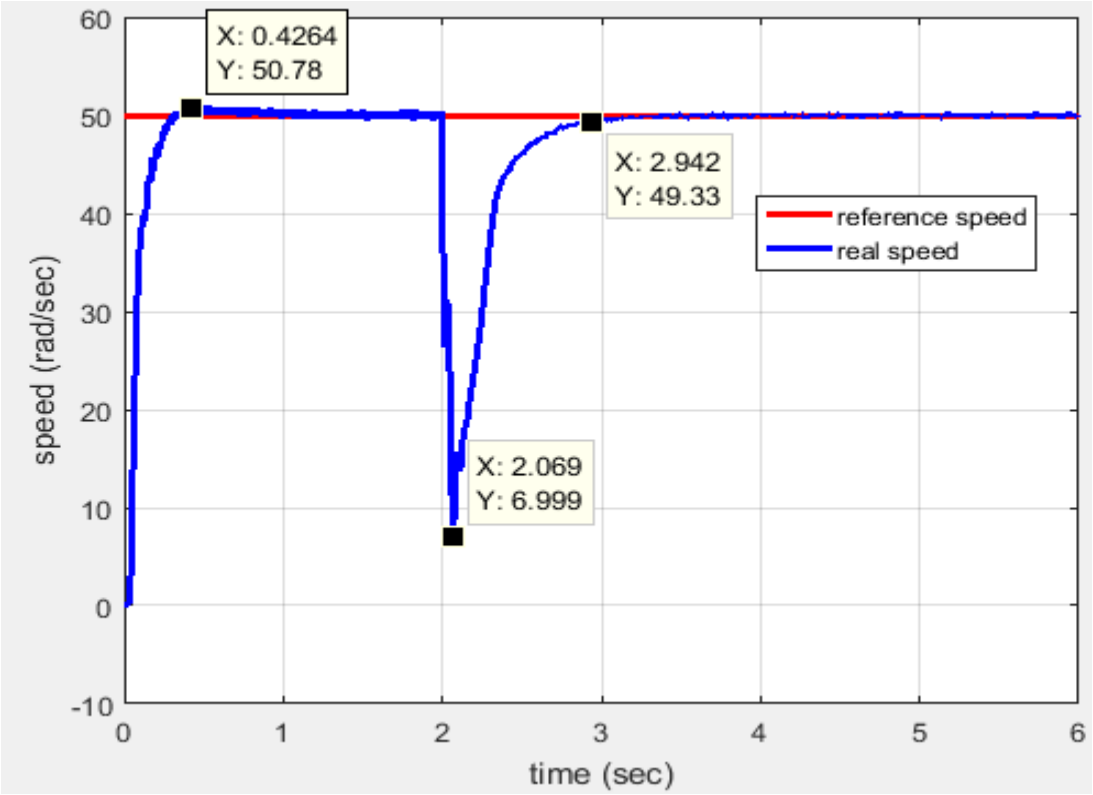

Figure 24. The motor response time at the low speed based on PI Controller.

It can be seen from figure 24 that the drive system achieves a response with a setting time of 0.4sec. The motor performance was poor at the moment of applying the load torque as the speed reached a value of 7rad/sec, and the motor needed 1sec to return to the reference speed. This can be explained by the fact that the flux amplitude was low (0.76wb), as shown in figure 25.

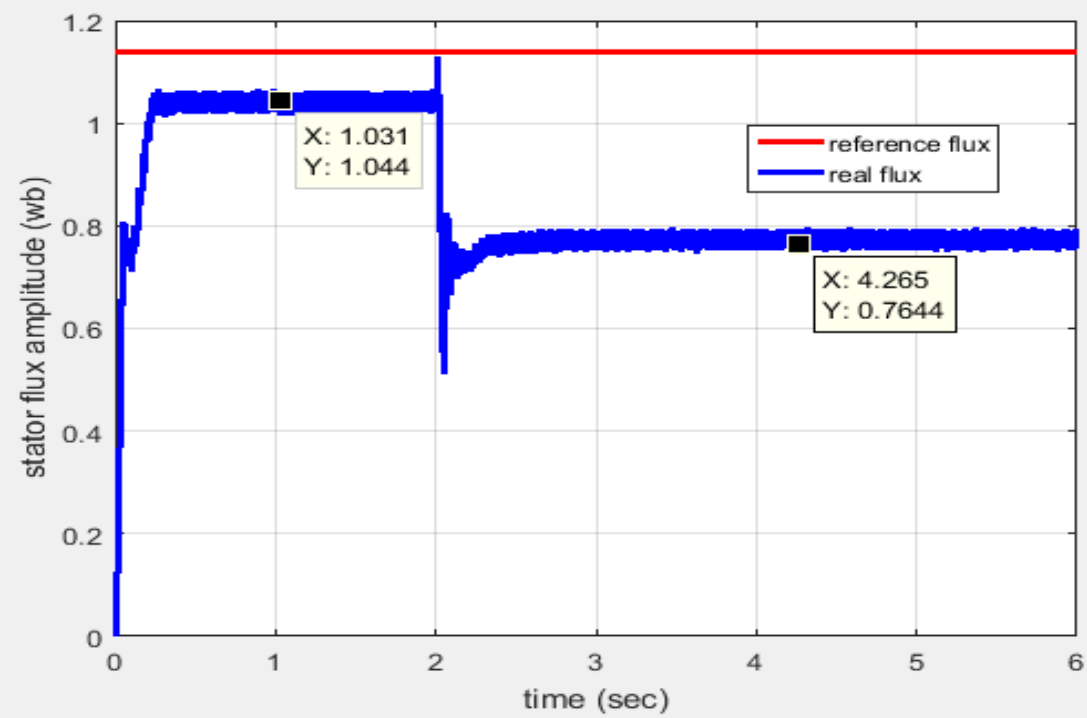

Figure 25. The motor response time for the stator flux at the low speed based on PI Controller.

Figure 26 shows the response time for the electromagnetic torque when the speed is regulated at a low value using a speed V/F control system based on PI Controller.

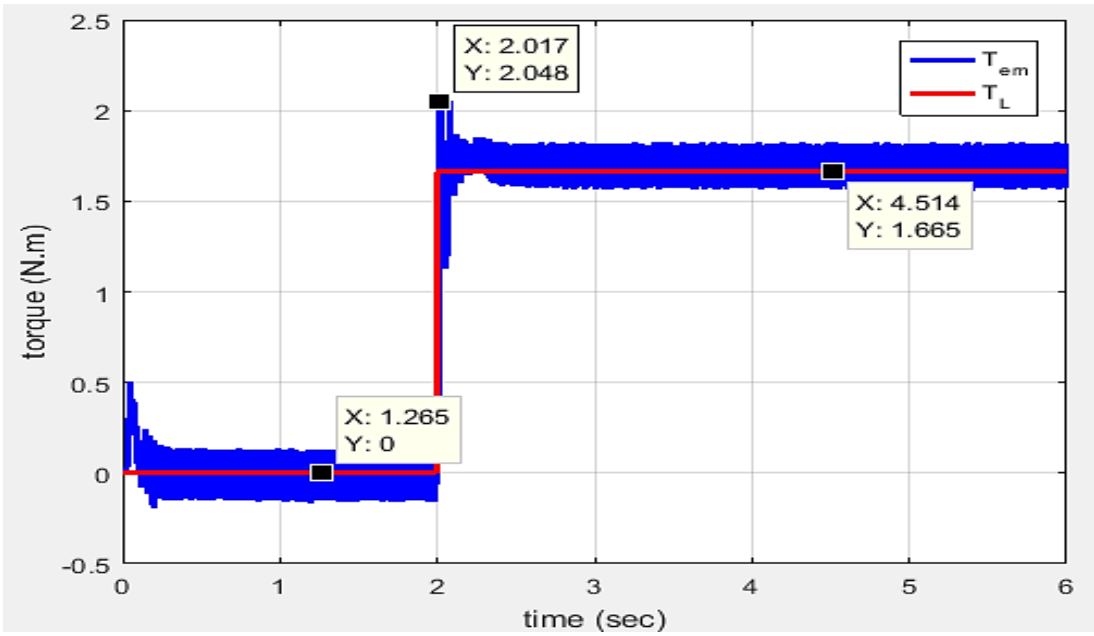

Figure 26. The motor response time for the electromagnetic torque at the low speed based on PI Controller.

Figure 26 shows that the electromagnetic torque rises when the load torque is applied to a value of 2.04 N.m only because of the decreases in the flux value and then stabilizes at a value close to the load torque.

Figure 27 shows the voltage wave on the motor's first phase, where the voltage values are within acceptable limits.

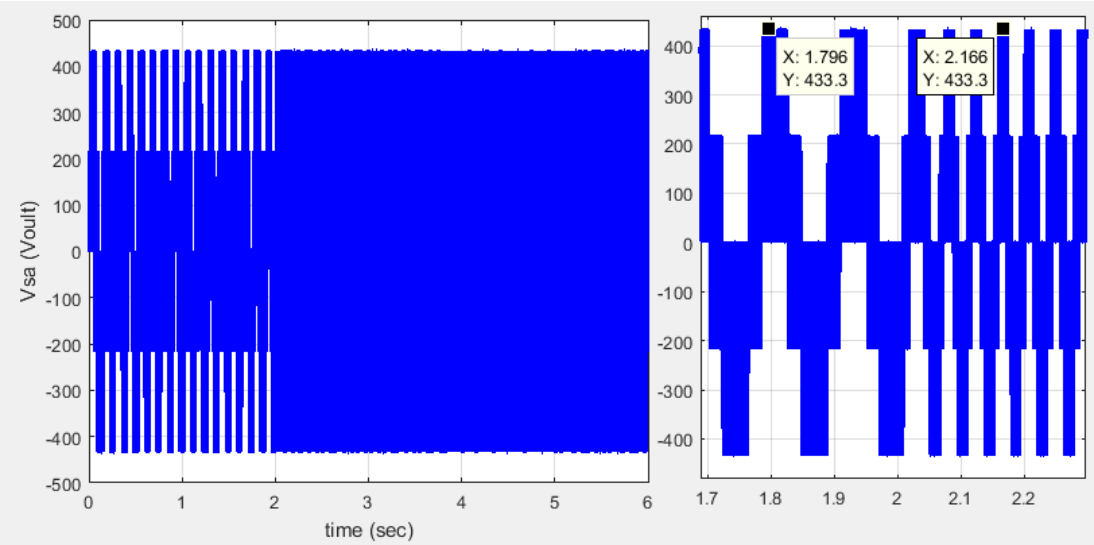

Figure 27. The applied voltages to the stator windings at a low speed based on PI Controller.

The current wave of the first phase of the motor is shown in figure 28. It can be seen that the values of current are within acceptable limits.

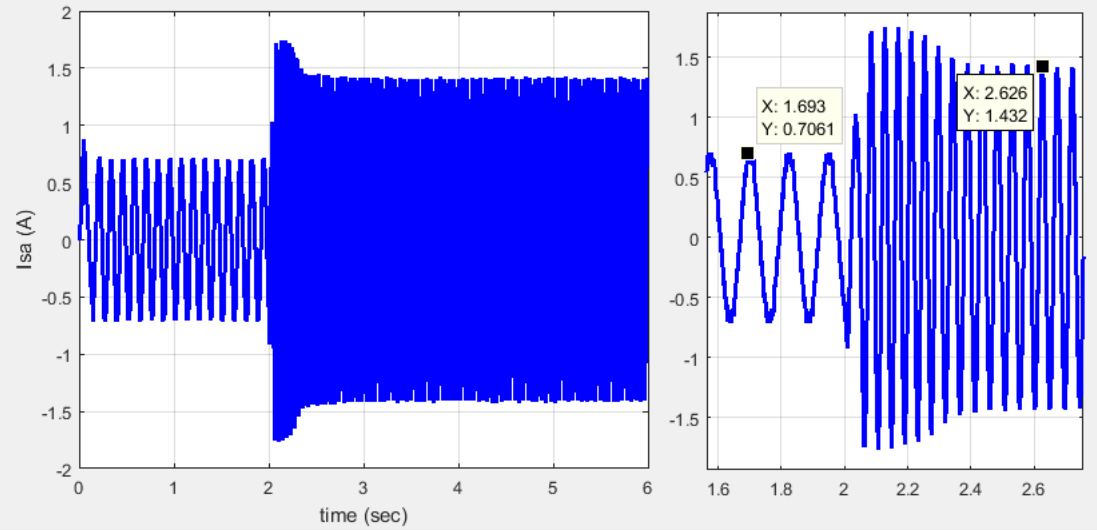

Figure 28. The current signal wave on the stator windings based on the PI controller at low speed.

3.6. Improving the speed V/F Control System based on PI Controller.

In the preceding paragraph, it is noted that the control system achieves a good response in regulating the speed, but the value of the magnetic flux is not fixed, causing vibration in the torque signal in transient cases; it is also noted that when working at low speeds, the motor performance is poor in the transient cases related to the change of load torque.

The change of magnetic flux can be reduced by modifying the control law so that a limit value was added to compensate for the voltage drop on the stator resistance, which was neglected when deducing the control law. This limit must be related to the load torque, considering that the goal is to reduce its vibration. This limit can be represented by the frequency of the rotor voltage, which increases with increasing load torque. Then, the voltage amplitude can be calculated as follows:

$$V_s = \omega_s + \omega_{\mathrm{sl}} \tag{3.10}$$

3.6.1 Simulation results of an enhanced Speed V/F control system based on PI controller when regulating the speed at a high value.

A simulation of an enhanced Speed V/F control system based on a PI controller was carried out in order to regulate the motor speed at the value of 50rad/sec., and the load torque was applied at the moment of 3sec.

Figure 29 shows the speed response time using a speed-enhanced PI controller.

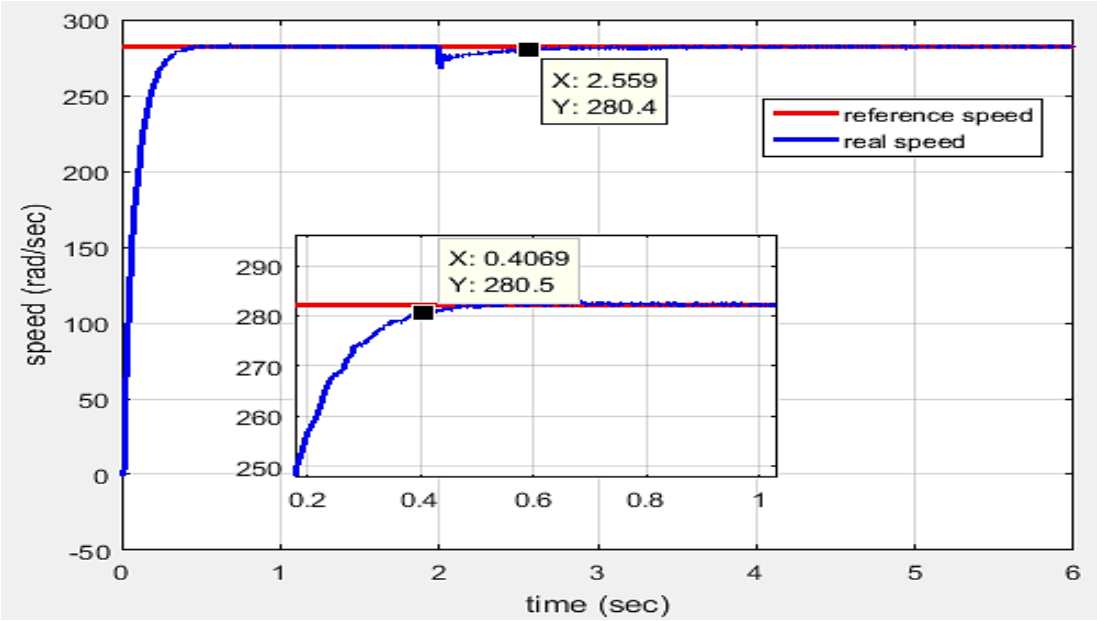

Figure 29. The motor response time at high speed based on PI Controller.

It is noticed from figure 29 that there is no change in the response time characteristics for speed regulation, where the setting time is 0.4sec., and the motor needs 0.56sec. in order to overcome the load torque

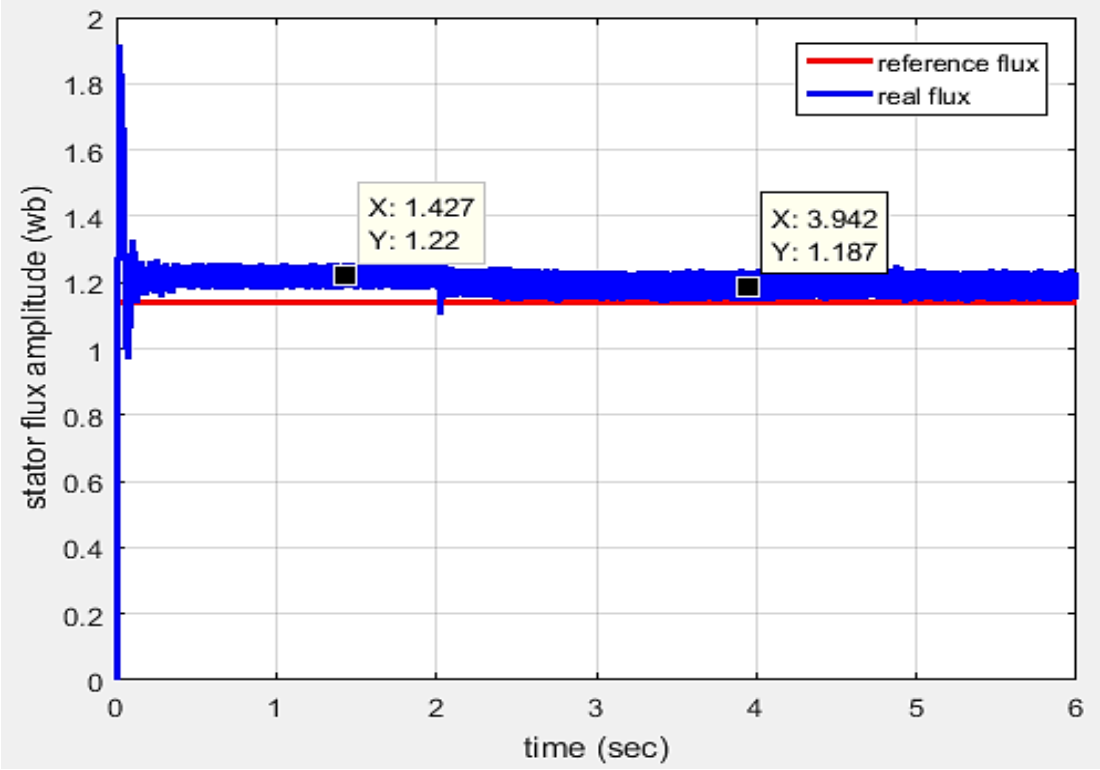

Figure 30. The response time for the flux at high speed based on the enhanced PI Controller.

Noticed in figure 30 that the obtained magnetic flux is bigger than the nominal value before and after applying the load torque.

Figure 31 shows the response time for the electromagnetic torque when the speed is regulated at a high value using an enhanced Speed V/F control system based on the PI controller

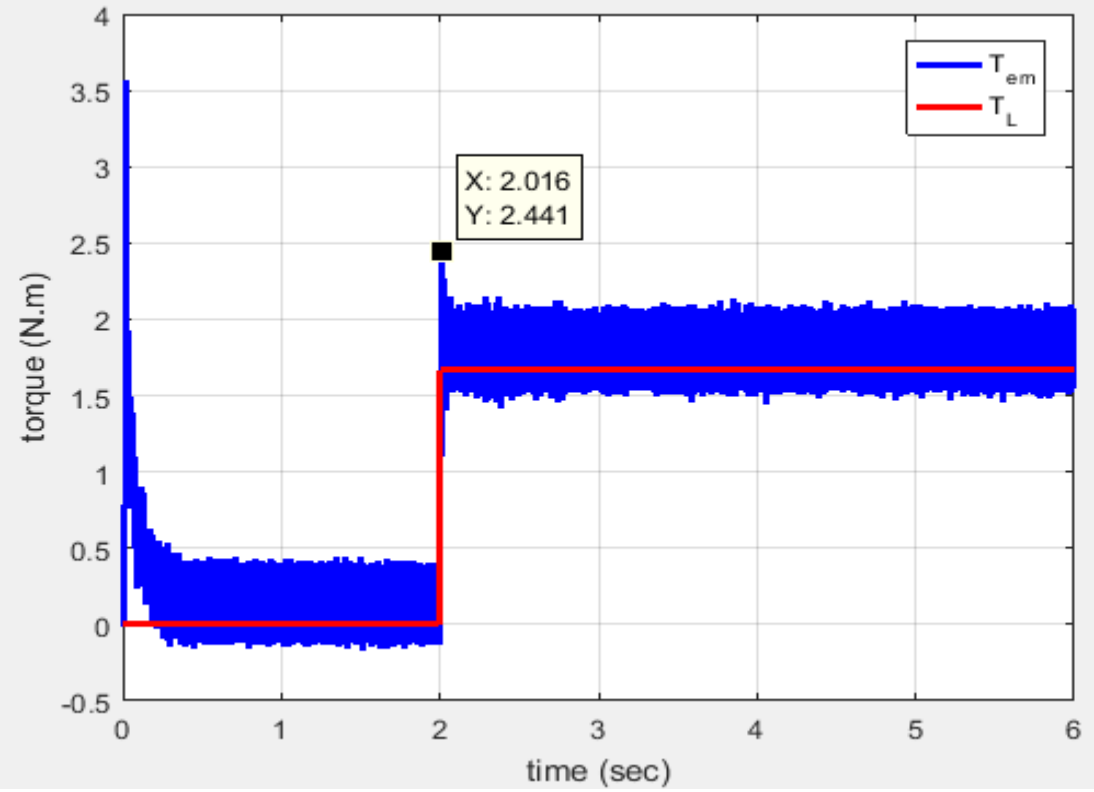

Figure 31. The response time for the electromagnetic torque based on the PI controller at high speed

It can be seen from Figure 31 that the electromagnetic moment rises when the load torque is applied to the value of 2.4 N.m and then stabilizes at a value that is close to the load torque.

The voltage wave on the first phase of the motor is shown in figure 32. It can be seen that the values of voltage are within acceptable limits.

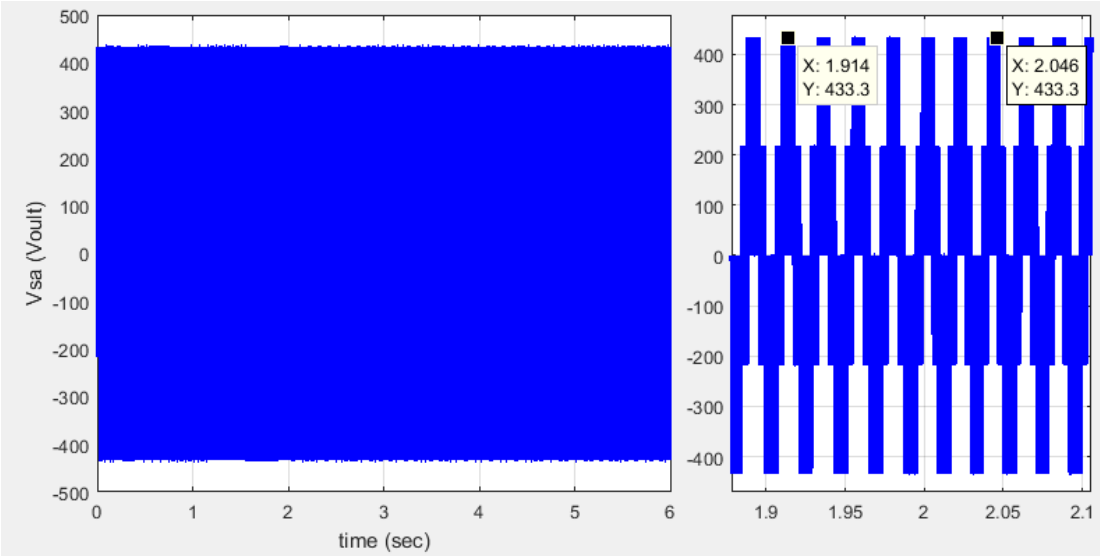

Figure 32. The applied voltages to the stator windings based on the PI enhanced Speed controller at high speed.

The current wave of the first phase of the motor is shown in figure 33. It can be seen that the values of current are within acceptable limits.

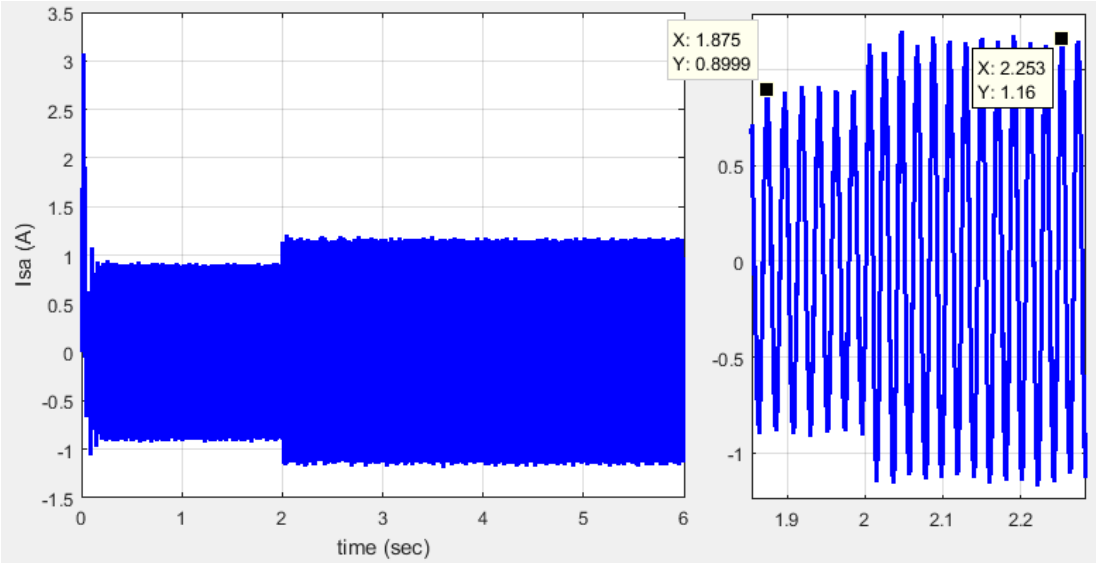

Figure 33. The consumed current by the stator windings based on an enhanced PI controller at high speed.

3.6.2 Simulation results of an enhanced Speed V/F control system based on PI controller when the speed is at a low value

A simulation of using an enhanced Speed V/F control system based on a PI controller was carried out in order to regulate the motor speed at the value of 50rad/sec, and the load torque was applied at the moment of 2sec**.**

Figure 34 shows the response time for speed regulation at 50rad/sec using an enhanced Speed V/F control system based on a PI controller.

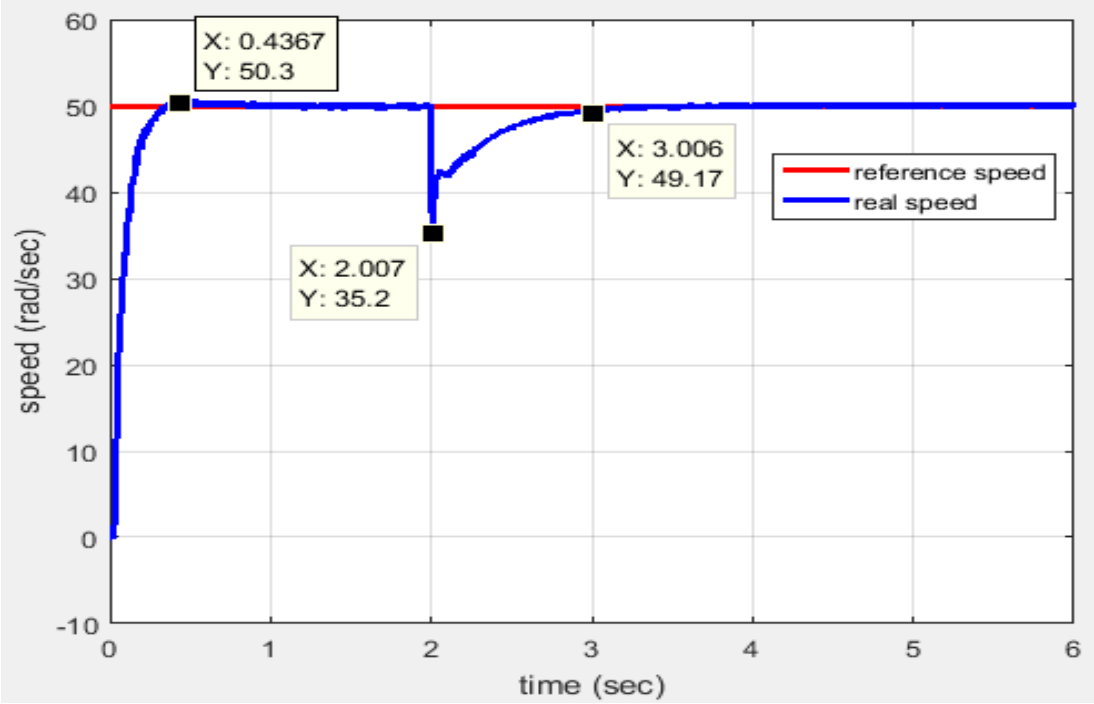

Figure 34. The speed response time based on enhanced PI controller at low speed.

It is noticed in figure 34 that the setting time for speed regulation is equal to 0.4sec, and the performance of the motor at the moment of applying the load torque was better compared to the previous case (figure 24), where the speed decreased to 35rad/sec while in the previous case, it reached 7rad/sec, and this is due to the increase of the magnetic flux as shown in figure 35.

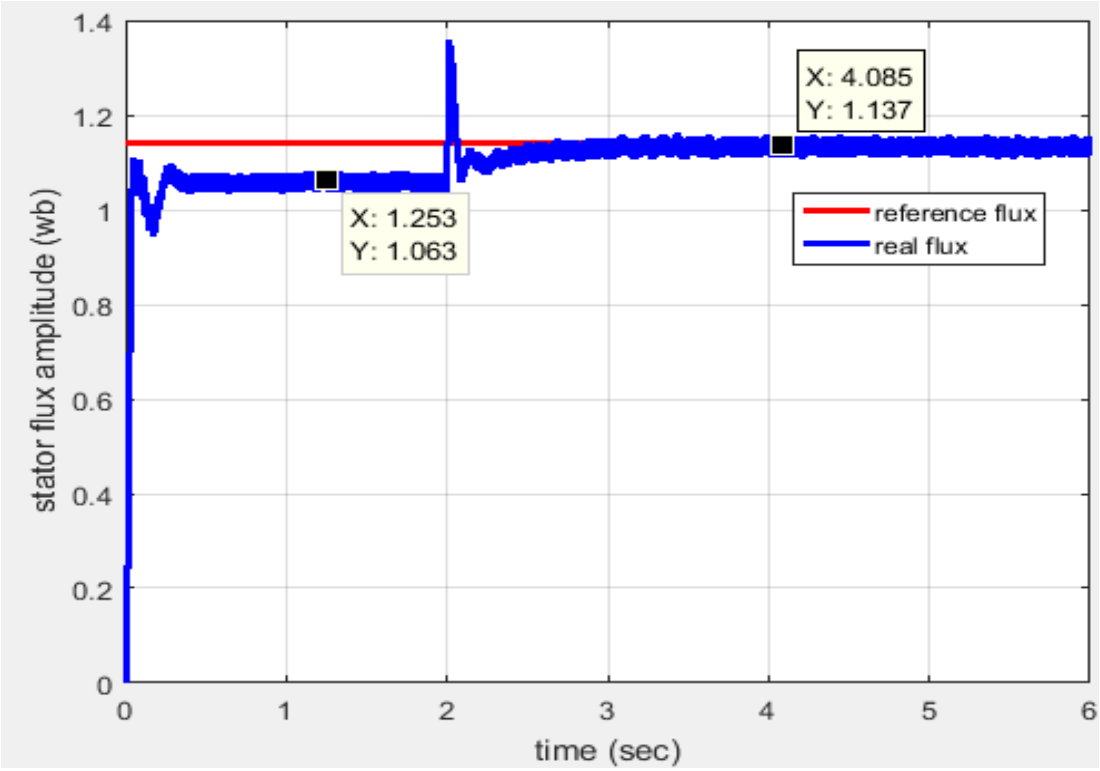

Figure 35. The flux response time based on the enhanced Speed PI controller at low speed

It is noticed in figure 35 that the magnetic flux maintained is close to the nominal value before applying the load torque. It is equal to the nominal value after applying the load torque; this has improved the motor's performance.

Figure 36 shows the response time for the electromagnetic torque with speed regulation at 50rad/sec using an enhanced Speed V/F control system based on a PI controller.

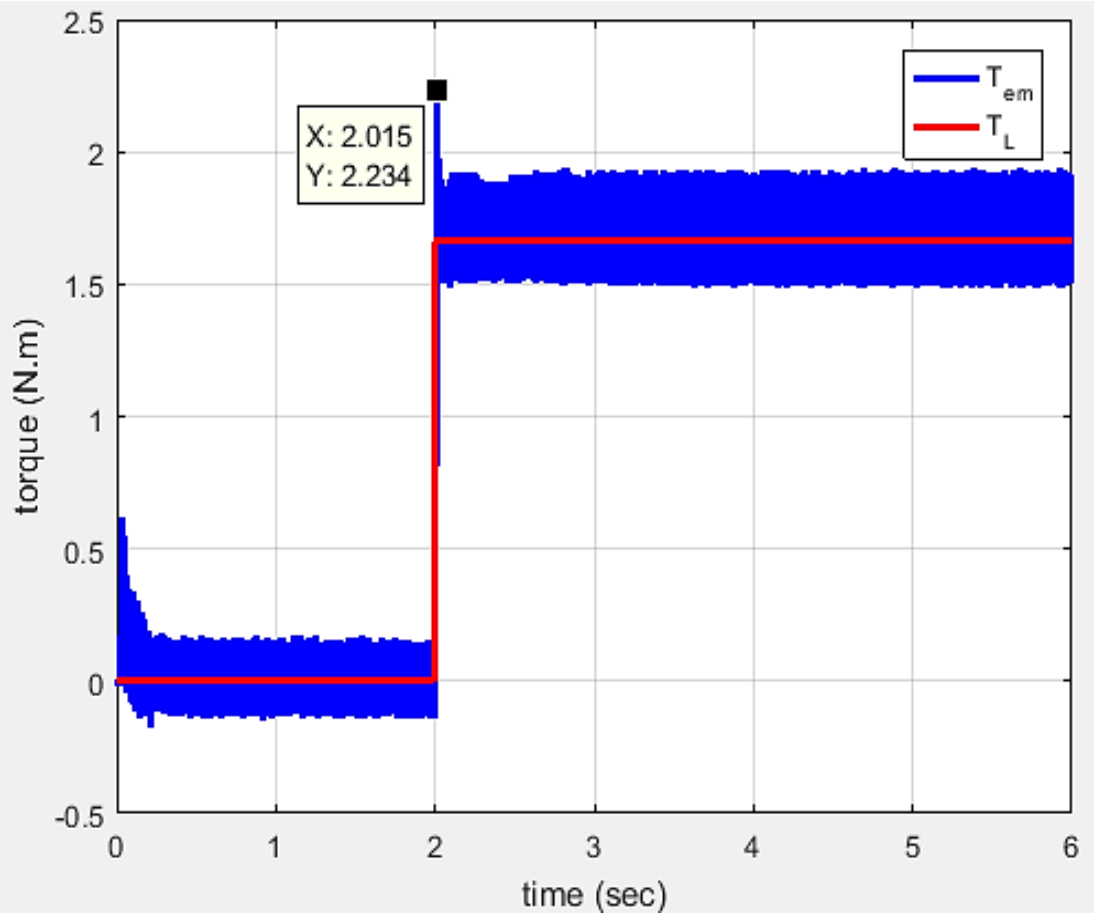

Figure 36. The electromagnetic torque response time based on the PI-enhanced speed controller at low speed.

Can be seen from figure 36 that the electromagnetic torque rises when the load torque is applied to a value of 2.23 N.m and then stabilizes at a value close to the load torque. The voltage wave on the first phase of the motor is shown in figure 37. It can be seen that the values of voltage are within acceptable limits.

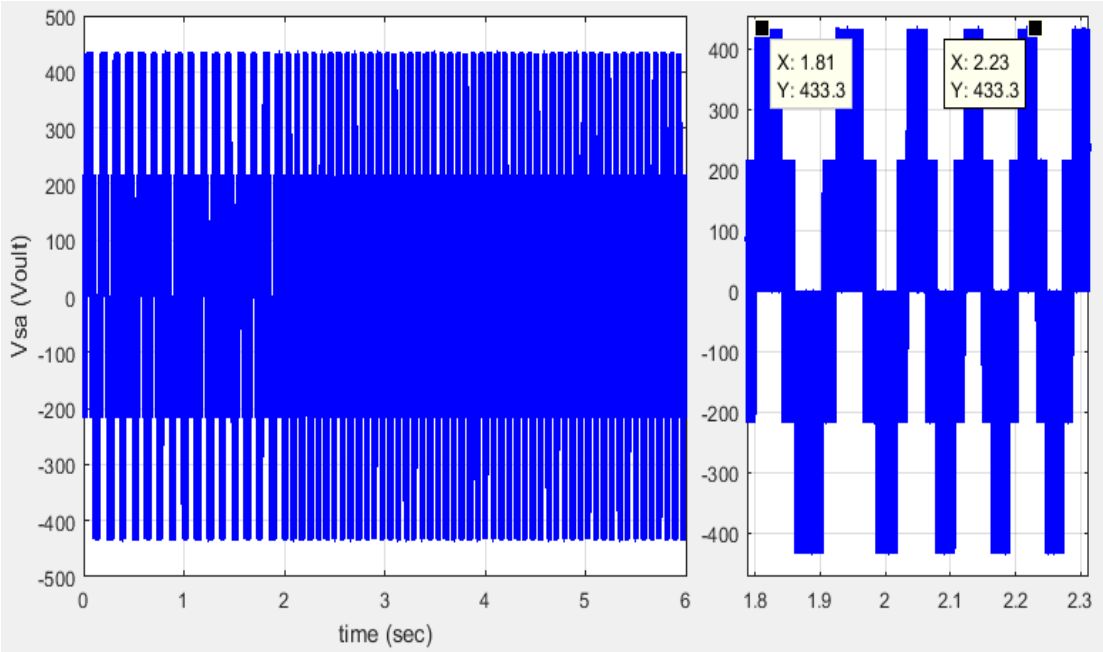

Figure 37. The applied voltages to the stator windings based on the PI controller enhanced Speed at low speed.

The current wave of the first phase of the motor is shown in figure 38. It can be seen that the values of current are within acceptable limits.

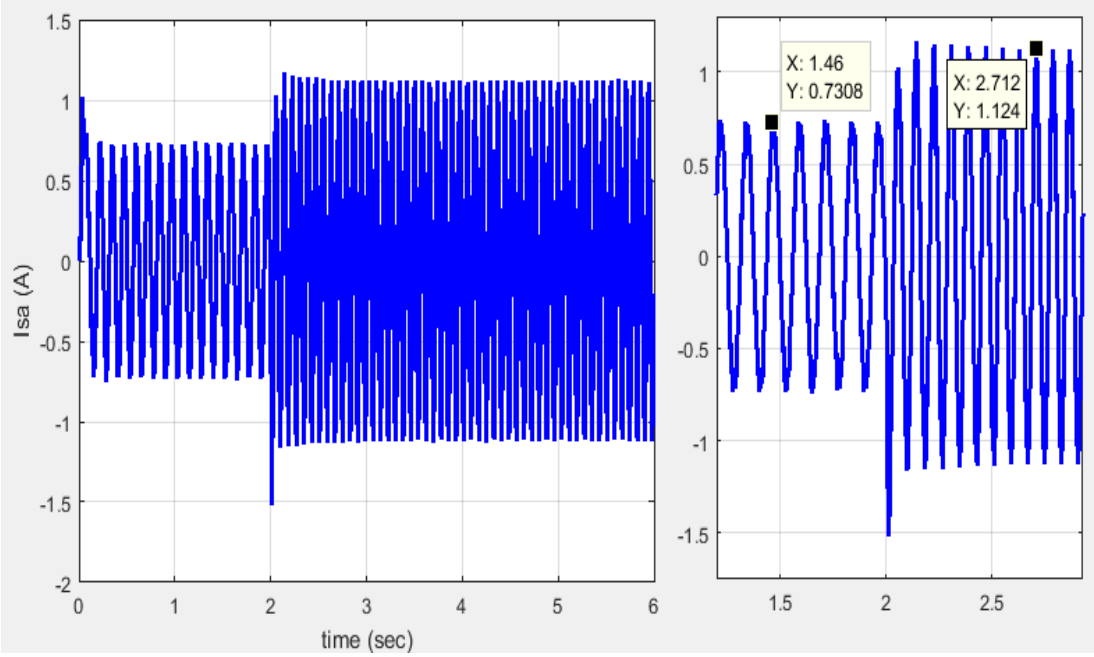

Figure 38. Low enhanced speed PI controller applied stator winding current.

Table 2 compares a speed V/F control system based on a PI controller and an enhanced Speed V/F control system based on a PI controller for speed regulation at high speed.

Table 2. Comparison Results of PI controller systems at High-speeds.

Controller technique	**Settling time**	**Overcoming load time**	**|Qs|**	**torque vibration**
a Speed V/F control system based on PI controller	0.4sec	0.56sec	1.2-1.1	small
an Enhanced Speed V/F control system based on PI controller	0.4sec	0.56sec	1.2-1.18	small

Table 3 compares a speed V/F control system based on a PI controller and an enhanced Speed V/F control system based on a PI controller for speed regulation at low speed.

Table 3. Comparison Results of PI controller systems at Low-speeds.

Controller technique	**Settling time**	**Overcoming load time**	**|Qs|**	**torque vibration**
a Speed V/F control system based on PI controller	0.43sec	1sec	1.04-0.76	small
an Enhanced Speed V/F control system based on PI controller	0.43sec	1sec	1.06-1.14	small

CHAPTER FOUR
CONTROL OF IM USING FUZZY LOGIC

4.1. Introduction

Fuzzy logic is a branch of artificial intelligence that reflects how a person thinks and tries to formulate his thoughts with words to make a decision, and it aims to create intelligent technologies that are closer to the human mind (Arulmozhiyal et al., 2009; Devi et al., 2014; Lesani et al., 2013).

Algebraic logic uses a very sharp differentiation, it is concerned with limits, while in fuzzy logic, the limits are fuzzy, so some issues must be judged gradually based on something, where each element belongs quite well or belongs to a certain degree of belonging or may not belong to a group-specific. As shown in Figure 39, in algebraic logic, only two values (1 or 0) are treated, while in fuzzy logic, a wide range of real values is treated, as it includes all real numbers in the range (0-1) where 0 means absolutely false, and 1 means absolutely true, in the fuzzy logic, there is a gradation of judgment according to the gradation of colors for this example.

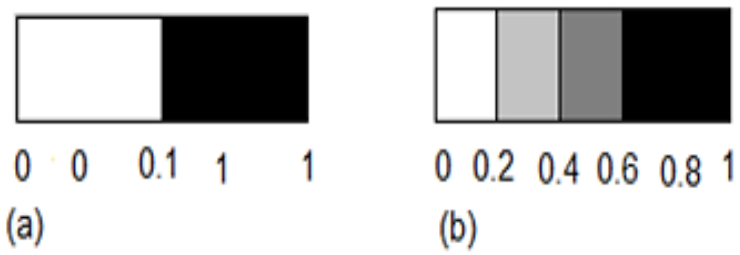

Figure 39. A value domain in algebraic logic, b- value domain in fuzzy logic

4.2. Terms in fuzzy logic

4.2.1 Fuzzy Sets

The basic idea of the fuzzy group is that the elements follow the fuzzy group with certain degrees of Membership, taken in the field [0 1]. Therefore, the principle followed by the fuzzy group is not only either true or false, but it can be partly true (or partly false) when any degree of Membership.

The degree of Membership is taken as a real number in the field [0 1] and is represented on the vertical axis and expresses the extent to which an element belongs to a group.

4.2.2. Linguistic variable

The principle of fuzzy group theory is based on the idea of linguistic variables. Linguistic variables are fuzzy variables, as each basic or subgroup fuzzy group expresses the linguistic value of an appropriate linguistic variable. For example, “the basic group is the weather, and the subgroups are (hot-cold-moderate).

"Hot weather" is a linguistic variable, and hot is a linguistic value. The range of potential values of a variable presents the global set of these variables, the global set of the variable "Weather" can range between 20-90°C and include fuzzy subgroups such as very hot-hot-moderate-cold-very cold. Each fuzzy subgroup also expresses a linguistic value for the accompanying linguistic variable (Devi et al., 2014; Lesani et al., 2013; Uddin et al., 2022).

4.2.3. Functions of Membership

One of the most important processes used in building the fuzzy system is to make the entrances fuzzy by adding them to fuzzy groups with membership dependencies determined according to the situation. These membership dependencies take various forms like trapezoidal, triangular, and gaussian. The choice of the shape of the membership functions depends primarily on the designer's experience of the studied system, but the triangular or trapezoidal shape can often provide the appropriate presentation of expert information and, at the same time, significantly simplify the calculation process. The distribution of membership dependents must be taken into account to cover the entire field, i.e., for each real income, a degree of Membership to at least one member. If the income does not raise any rule, an error will appear in the control logic, so the membership functions must overlap in all the studied fields until the fuzzy system responds smoothly, and the degree of overlap is determined by professional experience (Farah et al., 2021; Verma et al., 2018).

4.2.4 Laws of fuzzy Groups

Fuzzy set laws can be defined as a set of conditional sentences as:

If x is A, Then y is B. Where x and y are linguistic variables, A and B are language values determined by the main fuzzy groups X and Y, respectively.

Let's show the difference between fuzzy and classic group rules:

If w>1500, Then I is small

If w<1500, Then I is large

In the Boolean system, when the speed is greater than 1500 rpm, that makes the current (I) small; the speed changes from 0 to 1500, but the current (I) can take a small or large value.

If w is fast, then I is small

If w is low, then I is large

In the fuzzy system, the speed changes from 0 to 1500, but this range includes many fuzzy groups (fast-slow - very fast "......), and the current includes several groups.

It can be seen that the rule includes two parts: The first part is the estimation of the previous rule (if-part), and the second part applies the result to the next rule then-part (Arulmozhiyal et al., 2009; Devi et al., 2014; Lesani et al., 2013).

4.2.5 Fuzzy inference process

There are several steps to do the fuzzy inference operation, as shown in figure 40, and they are:

1- Converting the numerical income variables to a fuzzy value (Fuzzification) by determining the degree of Membership of the income element to the fuzzy group.

2- Evaluating the rule of experience by applying a fuzzy coefficient (AND, OR) in the If rule part and then linking the formula of the previous rule part with the next.

3- Assembling the rules exits.

4- Fuzzy by converting the fuzzy output variables into numerical values (Defuzzification). (akhila et al., 2016;Arulmozhiyal et al., 2009;Lesani et al., 2013).

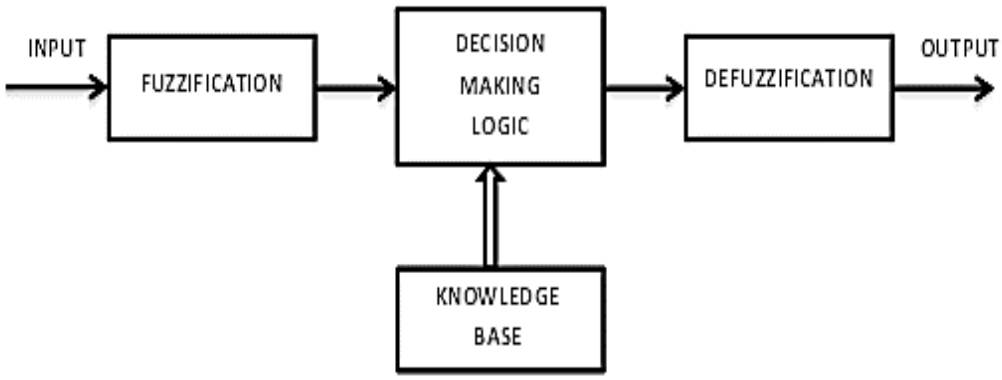

Figure 40. Fuzzy inference process (Moutchou et al., 2021).

4.3. Speed V/f control system based on Fuzzy PI controller

The block diagram of the proposed fuzzy PI control system is shown in figure 41, and the structure of the fuzzy PI controller is shown in figure 42.

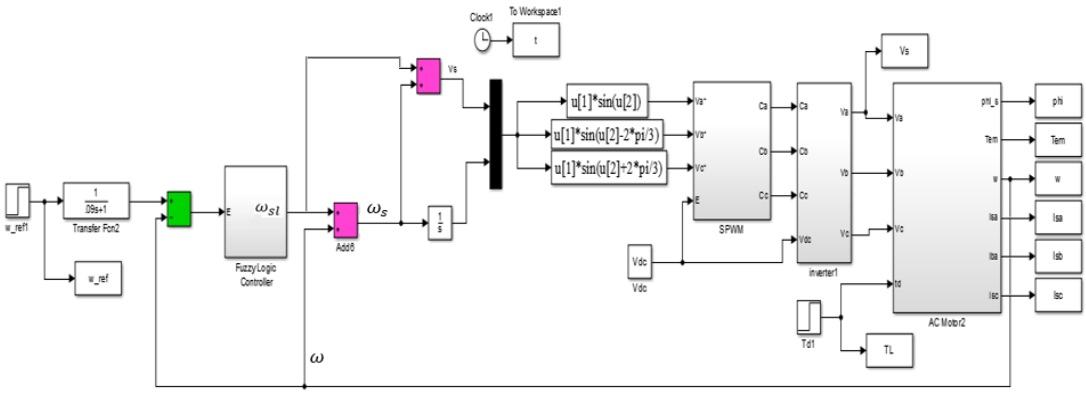

Figure 41. The block diagram of a speed V/F control system using fuzzy PI

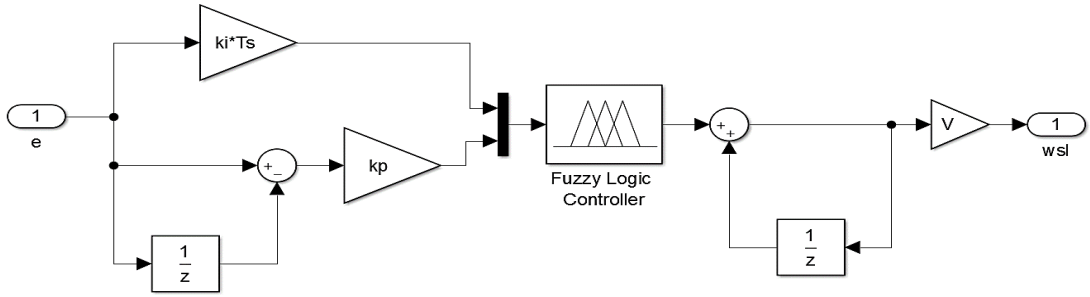

Figure 42. Structure of the fuzzy PI controller (Araria et al., 2020; Arulmozhiyal et al., 2009)

The fuzzy PI controller will be designed based on:

1- Mamdani method

2- Sugino method

4.4. Speed V/f control system using fuzzy PI based on the Mamdani method

The controller will first be designed based on the Mamdani method, where the membership functions of the input and output signals for the Mamdani method are shown in figures 43, 44, and 45.

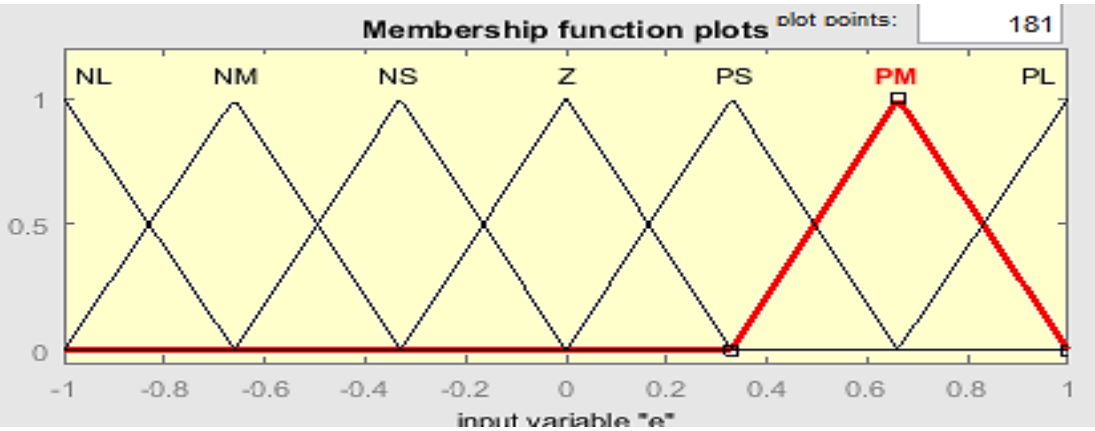

Figure 43. The membership functions of the speed error for fuzzy PI controller based on the Mamdani method in speed V/f control system.

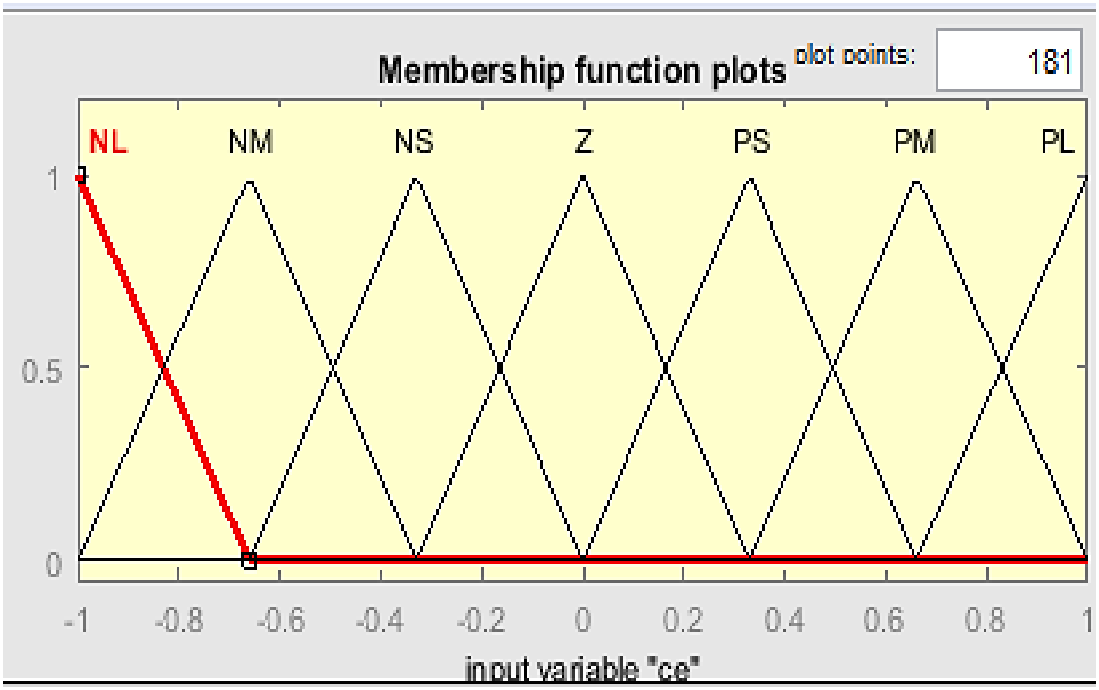

Figure 44. The membership functions of the speed for fuzzy PI controller based on the Mamdani method

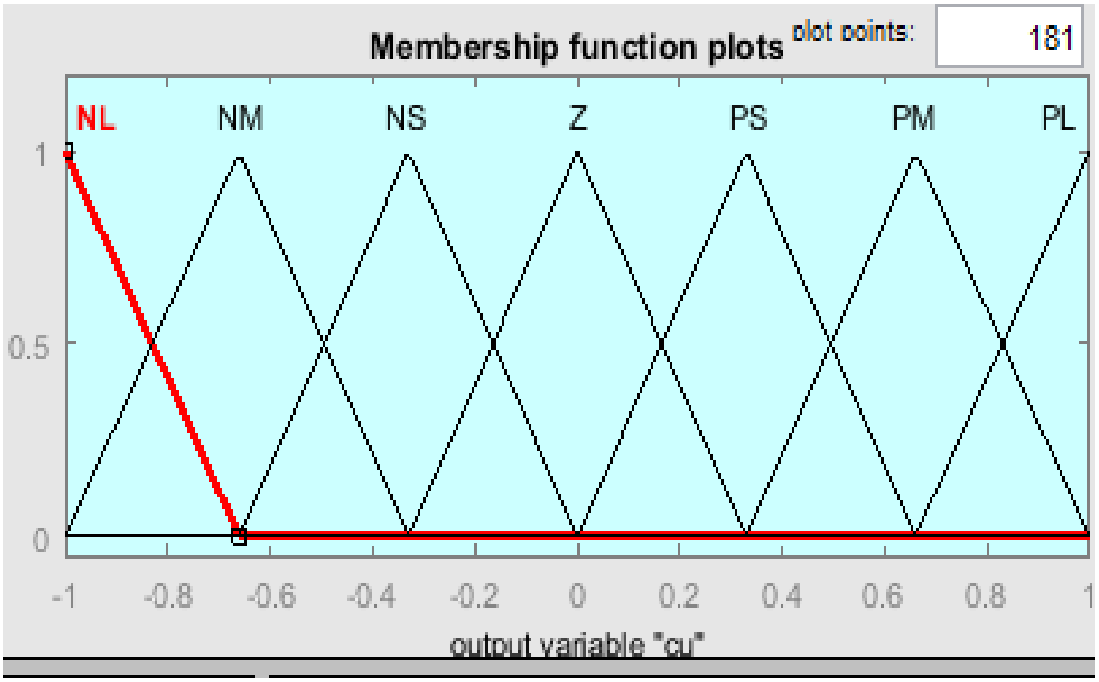

Figure 45. The membership functions of the change output for fuzzy PI controller based on the Mamdani method

The rule base is shown in Table 4.

Table 4. Rule base for speed fuzzy PI controller.

ce/e	NB	NM	NS	Z	PS	PM	PB
NB	NB	NB	NB	NB	NM	NS	Z
NM	NB	NB	NB	NM	NS	Z	PS
NS	NB	NB	NM	NS	Z	PS	PM
Z	NB	NM	NS	Z	PS	PM	PB
PS	NM	NS	Z	Z	PM	PB	PB
PM	NS	Z	PS	PM	PB	PB	PB
PB	Z	PS	PM	PB	PB	PB	PB

4.4.1 Simulation results of a Speed using fuzzy PI based on the Mamdani method at high speed.

A simulation of the speed V/F control system using fuzzy PI based on the Mamdani method when regulating the motor speed at a nominal value equal to 282rad/sec. The load torque is applied at the moment 2sec.

Figure 46 shows the response time of the speed V/F control system using fuzzy PI based on the Mamdani method when regulating the motor speed at a nominal value equal to 282rad/sec

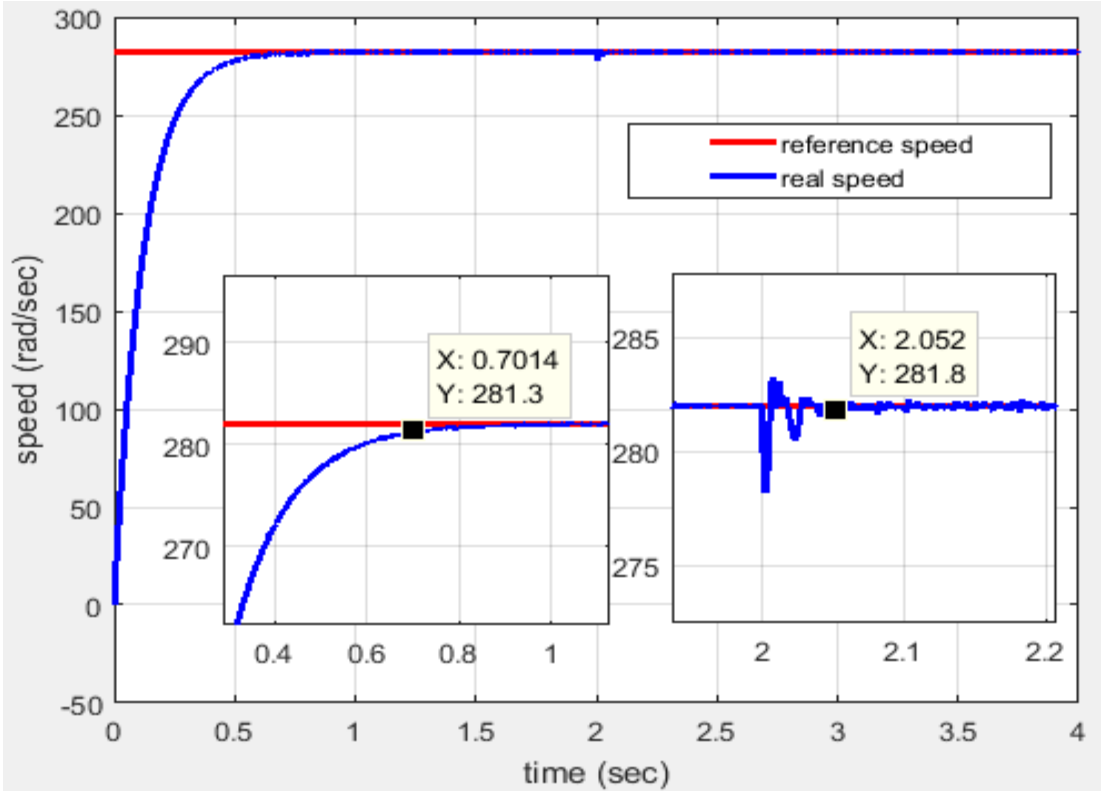

Figure 46. The speed response time using fuzzy PI based on the Mamdani method at 282rad/sec speed.

It is noticed from figure 46 that the speed V/F control system using fuzzy PI based on the Mamdani method has a greater ability to overcome the load torque where the motor needs less than 0.1sec to return to the reference speed while it needs 0.56sec for using PI controller, but the settling time is 0.7sec, it is bigger than settling time for using a PI controller.

Figure 47 shows the response time for the flux when the speed is regulated at a nominal value equal to 282rad/sec using a speed fuzzy PI V/F control system based on the Mamdani method.

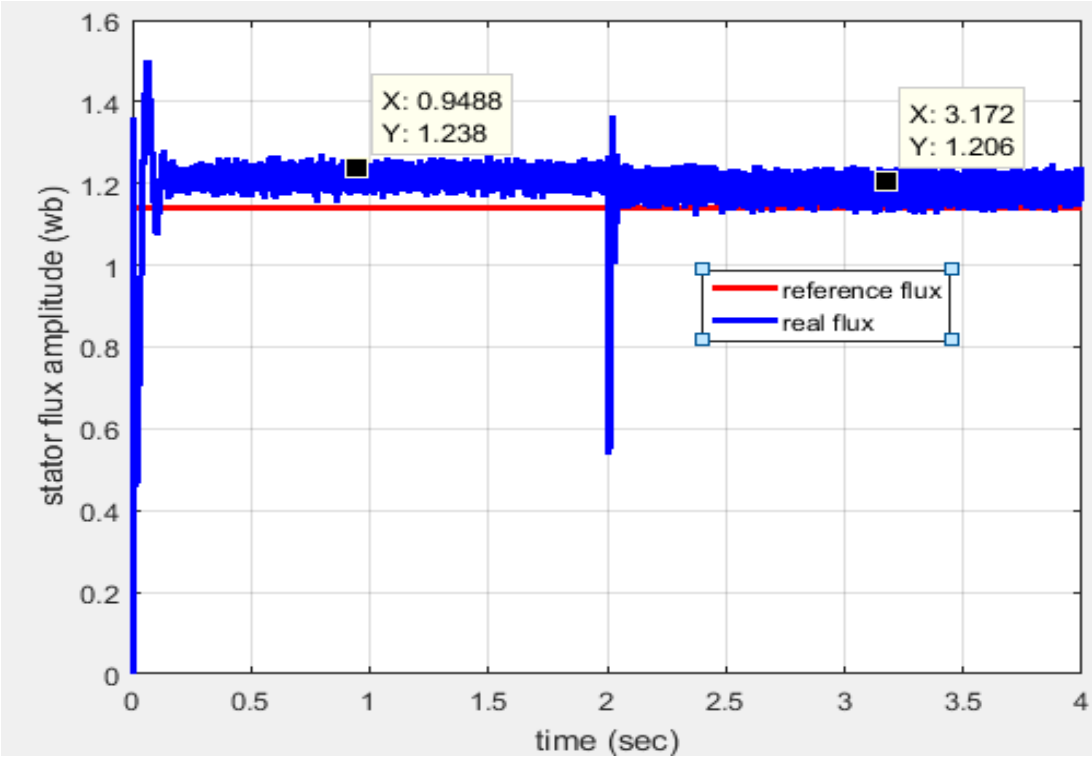

Figure 47. The flux response time using fuzzy PI based on the Mamdani method at 282rad/sec speed

It is noticed from figure 47 that the flux amplitude was equal to 1.23wb before applying the load torque, and it is equal to 1.2 after that. This matter contributed to the presence of a small vibration in the torque in the transient case, as shown in figure 48.

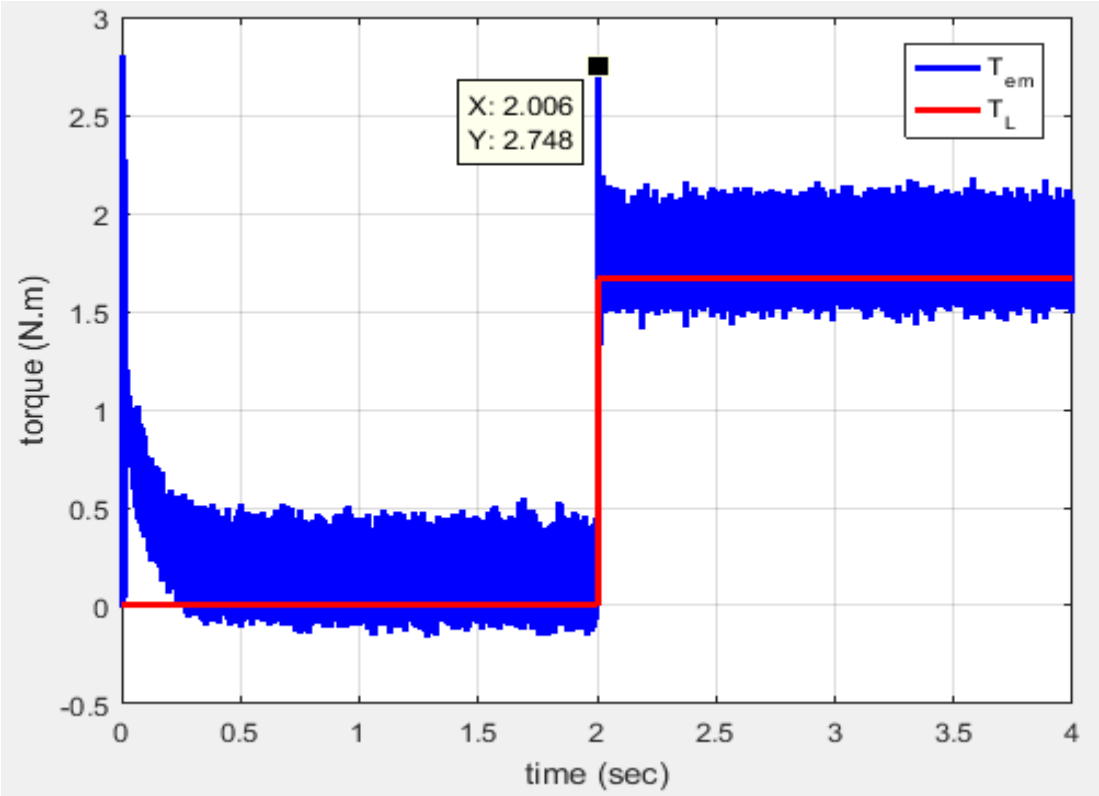

Figure 48. The electromagnetic torque response time using a fuzzy PI based on the Mamdani method at 282rad/sec speed**.**

The voltage wave on the first phase of the motor is shown in figure 49. It can be seen that the values of voltage are within acceptable limits.

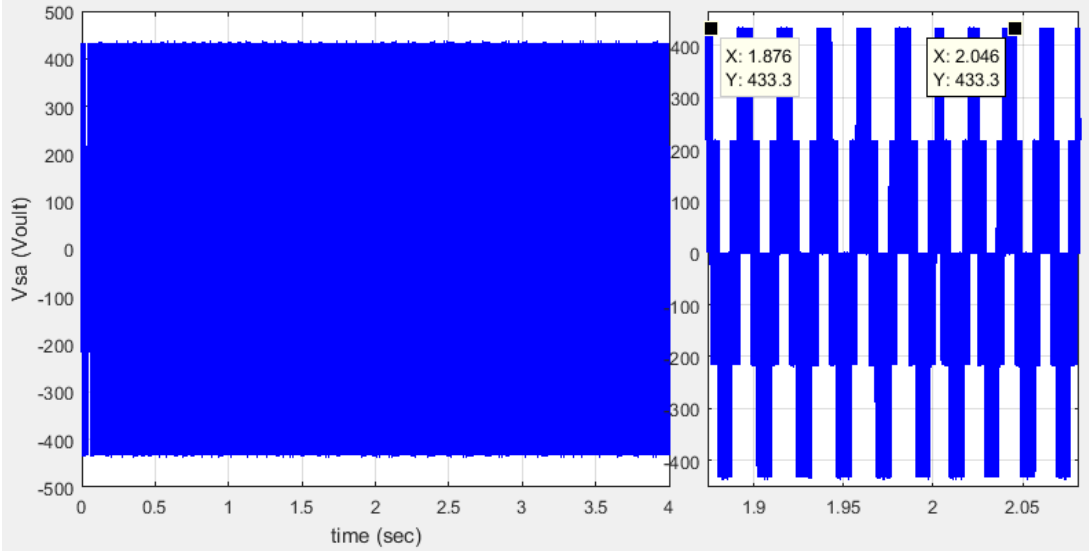

Figure 49. The applied voltages to the stator windings using fuzzy PI control based on the Mamdani method at 282rad/sec speed.

The current wave of the first phase of the motor is shown in figure 50. It can be seen that the values of current are within acceptable limits.

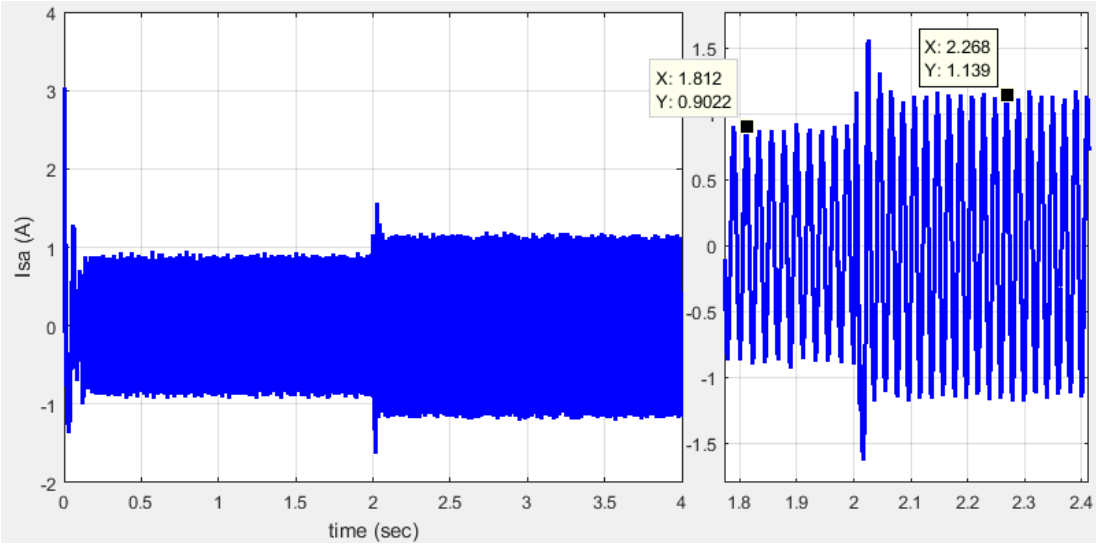

Figure 50. The applied current to the stator windings using a fuzzy PI control based on the Mamdani method at 282rad/sec speed.

4.4.2. Simulation Speed results using fuzzy PI based on the Mamdani method at a low speed.

A simulation of speed V/F control system using fuzzy PI based on the Mamdani method when regulating the motor speed at 50rad/sec and the load torque is applied at the moment 2sec.

Figure 46 shows the response time of the speed V/F control system using fuzzy PI based on the Mamdani method when regulating the motor speed at 50rad/sec

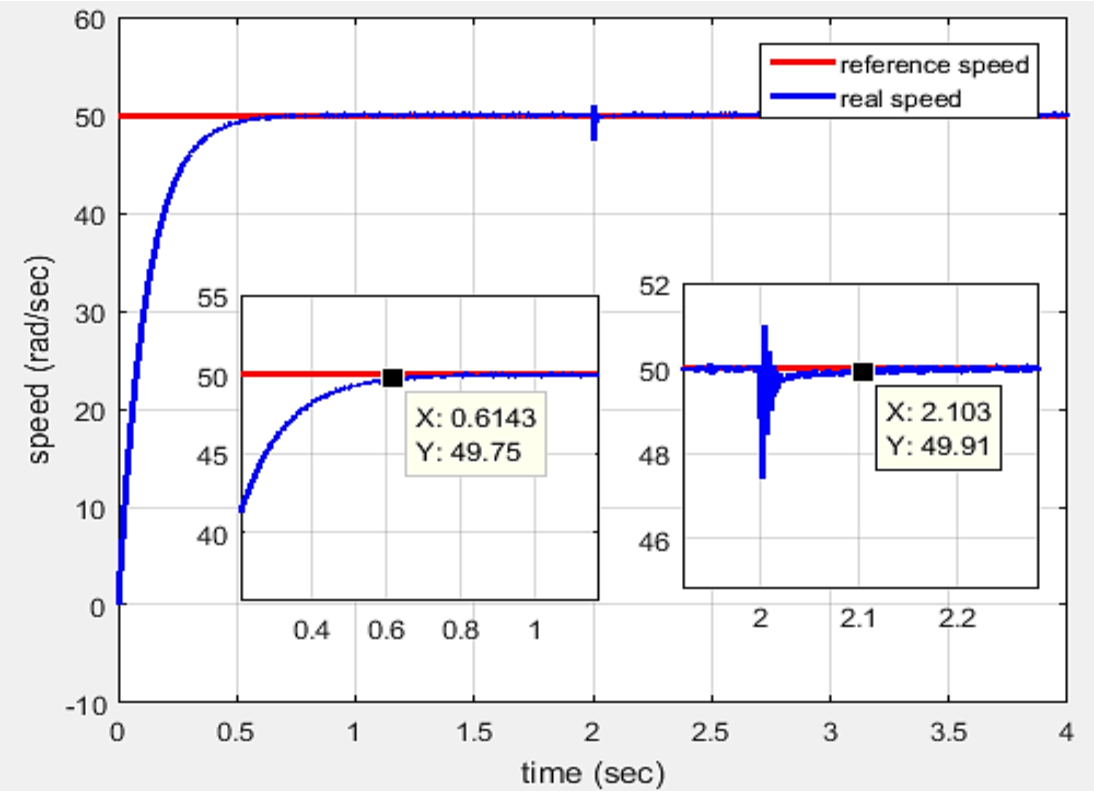

Figure 51. The speed response time using fuzzy PI based on the Mamdani method at 50rad/sec speed.

It is noticed from figure 51 that the speed V/F control system using fuzzy-PI based on the Mamdani method has a greater ability to overcome the load torque where the motor needs less than 0.1sec to return to the reference speed. It needs 0.5sec to use the PI controller, but the settling time is 0.6sec. It is bigger than the settling time for using the PI controller.

Figure 52 shows the response time for the flux when the speed is regulated at 50rad/sec using a speed fuzzy PI V/F control system based on the Mamdani method.

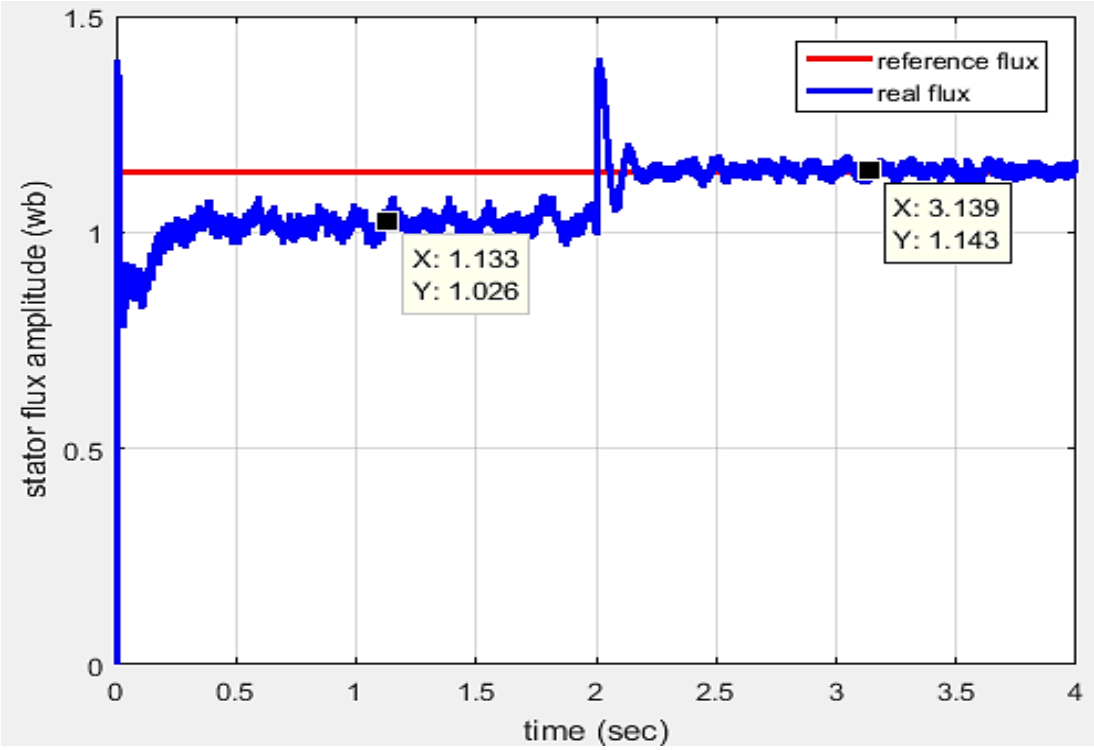

Figure 52. The flux response time using fuzzy PI based on the Mamdani method at 50rad/sec speed.

Noticed from figure 52 that the flux amplitude was equal to 1.026wb before applying the load torque, and it is equal to 1.14 after the moment of loading. This matter contributed to large vibration in the torque in the transient case, as shown in figure 53.

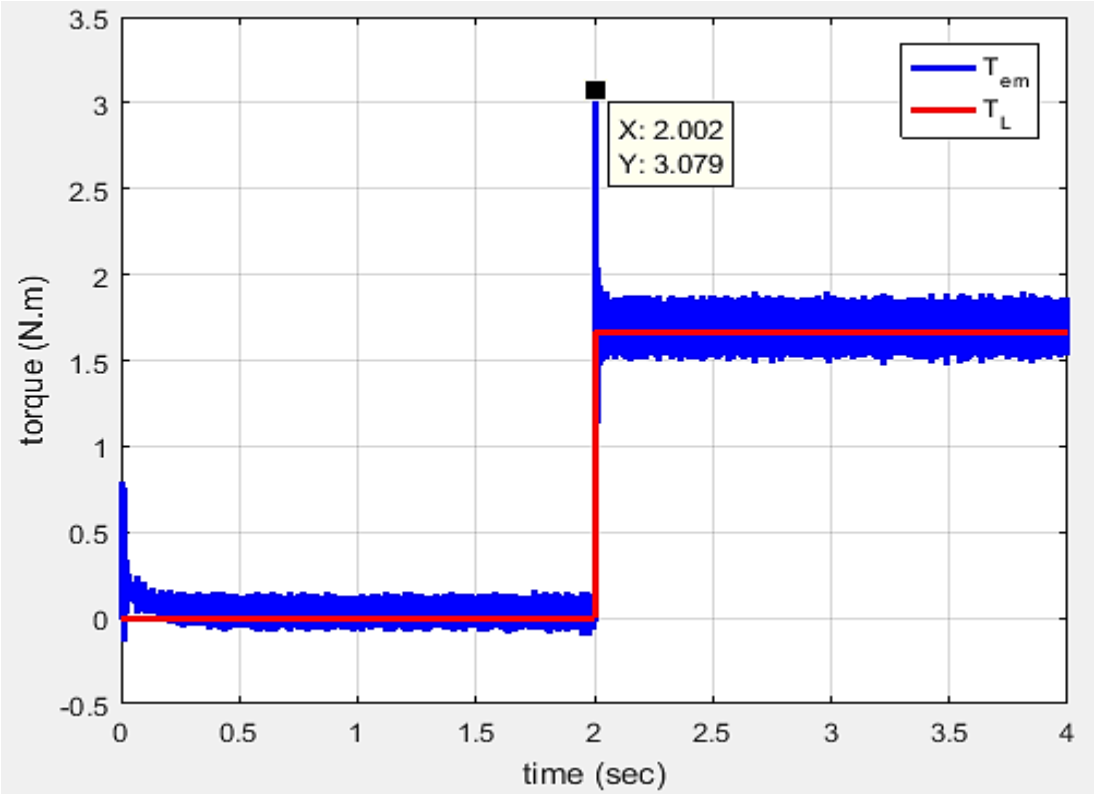

Figure 53. The electromagnetic torque response time using fuzzy PI control based on the Mamdani method at 50rad/sec speed.

The voltage wave for the first phase is shown in Figure 54. It can be seen that the values of current are within acceptable limits.

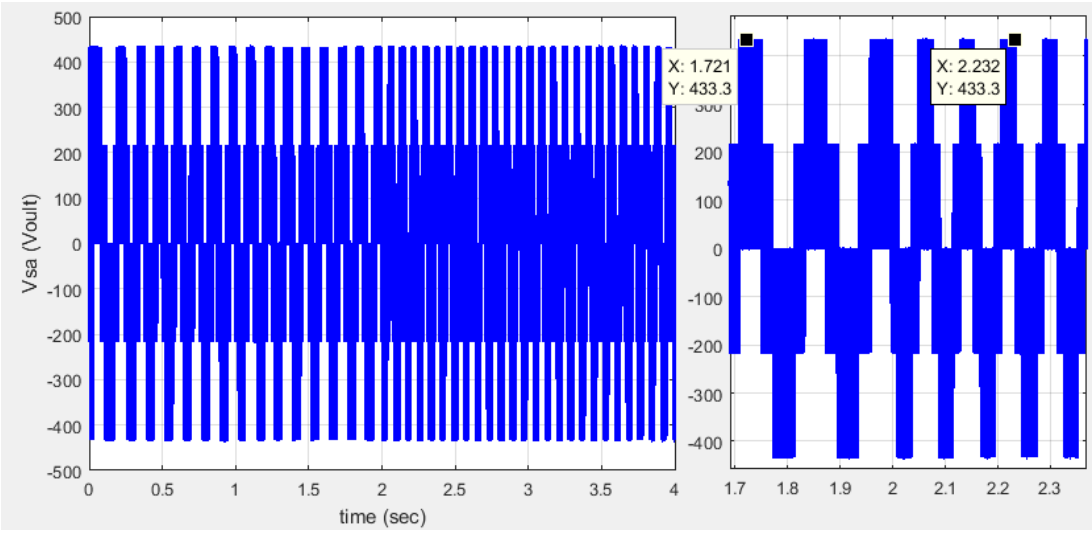

Figure 54. The applied voltages to the stator windings using a speed fuzzy PI control based on the Mamdani method at 50rad/sec.

The current wave of the first phase of the motor is shown in figure 55. It can be seen that the values of current are within acceptable limits.

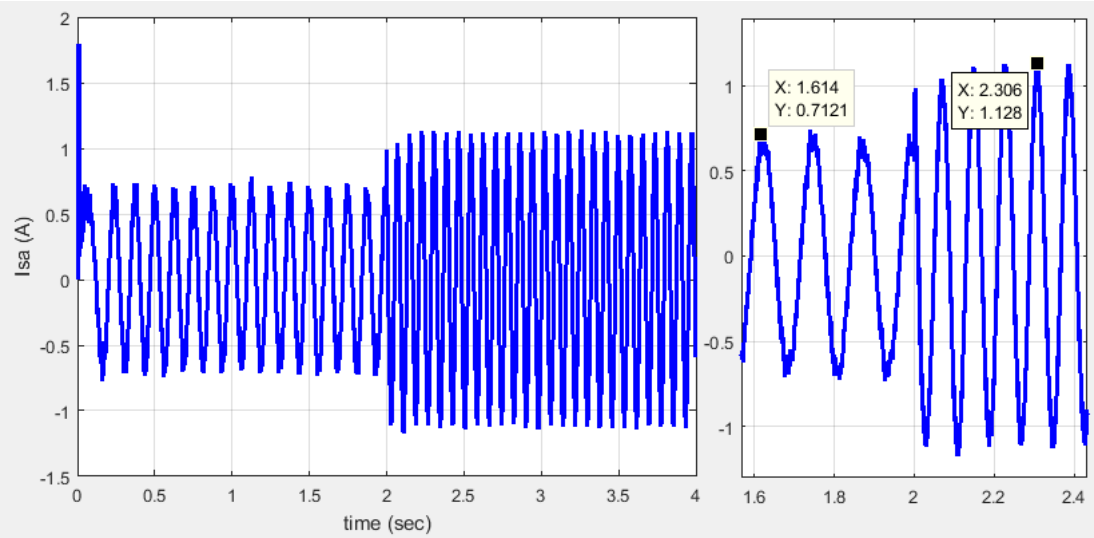

Figure 55. The applied current to the stator windings using a speed fuzzy PI control based on the Mamdani method at 50rad/sec speed.

4.5. Speed V/f control using fuzzy PI based on the Sugino method

In this step, the controller will be designed based on the Sugino method, where the membership functions of the input and output signals of the Sugino method are shown in figures 56, 57, and 58.

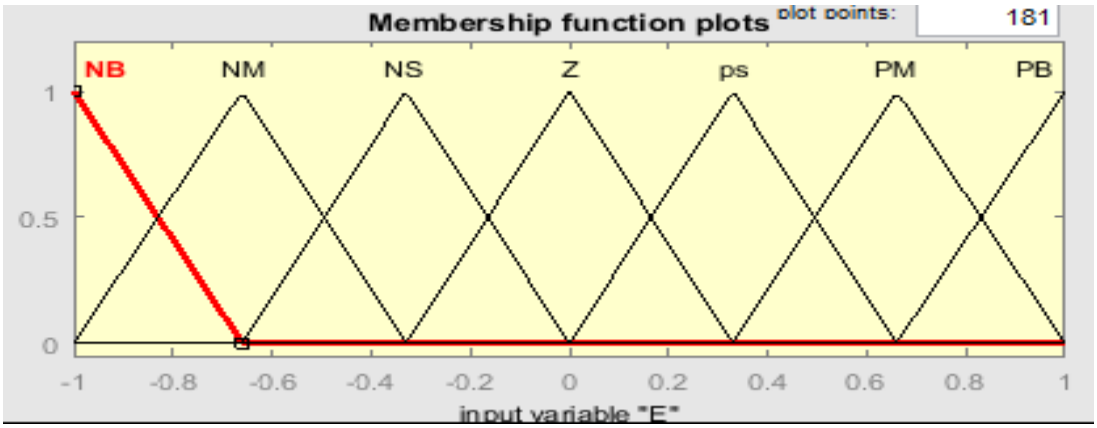

Figure 56. The Membership functions of the speed error for fuzzy PI controller based on Sugino method

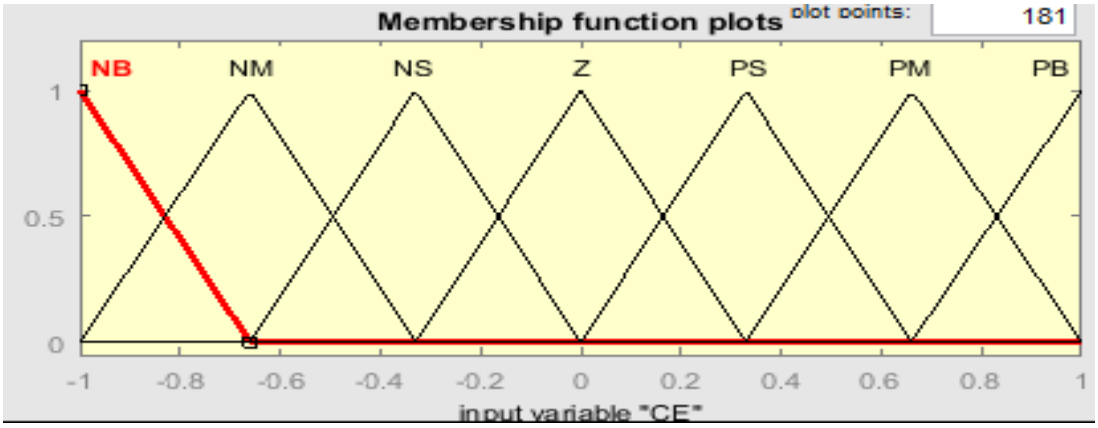

Figure 57. The Membership functions of the speed error change for the fuzzy PI controller based on the Sugino method

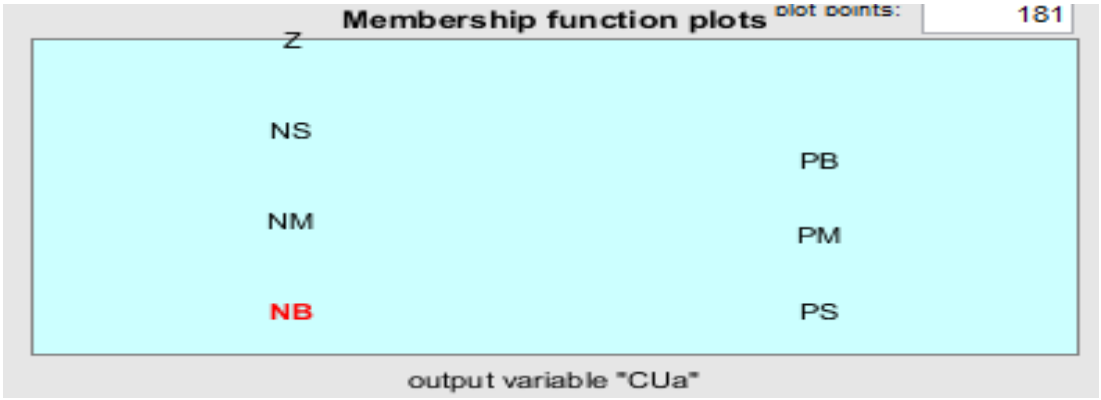

Figure 58. The Membership functions of the change output for fuzzy PI controller based on Sugino method

4.5.1 Simulation Speed results of V/f control using fuzzy PI based on the Sugino method at high speed.

A simulation of speed V/F control system using fuzzy PI based on the Sugino method when regulating the motor speed at a nominal value equal to 282rad/sec and the load torque is applied at the moment 2sec.

Figure 46 shows the response time of the speed V/F control system using fuzzy PI based on the Sugino method when regulating the motor speed at a nominal value equal to 282rad/sec

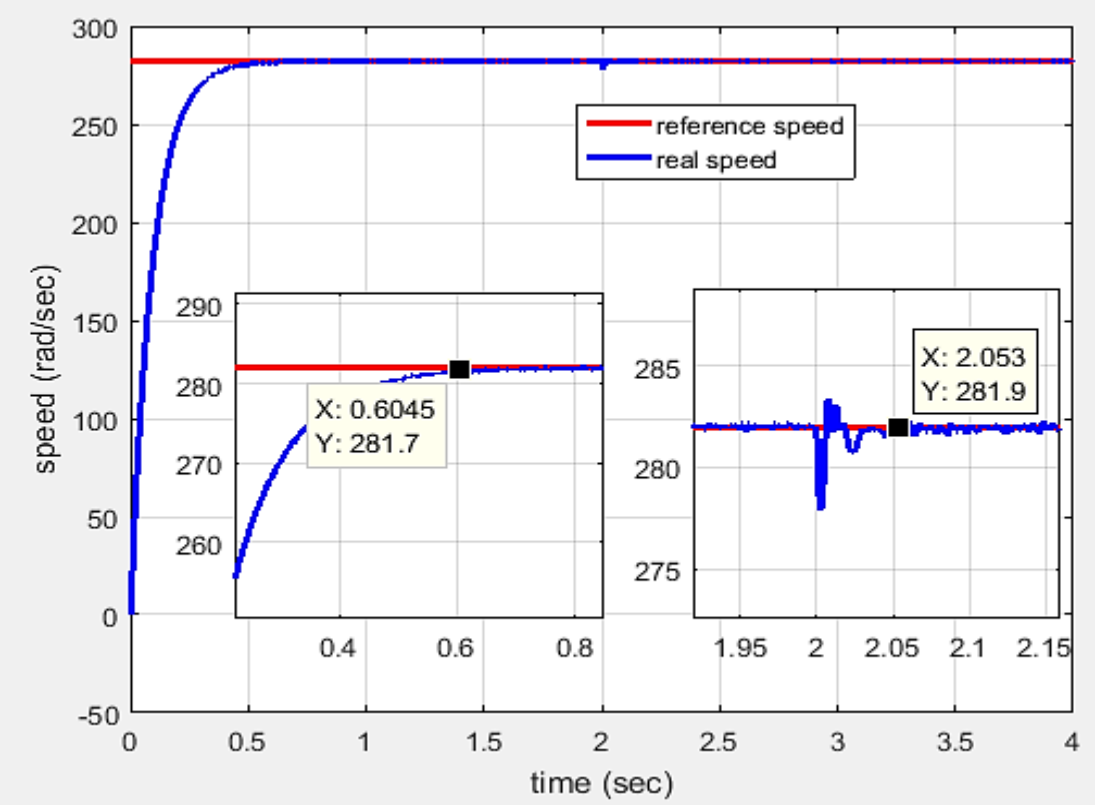

Figure 59. The speed response time using fuzzy PI based on the Sugino method at 282rad/sec speed.

Figure 59 shows that the speed V/F control system using fuzzy PI based on the Sugino method has a settling time (ts=0.6sec) it is smaller than the settling time for the speed V/F control system using fuzzy PI based on the Mamdani method, but it has the same ability to overcome the load torque where the motor needs less than 0.1sec to return to the reference speed.

Figure 60 shows the response time for the flux when the speed is regulated at 282rad/sec using a speed fuzzy PI V/F control system based on the Sugino method.

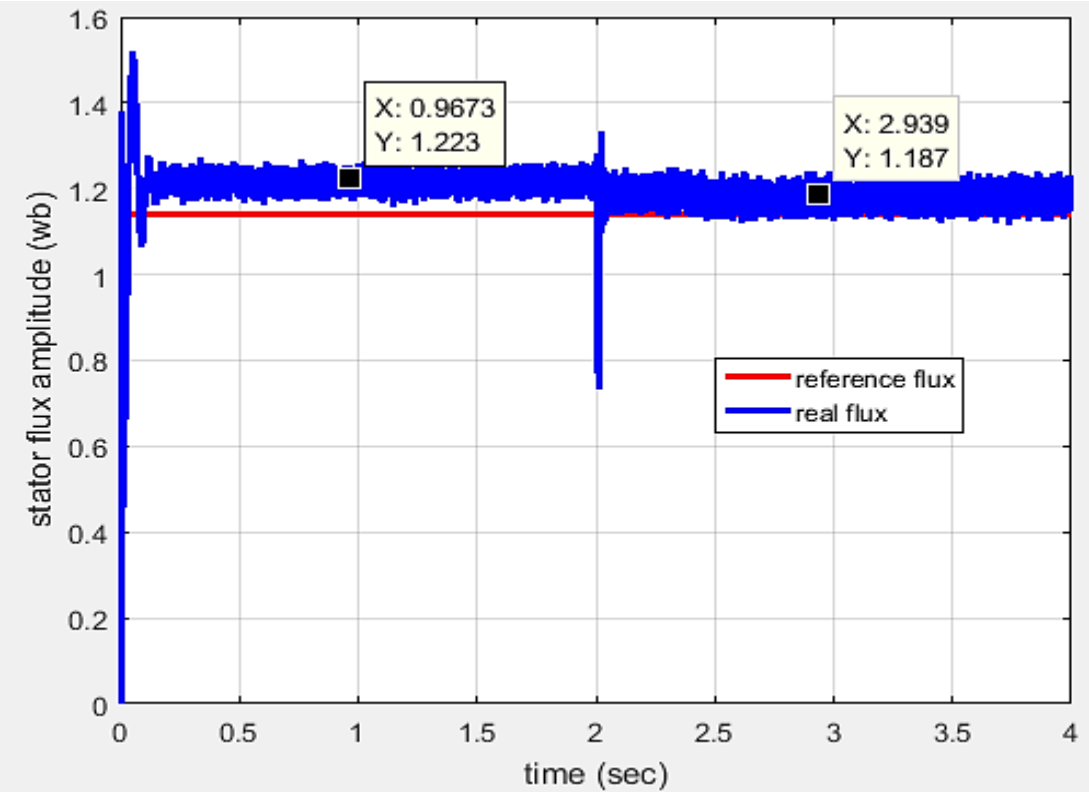

Figure 60. The flux response time using fuzzy PI control based on the Sugino method at 282rad/sec speed

As shown in figure 60 the amplitude of the flux was equal to 1.22wb before applying the load torque, and it is equal to 1.18 after that, so there is a small vibration in the torque in the transient case as shown in figure 61.

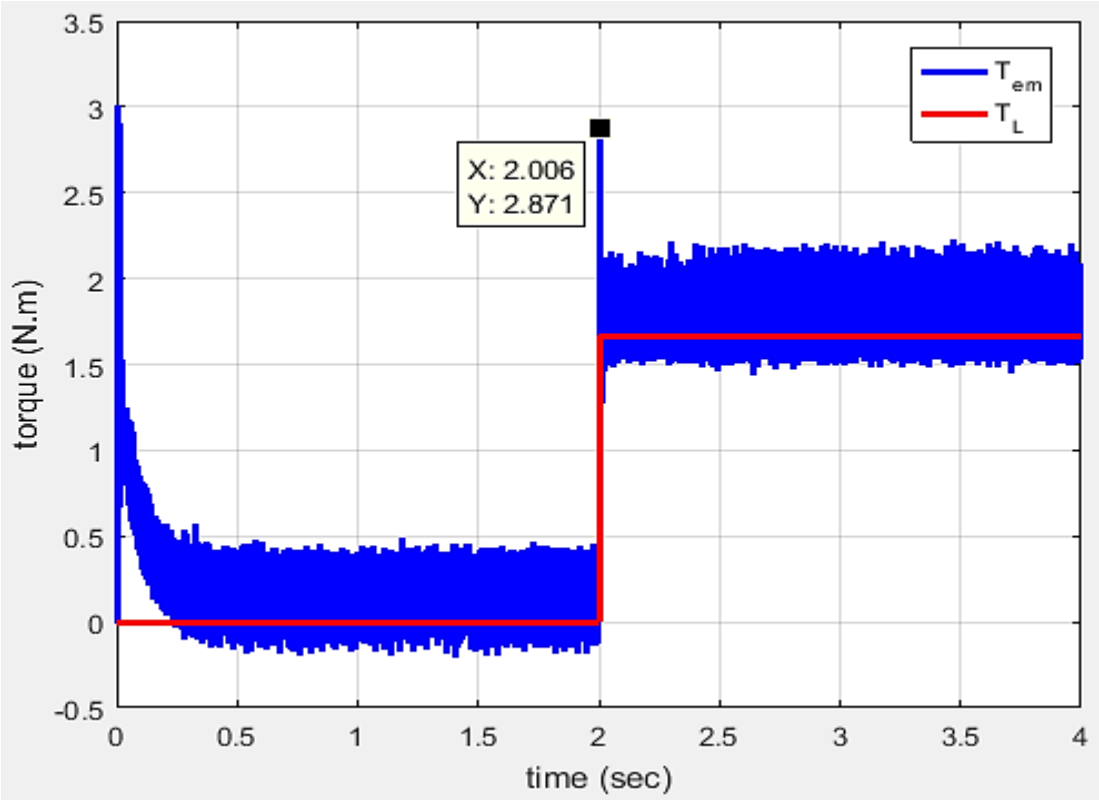

Figure 61. The electromagnetic torque response time using fuzzy PI control based on the Sugino method at 282rad/sec speed

The voltage wave on the first phase of the motor is shown in figure 62. It can be seen that the values of voltage are within acceptable limits.

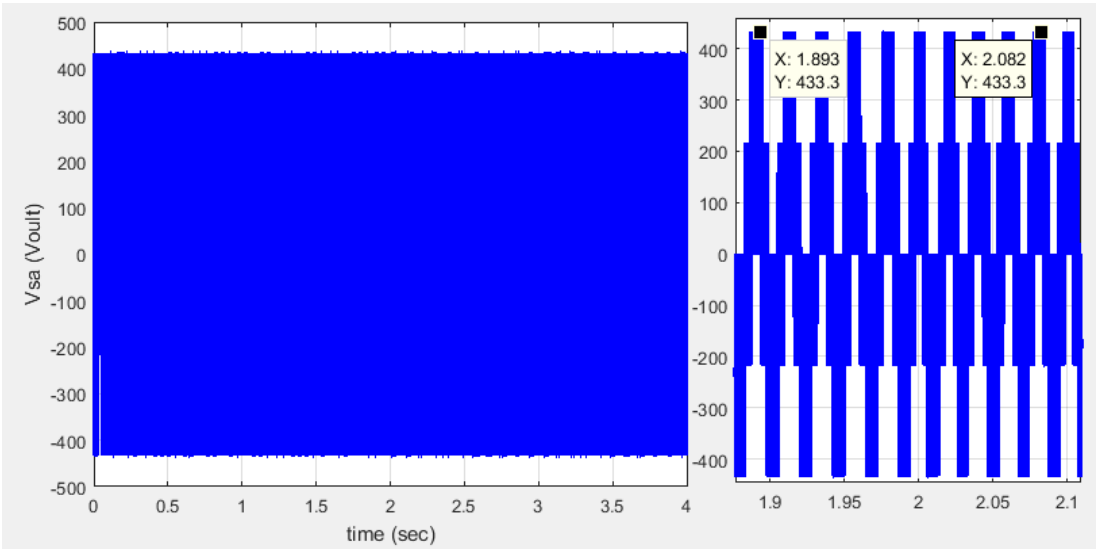

Figure 62. The applied voltages to the stator windings using fuzzy PI control based on the Sugino method at 282rad/sec

The current wave of the first phase of the motor is shown in figure 63. It can be seen that the values of current are within acceptable limits.

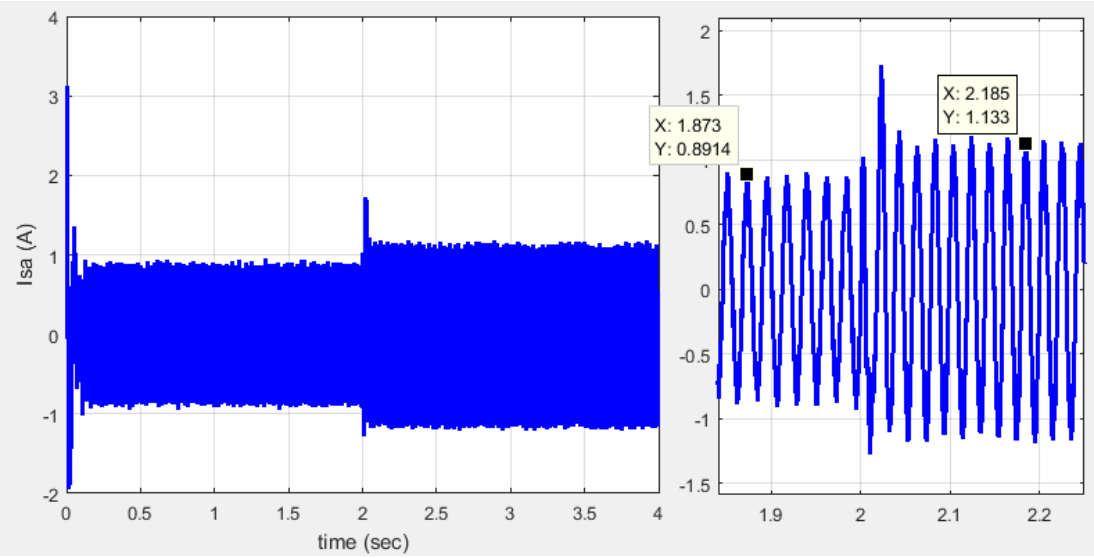

Figure 63. The current applied to the stator windings using fuzzy PI control based on the Sugino method at 282rad/sec speed

4.5.2 Simulation Speed results using fuzzy PI control based on the Sugino method at a low speed

A simulation of the speed V/F control system using fuzzy PI based on the Sugino method when regulating the motor speed at 50rad/sec and the load torque is applied at the moment 2sec.

Figure 46 shows the response time of the speed V/F control system using fuzzy PI based on the Sugino method when regulating the motor speed at 50rad/sec

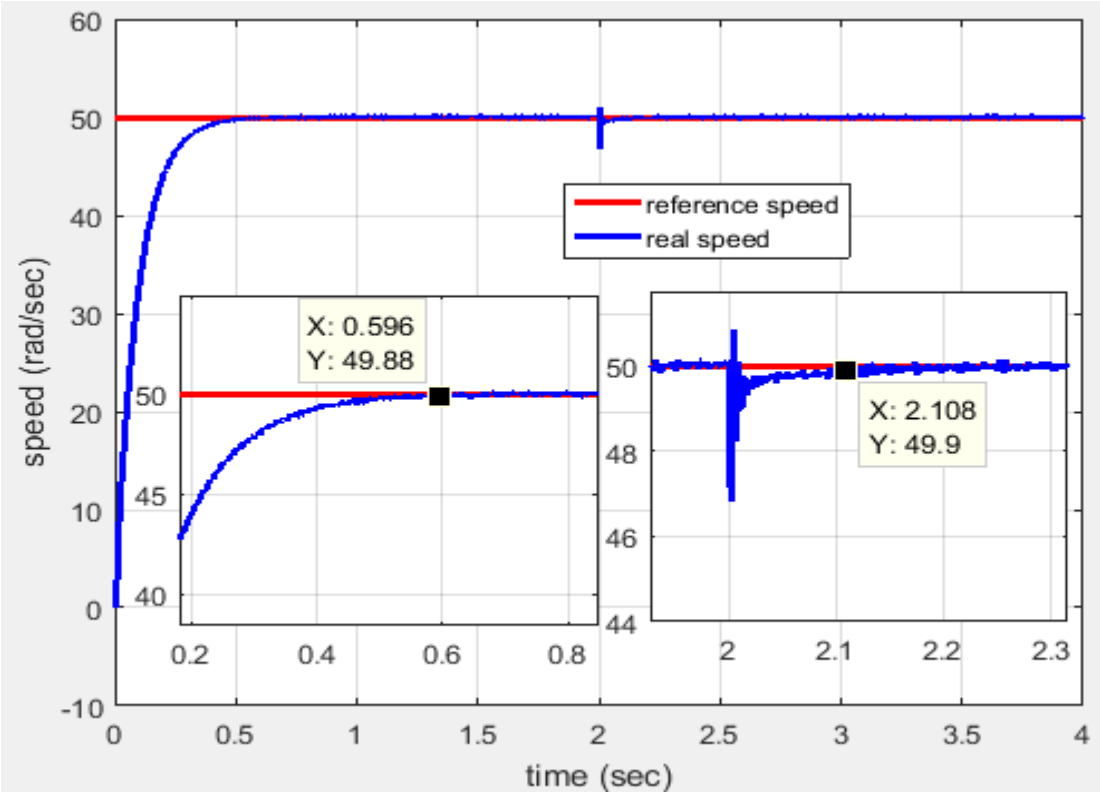

Figure 64. The speed response time using fuzzy PI control based on the Sugino method at 50rad/sec speed

It is noticed in figure 64 that the speed V/F control system using fuzzy PI based on the Sugino method has the same settling time as the speed V/F control system using fuzzy PI based on the Mamdani method (ts=0.6sec) and has the same ability to overcome the load torque where the motor needs less than 0.1sec to return to the reference speed.

Figure 65 shows the response time for the flux when the speed is regulated at 50rad/sec using a speed fuzzy PI V/F control system based on the Sugino method.

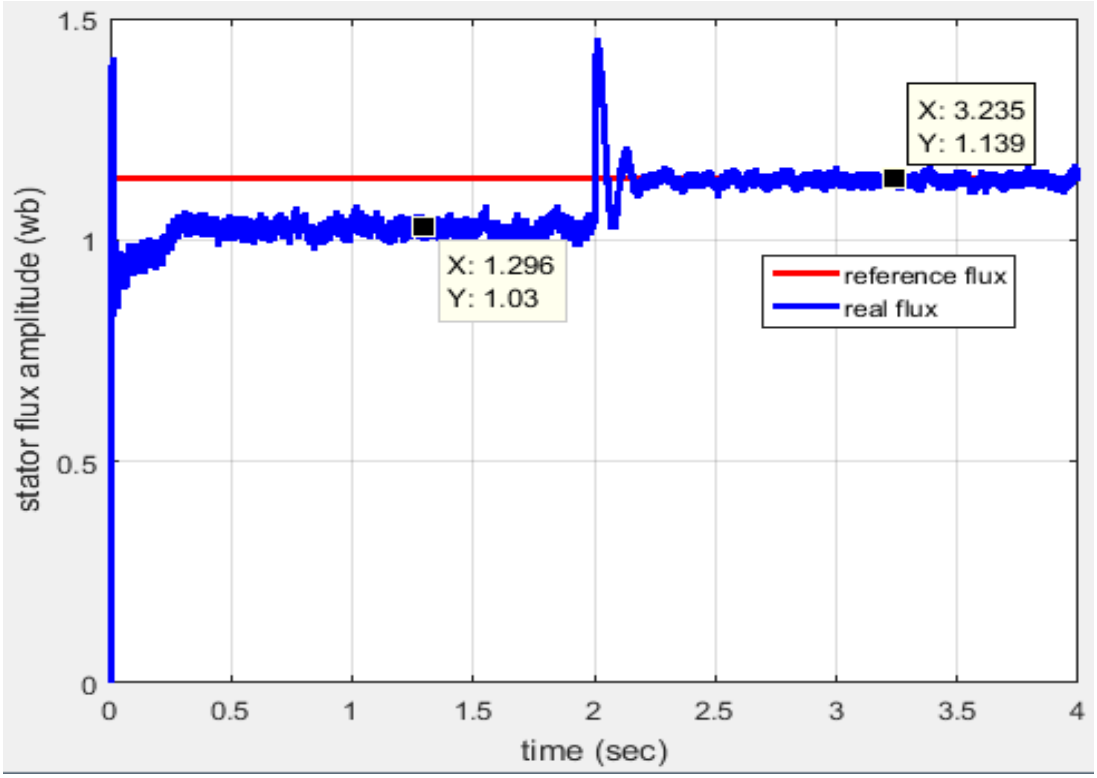

Figure 65. The flux response time using fuzzy PI control based on the Sugino method at 50rad/sec speed.

It is noticed from figure 65 that the amplitude of the flux was equal to 1.03wb before applying the load torque, and it is equal to 1.14 after that, and this matter contributed to the presence of a large vibration in the torque in the transient case as shown in figure 66.

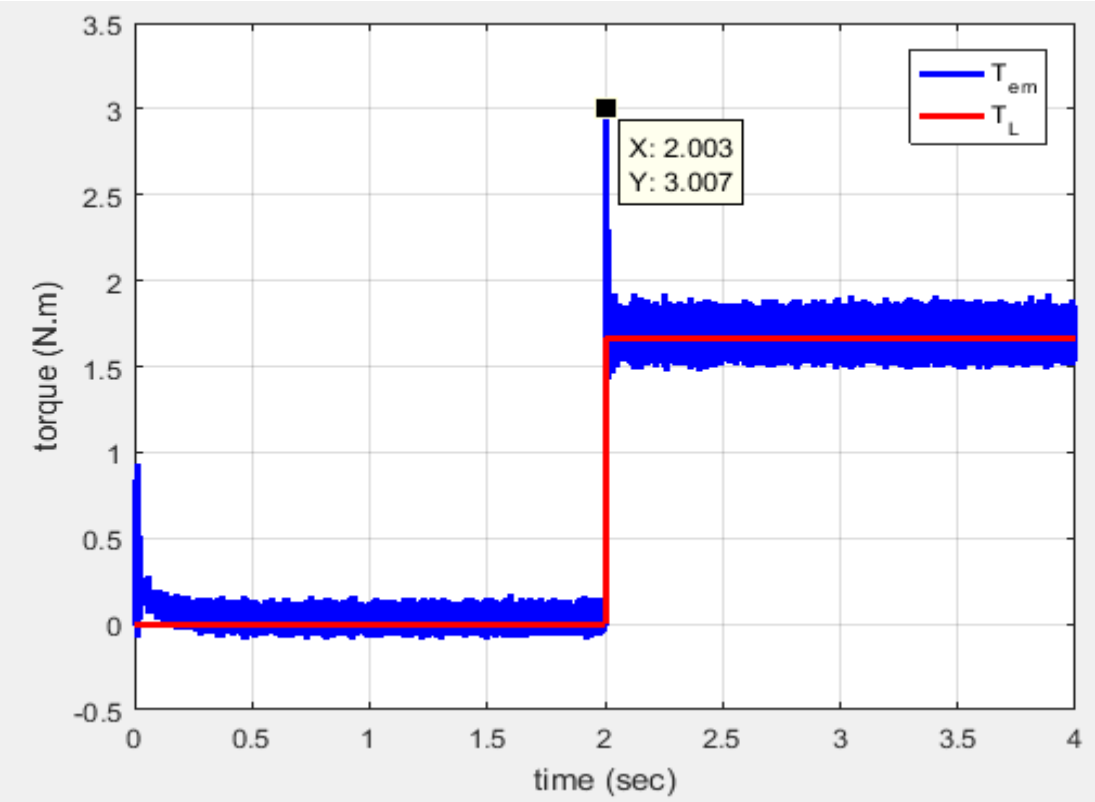

Figure 66. The electromagnetic torque response time using fuzzy PI control based on the Sugino method at 50rad/sec speed

The voltage wave on the first phase of the motor is shown in figure 67. It can be seen that the values of voltage are within acceptable limits.

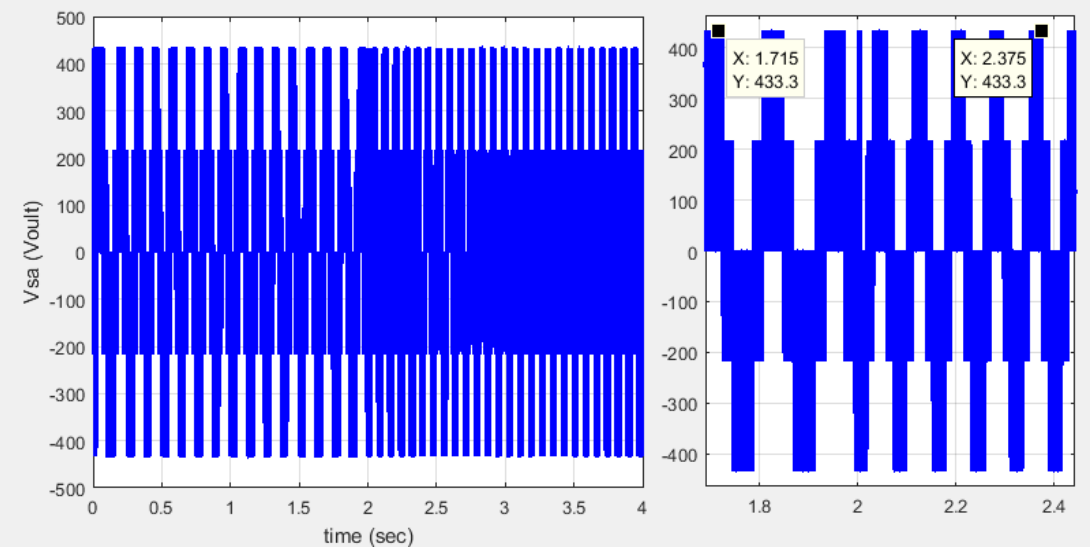

Figure 67. The applied voltages to the stator windings using fuzzy PI control based on the Sugino method at 50rad/sec speed

The current wave of the first phase of the motor is shown in figure 68. It can be seen that the values of current are within acceptable limits.

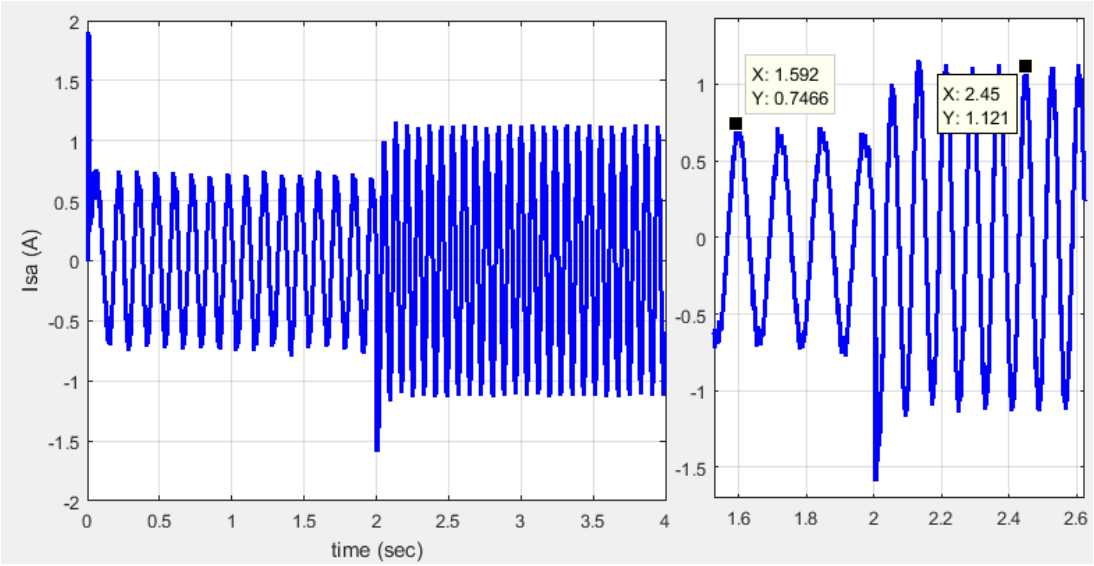

Figure 68. The applied current to the stator windings using fuzzy PI control based on the Sugino method at 50rad/sec speed.

4.6. Flux and Speed, V/F control system, using fuzzy PI based on Sugino method

The constant voltage amplitude relationship can be written as follow in equation (4.9) to improve the dynamic performance and maintain a constant value of the magnetic flux.

$$V_s = \omega_s + \delta \tag{4.9}$$

Where δ is a voltage amplitude correction signal.

Figure 69 shows the block diagram of the proposed speed and flux control system using fuzzy PI.

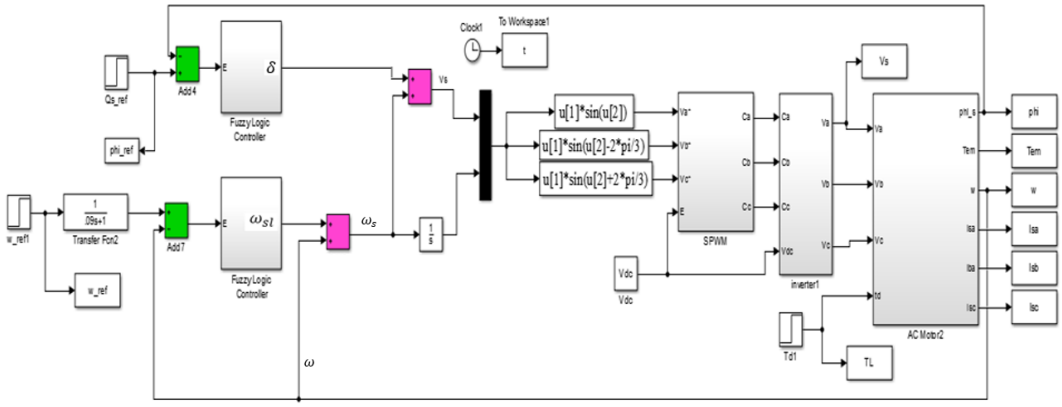

Figure 69. The block diagram of the Flux and Speed control system using fuzzy PI

The speed and flux controllers will be designed based on the Sugino method, where the membership functions of the input and output signals for the Sugino method are shown in the figures there below

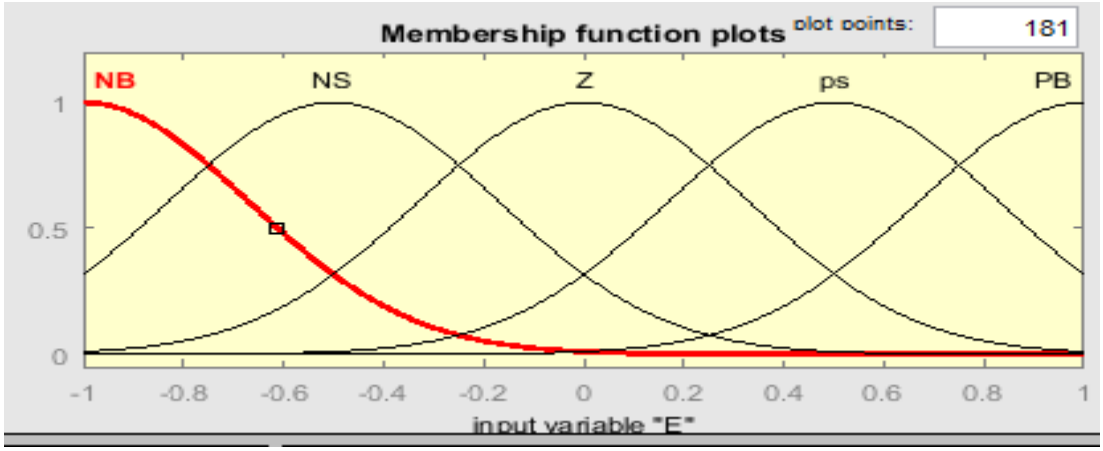

Figure 70. The Membership functions of the error for fuzzy PI controller based on Sugino method in Flux and speed

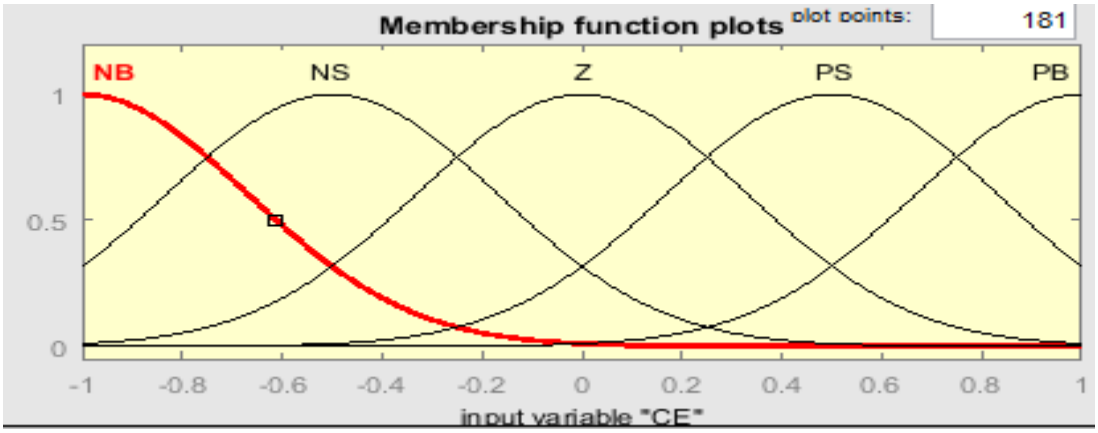

Figure 71. The Membership functions of the speed error change for fuzzy PI controller based on Sugino method in Flux and speed

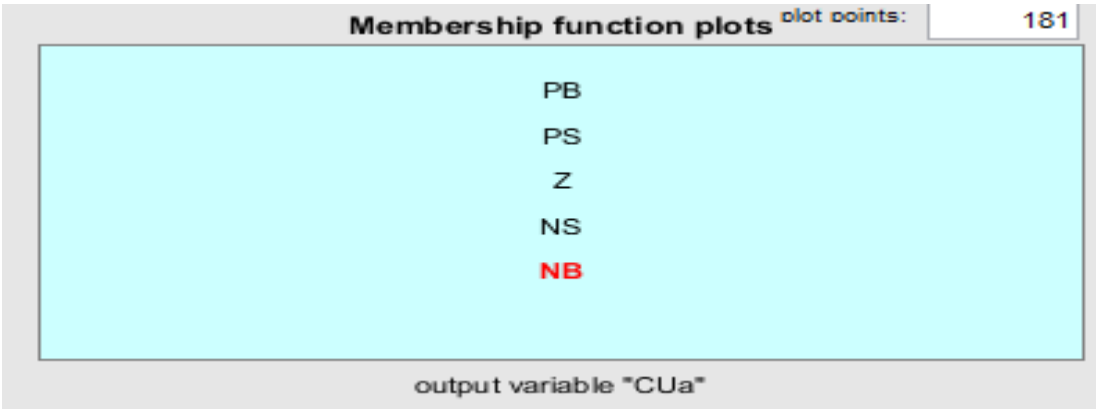

Figure 72. The Membership functions of the change output for fuzzy PI controller based on Sugino method in Flux and speed

The rule base is shown in Table 5.

Table 5. Rule base for speed and flux fuzzy PI controllers

Ce/e	NB	NS	Z	PS	PB
NB	NB	NB	NB	NM	Z
NS	NB	NM	NS	Z	PM
Z	NB	NS	Z	PS	PB
PS	NM	Z	PS	PM	PB
PB	Z	PM	PB	PB	PB

4.6.1 Simulation results of Flux and Speed using fuzzy PI based on the Sugino method at a high speed

A simulation of Flux and speed V/F control system using fuzzy PI based on Sugino method when regulating the motor speed at a nominal value equal to 282rad/sec and the load torque is applied at the moment 2sec.

Figure 73 shows the response time of Flux and speed V/F control system using fuzzy PI based on the Sugino method when regulating the motor speed at a nominal value equal to 282rad/sec.

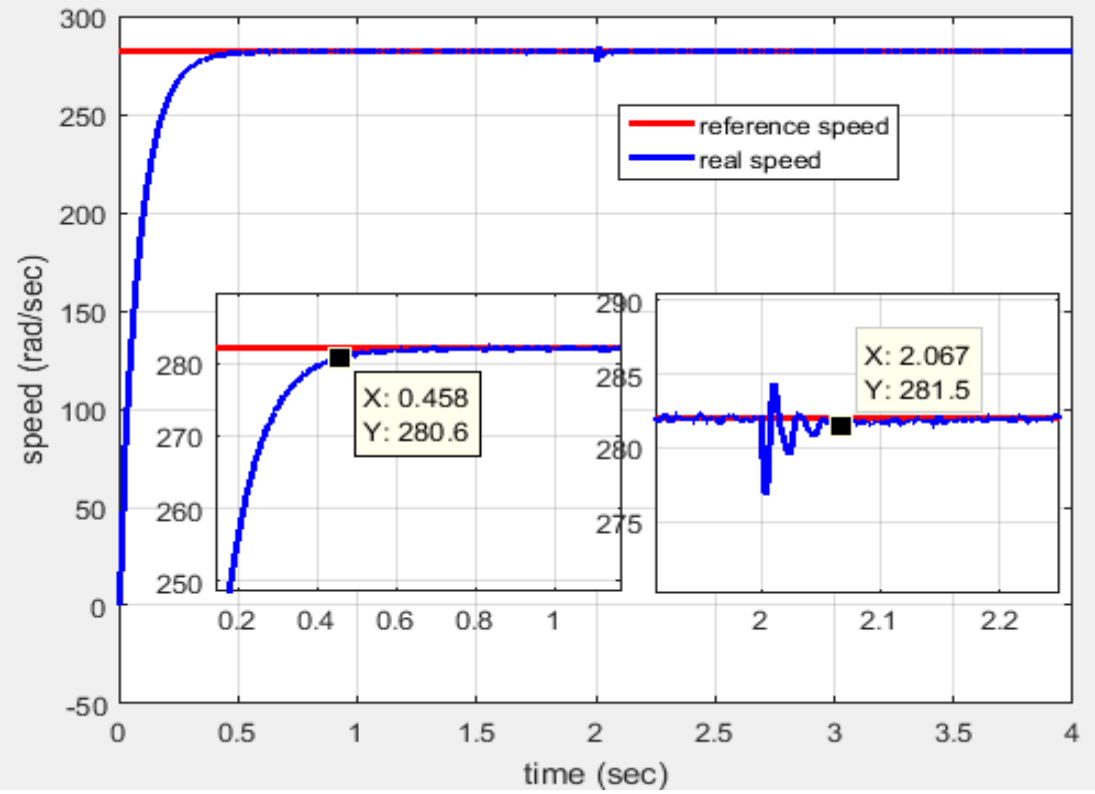

Figure 73. The flux and speed response time using fuzzy PI based on Sugino method at 282rad/sec speed

It is noticed from figure 73 that Flux and speed V/F control system using fuzzy PI based on the Sugino method has a settling time (ts=0.45sec) it is smaller than the settling time for speed V/F control system using fuzzy PI based on the Sugino method, but it has the same ability to overcome the load torque where the motor needs less than 0.1sec to return to the reference speed.

Figure 74 shows the response time for the flux when the speed is regulated at 282rad/sec using a speed fuzzy PI V/F control system based on the Sugino method.

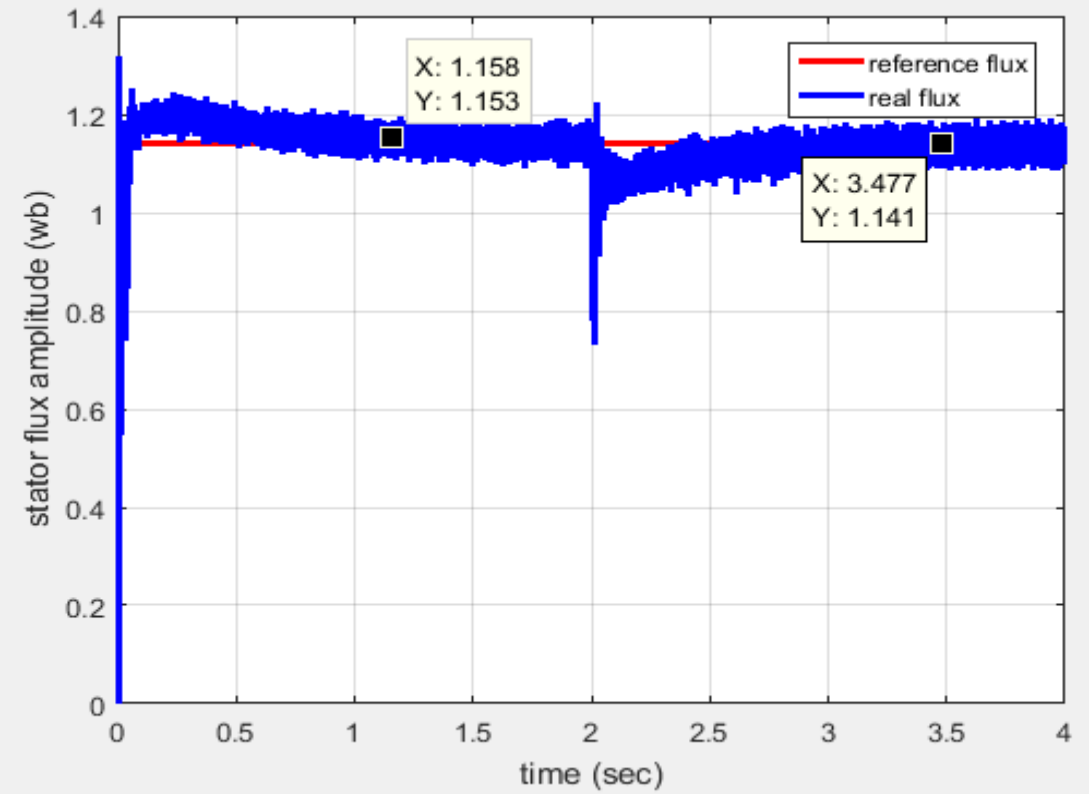

Figure 74. The flux response time using Flux and speed fuzzy PI control based on the Sugino method at 282rad/sec speed

It is noticed from figure 74 that the Flux and speed V/F control system using fuzzy PI based on the Sugino method maintains a constant value of ($\Phi_s = 1.14$ wb), unlike the speed V/F control system using fuzzy PI based on the Sugino method. This matter contributes to reducing vibrations in the electromagnetic torque, as shown in figure 75.

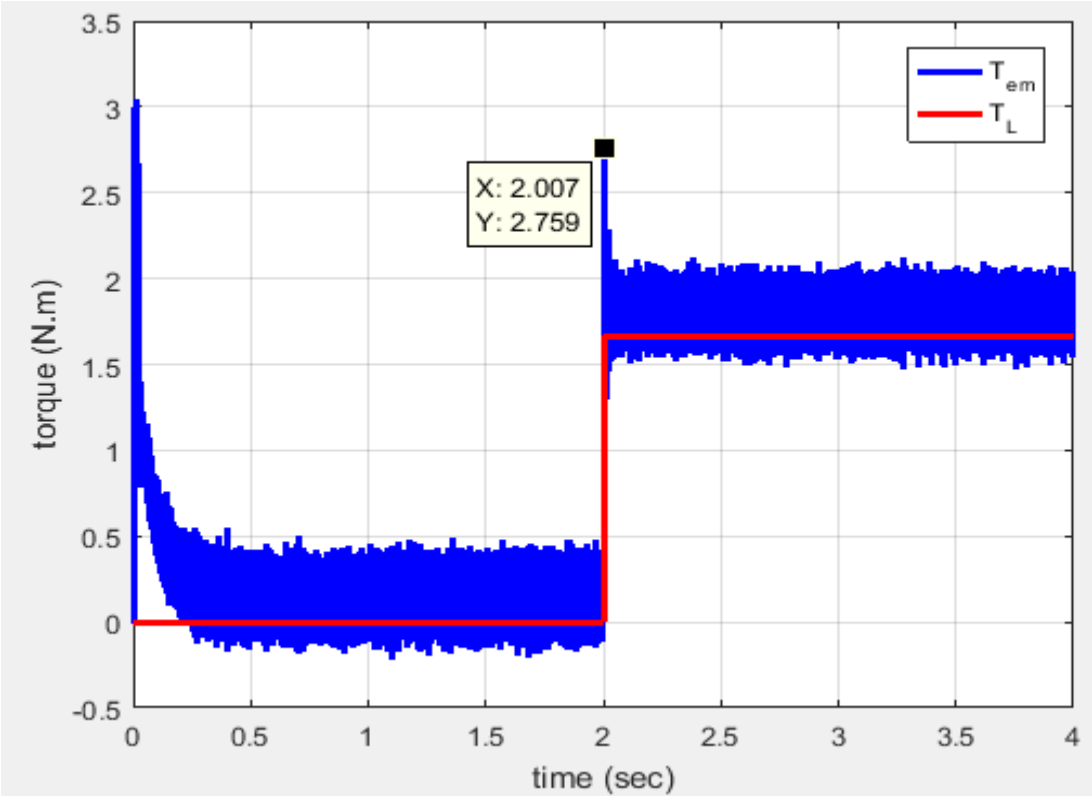

Figure 75. The electromagnetic torque response time using Flux and speed fuzzy PI control based on the Sugino method at 282rad/sec speed

The voltage wave on the first phase of the motor is shown in figure 76. It can be seen that the values of voltage are within acceptable limits.

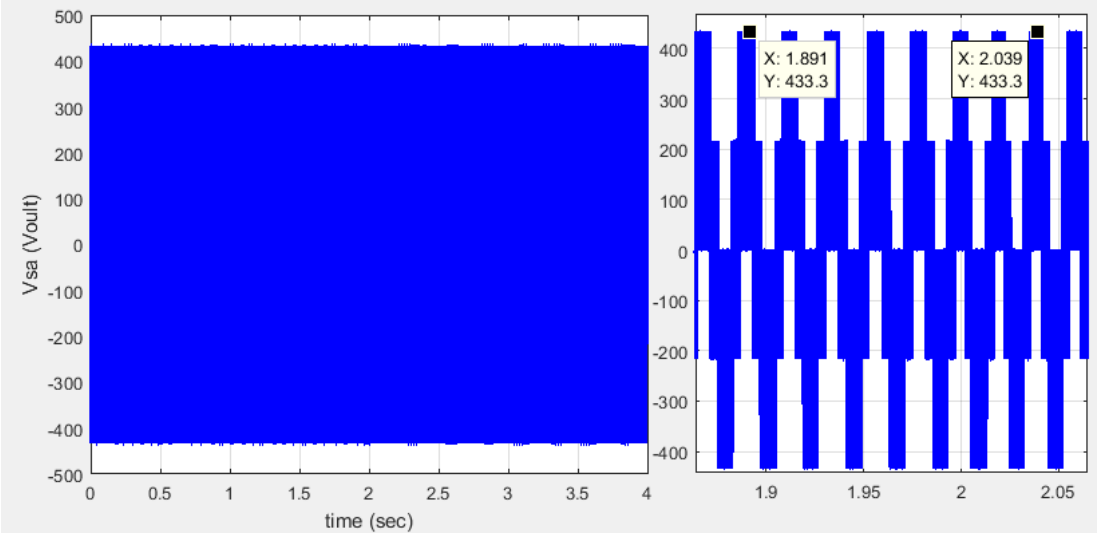

Figure 76. The applied voltages to the stator using Flux and speed fuzzy PI control based on the Sugino method at 282rad/sec speed

The current wave of the first phase of the motor is shown in figure 77. It can be seen that the values of current are within acceptable limits.

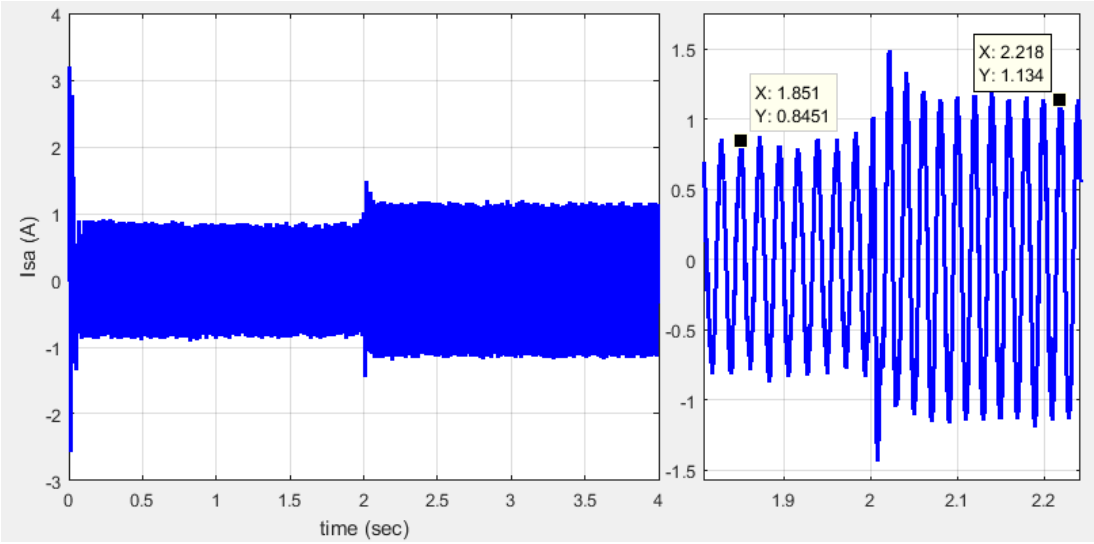

Figure 77. The applied current to the stator winding using Flux and speed fuzzy PI control based on the Sugino method at 282rad/sec speed

4.6.2. Simulation of the Flux and Speed results using fuzzy PI based on the Sugino method at a low speed

A simulation of Flux and speed V/F control system using fuzzy PI based on Sugino method when regulating the motor speed at a nominal value equal to 50rad/sec and the load torque is applied at the moment 2sec.

Figure 78 shows the response time of Flux and speed V/F control system using fuzzy PI based on the Sugino method when regulating the motor speed at a nominal value equal to 50rad/sec.

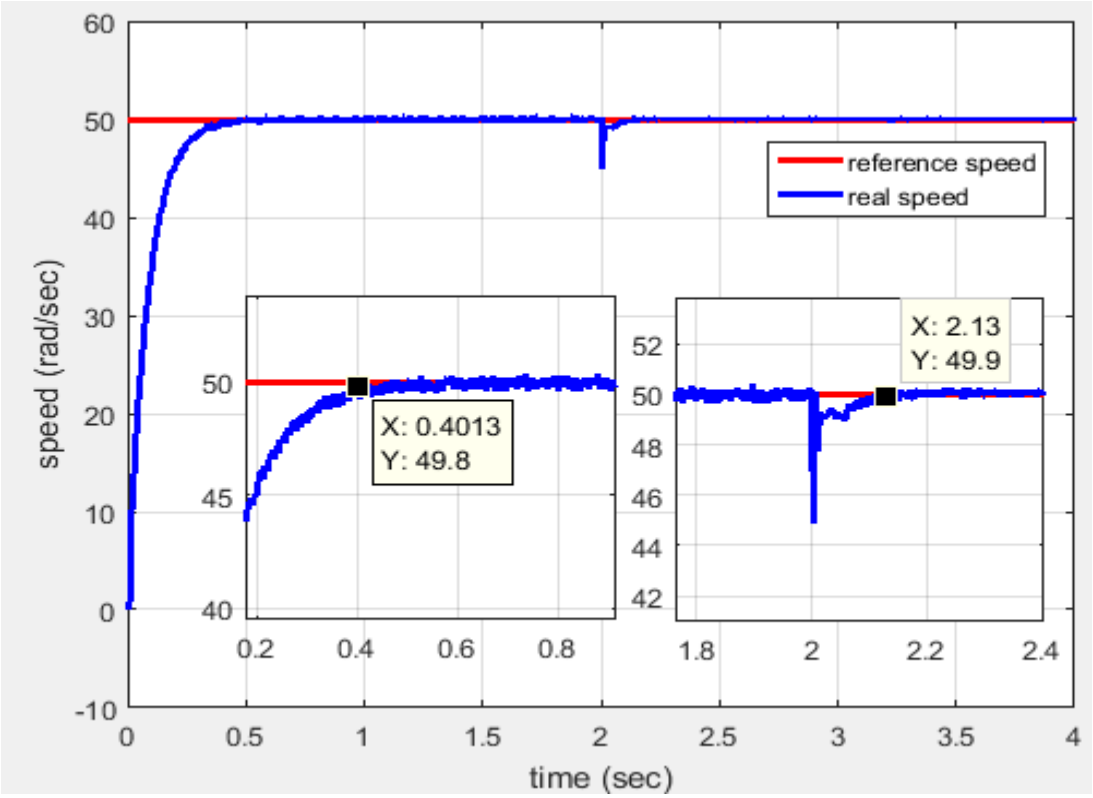

Figure 78. The Flux and speed response time control using fuzzy PI based on Sugino method at 50rad/sec speed

It is noticed from figure 78 that Flux and speed V/F control system using fuzzy PI based on the Sugino method has a settling time (ts=0.4sec) it is smaller than the settling time for speed V/F control system using fuzzy PI based on the Sugino method, but it has the same ability to overcome the load torque where the motor needs less than 0.1sec to return to the reference speed.

Figure 79 shows the response time for the flux when the speed is regulated at 50rad/sec using a speed fuzzy PI V/F control system based on the Sugino method.

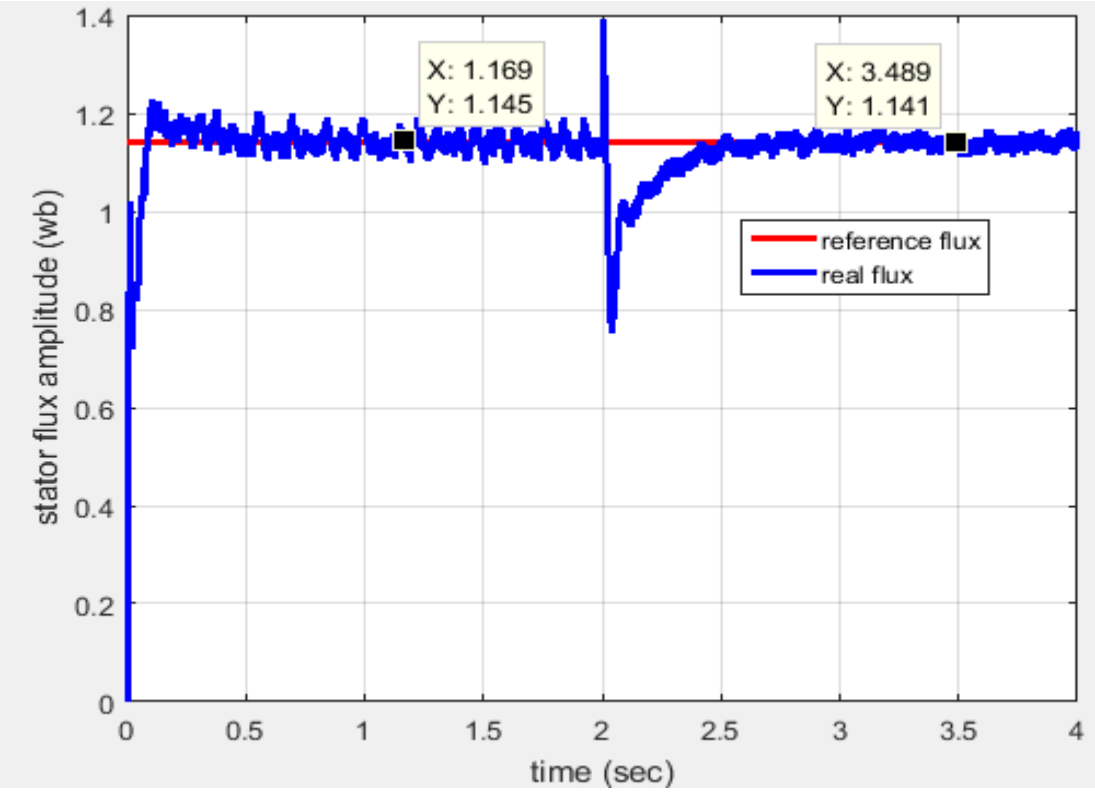

Figure 79. The flux response time using Flux and speed fuzzy PI control based on the Sugino method at 50rad/sec speed

It is noticed from figure 74 that the Flux and speed V/F control system using fuzzy PI based on the Sugino method maintains a constant value of ($\Phi_s = 1.14$ wb), unlike the speed V/F control system using fuzzy PI based on the Sugino method. This matter contributes to reducing vibrations in the electromagnetic torque, as shown in figure 75.

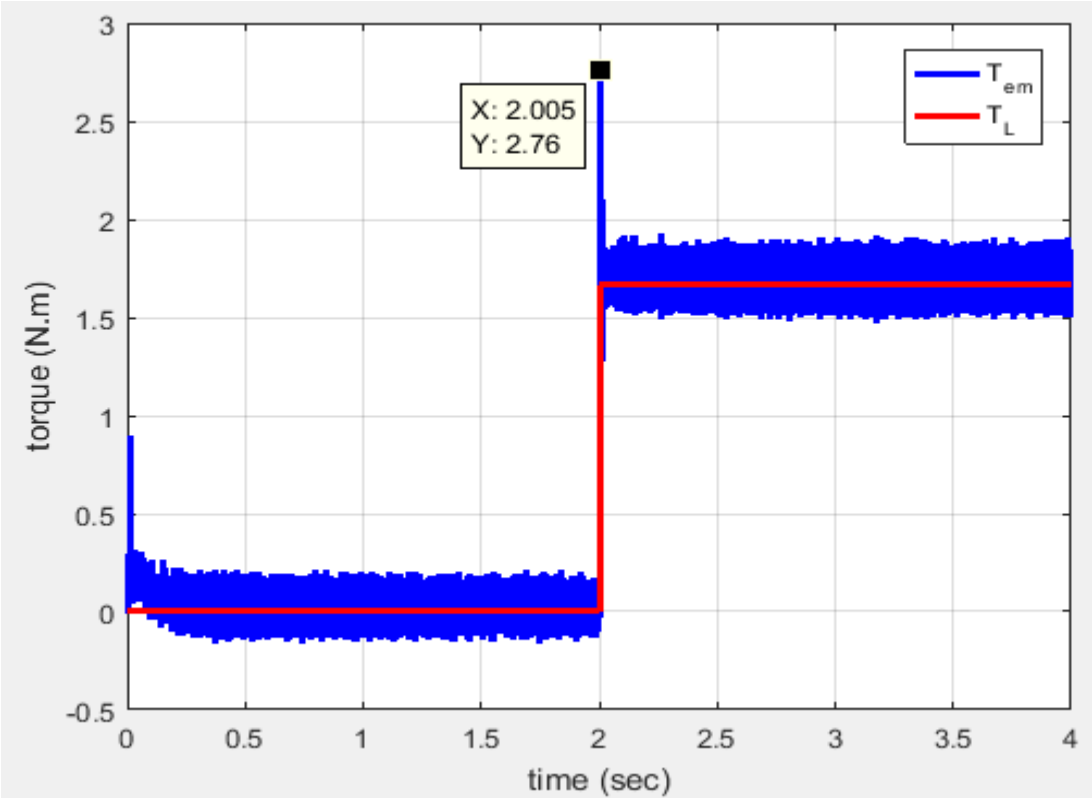

Figure 80. The electromagnetic torque response time using Flux and speed fuzzy PI control based on the Sugino method at 50rad/sec speed

The voltage wave on the first phase of the motor is shown in figure 81. It can be seen that the values of voltage are within acceptable limits.

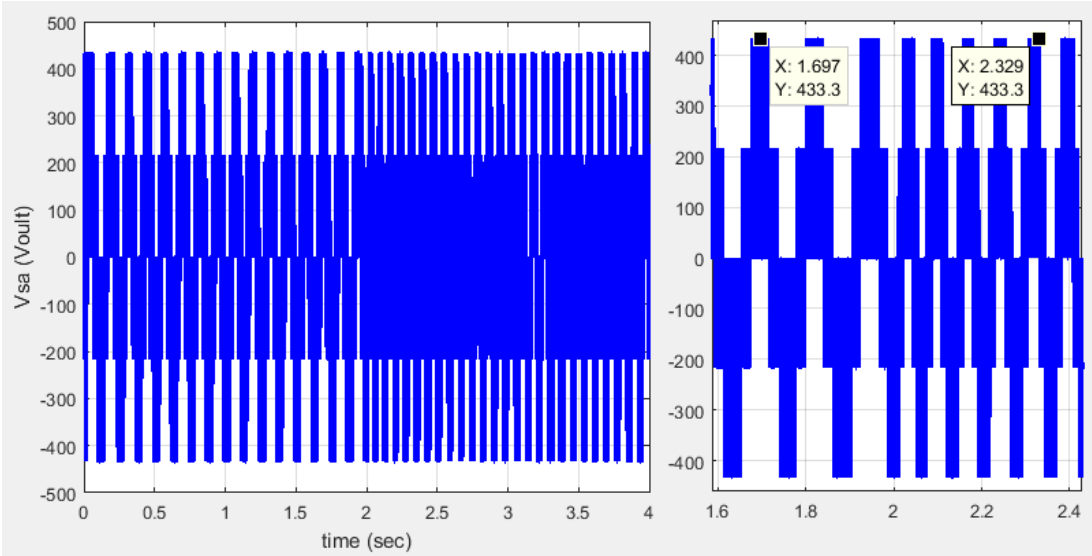

Figure 81. The applied voltages to the stator using Flux and speed fuzzy PI control based on the Sugino method at 50rad/sec

The current wave of the first phase of the motor is shown in figure 82. It can be seen that the values of current are within acceptable limits.

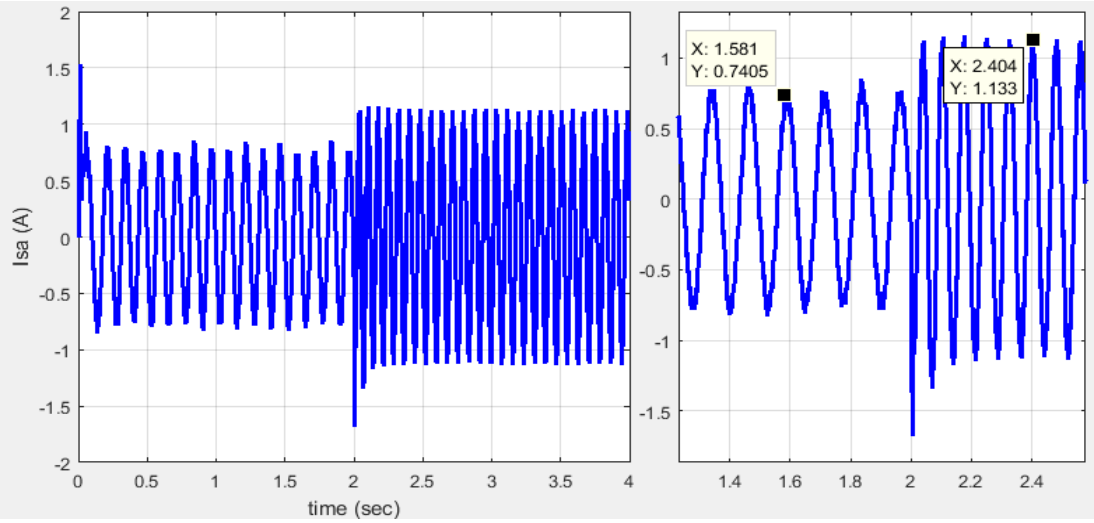

Figure 82. The current applied to the stator using Flux and speed fuzzy PI control based on the Sugino method at 50rad/sec

In Table 6, a speed V/F fuzzy PI control system based on the Mamdani method, a speed V/F fuzzy PI control system based on the Sugino method, and Flux and speed V/F fuzzy PI control system based on the Sugino method for speed regulation at high speed are compared.

Table 6. Comparison Results of fuzzy PI controller systems at High-speeds.

Controller technique	Settling time	Overcoming load time	|Qs|	torque vibration
speed V/F fuzzy PI control system based on the Mamdani method	0.7sec	0.05sec	1.23-1.2	large
speed V/F fuzzy PI control system based on the Sugino method	0.6sec	0.05sec	1.22-1.18	small
Flux and speed V/F fuzzy PI control system based on the Sugino method	0.45sec	0.05sec	1.14	small

Table 7 compares a speed V/F fuzzy PI control system based on the Mamdani method, a speed V/F fuzzy PI control system based on the Sugino method, and Flux and speed V/F fuzzy PI control system based on the Sugino method for speed regulation at low speed.

Table 7. Comparison Results of fuzzy PI controller systems at Low-speeds.

Controller technique	**Settling time**	**Overcoming load time**	**|Qs|**	**torque vibration**
speed V/F fuzzy PI control system based on the Mamdani method	0.6sec	0.1sec	1.02-1.14	large
speed V/F fuzzy PI control system based on the Sugino method	0.6sec	0.1sec	1.03-1.14	large
Flux and speed V/F fuzzy PI control system based on the Sugino method	0.4sec	0.1sec	1.14	small

CHAPTER FIVE
CONCLUSIONS AND RECOMMANDATION

5.1 Conclusions

This thesis studied and simulated a scalar V/F control system of induction motor. The control system was initially designed based on PI controllers. While its performance was poor at low speeds in; torque vibration, the time to overcome load torque, setting time, and during transient conditions, in contrast, the performance was good at high speeds, but the magnetic saturation issue arises here, as well as the flux value being higher than the nominal value, which leads to a decrease in motor efficiency, increasing losses. Thus, the motor will need economic cooling systems. In the next stage, the scalar V/F control system was designed using a fuzzy PI controller, where both Mamdani and Sugino methodologies were relied on with seven membership functions for each of the two input signals (error and error change) and the output signal (slide frequency change). The simulation results showed the effectiveness of the control system and a great ability to overcome the load torque and reduce the vibration of the torque in transient conditions. However, the need still exists to solve the magnetic saturation problem. Thus, the control system is designed based on Sugino's methodology, using five membership functions for each input and output signal to regulate speed and magnetic flux. The results confirmed that the suggested control system is quite effective.

5.2 Recommendations

For the practical implementation of the proposed control system (Flux and speed V/F control system based on fuzzy-PI techniques), a robust magnetic flux estimator will need to be developed. Also the magnetic flux is a physical amount that is not measured in an induction motor control system. Open-loop estimators give inaccurate flux estimates when stator resistance changes, causing drive systems to fail. The second issue that requires sufficient consideration is the harmonic content in an electronic inverter. Advanced PWM techniques like space vector plus width modulation or superior performance converters such as multi-level converters can reduce it.

REFERENCES

Aggarwal, A., Rai, J. N., & Kandpal, M. (2012). Comparative Study of Speed Control of Induction Motor Using PI and Fuzzy Logic Controller. IOSR Journal of Electrical and Electronics Engineering Ver. I, 10(2), 2278–1676. Retrieved from www.iosrjournals.org

Agrawal, A., Lodhi, R. S., & Nema, P. (2019). Indirect vector control for induction motor drive using two-level and five-level inverter. International Journal of Applied Power Engineering (IJAPE), 8(2), 134. https://doi.org/10.11591/ijape.v8.i2.pp134-144

Akhila, E., Kumar, N. P., & Isha, T. B. (2016). Fuzzy logic and PI controls in speed control of induction motor. Advances in Intelligent Systems and Computing (Vol. 397, pp. 987–1001). Springer Verlag. https://doi.org/10.1007/978-81-322-2671-0_93

Araria, R., Berkani, A., Negadi, K., Marignetti, F., & Boudiaf, M. (2020). Performance analysis of DC-DC converter and DTC-based fuzzy logic control for power management in electric vehicle application. Journal Europeen Des Systemes Automatises, 53(1), 1–9. https://doi.org/10.18280/jesa.530101

Arulmozhiyal, R., Baskaran, K., Devarajan, N., & Kanagaraj, J. (2009). Space vector pulse width modulation-based induction motor speed control using FPGA. 2009 2nd International Conference on Emerging Trends in Engineering and Technology, ICETET 2009, 1(1), 742–747. DOI: 10.1109/ICETET.2009.208

Bharti, R., Kumar, M., & Prasad, B. M. (2019). V/F Control of Three Phase Induction Motor. Proceedings - International Conference on Vision Towards Emerging Trends in Communication and Networking, ViTECoN 2019, 1–4. DOI: 10.1109/ViTECoN.2019.8899420

Chen, M., & Zhang, W. (2015). H2 optimal speed regulator for vector-controlled induction motor drives. Proceedings of the 2015 27th Chinese Control and Decision Conference, CCDC 2015, 3, 1233–1236. DOI: 10.1109/CCDC.2015.7162106

Devi, K., Gautam, S., & Nagaria, D. (2014). Speed Control of 3-Phase Induction Motor Using Self-Tuning Fuzzy PID Controller and Conventional PID Controller. International Journal of Information & Computation Technology, 4(12), 1185–1193.

Divyasree & Binojkumar, P., & Binojkumar, A. C. (2017). Induction Motor Drive Using Space Vector PWM Technique. 2017 International Conference on Energy, Communication, Data Analytics and Soft Computing (ICECDS), 2946–2951.

Diyoke, G. C., C., O., & Aniagwu, U. (2016). Different Methods of Speed Control of Three-Phase Asynchronous Motor. American Journal of Electrical and

Electronic Engineering, Vol. 4, 2016, Pages 62-68, 4(2), 62–68. Retrieved from http://pubs.sciepub.com/ajeee/4/2/3/

Duranay, Z. B., Guldemir, H., & Tuncer, S. (2020). Implementation of a V/f Controlled Variable Speed Induction Motor Drive. EMITTER International Journal of Engineering Technology, 8(1), 35–48. https://doi.org/10.24003/emitter.v8i1.490

El-Zohri, E. H., & Mosbah, M. A. (2020). Speed Control of Inverter-Fed Induction Motor Using Hybrid Fuzzy-PI Controller. Proceedings of 2020 International Conference on Innovative Trends in Communication and Computer Engineering, ITCE 2020, 216–221. DOI: 10.1109/ITCE48509.2020.9047750

Farah, N., Talib, M. H. N., Ibrahim, Z. B., Abdullah, Q., Aydoğdu, Ö., Lazi, J. M., & Isa, Z. (2021). Fuzzy membership functions tuning for speed controller of induction motor drive: Performance improvement. Indonesian Journal of Electrical Engineering and Computer Science, 23(3), 1258–1270. https://doi.org/10.11591/ijeecs.v23.i3.pp1258-1270

Fereka, D., Zerikat, M., & Belaidi, A. (2018). MRAS Sensorless Speed Control of an Induction Motor Drive Based on Fuzzy Sliding Mode Control. In 2018 7th International Conference on Systems and Control, ICSC 2018 (pp. 230–236). Institute of Electrical and Electronics Engineers Inc. https://doi.org/10.1109/ICoSC.2018.8587844

Hannan, M. A., Ali, J. A., Ker, P. J., Mohamed, A., Lipu, M. S. H., & Hussain, A. (2018). Switching techniques and intelligent controllers for induction motor drive: Issues and recommendations. IEEE Access, 6(c), 47489–47510. DOI: 10.1109/ACCESS.2018.2867214

Hinkkanen, M., Tiitinen, L., Molsa, E., & Harnefors, L. (2022). On the Stability of Volts-per-Hertz Control for Induction Motors. IEEE Journal of Emerging and Selected Topics in Power Electronics, 10(2), 1609–1618. https://doi.org/10.1109/JESTPE.2021.3060583

https://doi.org/10.1109/ICACCM50413.2020.9212965

Karthik, D., & Chelliah, T. R. (2017). Analysis of scalar and vector control-based efficiency-optimized induction motors subjected to inverter and sensor faults. In Proceedings of 2016 International Conference on Advanced Communication Control and Computing Technologies, ICACCCT 2016 (pp. 462–466). Institute of Electrical and Electronics Engineers Inc. https://doi.org/10.1109/ICACCCT.2016.7831682

Lee, J. W. (2019). Novel Current Control Assisted V/F Control Method for High-Speed Induction Motor Drives. ICPE 2019 - ECCE Asia - 10th International Conference on Power Electronics - ECCE Asia, 3, 1293–1296. DOI: 10.23919/icpe2019-ecceasia42246.2019.8796956

Lee, K., & Han, Y. (2022). Reactive-Power-Based Robust MTPA Control for v/f Scalar-Controlled Induction Motor Drives. IEEE Transactions on Industrial Electronics, 69(1), 169–178. https://doi.org/10.1109/TIE.2021.3055183

Lesani, M. J., Mahmoudi, H., Ebrahim, M., Varzali, S., & Khaburi, D. A. (2013). Predictive torque control of induction motor based on improved fuzzy PI control method. 13th Iranian Conference on Fuzzy Systems, IFSC 2013, 1–5. DOI: 10.1109/IFSC.2013.6675649

Li, W., Xu, Z., & Zhang, Y. (2019). Induction, motor control system, based on FOC algorithm. In Proceedings of 2019 IEEE 8th Joint International Information Technology and Artificial Intelligence Conference, ITAIC 2019 (pp. 1544–1548). Institute of Electrical and Electronics Engineers Inc. https://doi.org/10.1109/ITAIC.2019.8785597

Mikhael, H., Jalil, H., & Ibrahim, I. (2016). Speed Control of Induction Motor using PI and V/F Scalar Vector Controllers. International Journal of Computer Applications, 151(7), 36–43. https://doi.org/10.5120/ijca2016911831

Mohammed, A. N., & Ghoneim, G. A. R. (2021). Fuzzy-PID Speed Controller Model-Based Indirect Field Oriented Control for Induction Motor. In Proceedings of 2020 International Conference on Computer, Control, Electrical, and Electronics Engineering, ICCCEEE 2020. Institute of Electrical and Electronics Engineers Inc. https://doi.org/10.1109/ICCCEEE49695.2021.9429623

Moutchou, M., Jbari, A., & Abouelmahjoub, Y. (2021). Implemented reduced induction machine fuzzy logic control based on DSpace-1104 r&d controller board. International Journal of Power Electronics and Drive Systems, 12(2), 1015–1023. https://doi.org/10.11591/ijpeds.v12.i2.pp1015-1023

Mugheri, N. H., & Keerio, M. U. (2021). An Optimal Fuzzy Logic-based PI Controller for the Speed Control of an Induction Motor using the V/F Method. Engineering, Technology & Applied Science Research, 11(4), 7399–7404. DOI: 10.48084/etasr.4255

Nishad, B. K., & Sharma, R. (2018). Induction Motor Control using Modified Indirect Field Oriented Control. India International Conference on Power Electronics, IICPE, 2018-December(2), 1–5. DOI: 10.1109/IICPE.2018.8709426

Pedra, J., Candela, I., & Sainz, L. (2009). Modeling of squirrel-cage induction motors for transient electromagnetic programs. IET Electric Power Applications, 3(2), 111–122. https://doi.org/10.1049/iet-epa:20080043

Pena, J. M., & Diaz, E. V. (2017). Implementation of V/f scalar control for speed regulation of a three-phase induction motor. Proceedings of the 2016 IEEE ANDESCON, ANDERSON 2016. DOI: 10.1109/ANDESCON.2016.7836196

Ping, L., & Lanying, H. (2006). Vector control-based speed sensorless control of induction motors using a sliding-mode controller. Proceedings of the World

Congress on Intelligent Control and Automation (WCICA), 1(03), 1942–1946. DOI: 10.1109/WCICA.2006.1712695

Sabir, A., & Ibrir, S. (2018). Induction motor speed control using the reduced-order model. Automatika, 59(3–4), 274–285. https://doi.org/10.1080/00051144.2018.1531963

Sharma, G., Parashar, D., & Chandel, A. (2020). Analysis of Dynamic Model of Three Phase Induction Motor with MATLAB/SIMULINK. In Proceedings - 2020 International Conference on Advances in Computing, Communication, and Materials, ICACCM 2020 (pp. 51–58). Institute of Electrical and Electronics Engineers Inc.

Shiravani, F., Alkorta, P., Cortajarena, J. A., & Barambones, O. (2022). An Enhanced Sliding Mode Speed Control for Induction Motor Drives. Actuators, 11(1). https://doi.org/10.3390/act11010018

Sudaryanto, A., Purwanto, E., Ferdiansyah, I., Nugraha, S. D., Qudsi, O. A., Rifadil, M. M. H., & Rusli, M. R. (2020). Design and Implementation of SVPWM Inverter to Reduce Total Harmonic Distortion (THD) on Three Phase Induction Motor Speed Regulation Using Constant V/F. 2020 3rd International Seminar on Research of Information Technology and Intelligent Systems, ISRITI 2020, 412–417. DOI: 10.1109/ISRITI51436.2020.9315353

Suetake, M., Da Silva, I. N., & Goedtel, A. (2011). Embedded DSP-based compact fuzzy system and its application for induction-motor V/f speed control. IEEE Transactions on Industrial Electronics, 58(3), 750–760. DOI: 10.1109/TIE.2010.2047822

Trabelsi, R., Khedher, A., Mimouni, M. F., & M'Sahli, F. (2012). Backstepping control for an induction motor using an adaptive sliding rotor-flux observer. Electric Power Systems Research, 93, 1–15. DOI: 10.1016/j.epsr.2012.06.004

Uddin, M. N., Radwan, T. S., & Rahman, M. A. (2002). Performances of fuzzy-logic-based indirect vector control for induction motor drive. IEEE Transactions on Industry Applications, 38(5), 1219–1225. https://doi.org/10.1109/TIA.2002.802990

Verma, P., Saxena, R., Chitra, A., & Sultana, R. (2018). Implementing fuzzy PI scalar control of induction motor. IEEE International Conference on Power, Control, Signals and Instrumentation Engineering, ICPCSI 2017, 1674–1678. DOI: 10.1109/ICPCSI.2017.8391998

RESUME

Personal Information

Surname, name : Mohammed AL-EZZI

Nationality : Iraq

Education

Degree	Education Unit	Graduation Date
Master	Electrical-electronic engineering	2022
Bachelor	Electrical engineering	2004/2005
High School	Al-jumhuria school	2000

Work Experience

Year	Place	Title
2000-2022	Baghdad and Kirkuk -Iraq	Electrical engineering

Foreign Language

Arabic – English

Publications